

STATUS OF THESIS

Title of thesis **A Study on the Potential of Amino Acid Salt as a Solvent for Acid Gas Removal**

I, **FAISAL HARRIS**

hereby allow my thesis to be placed at the Information Resource Center (IRC) of Universiti Teknologi PETRONAS (UTP) with the following conditions:

1. The thesis becomes the property of UTP
2. The IRC of UTP may make copies of the thesis for academic purposes only
3. This thesis classified as

Confidential

Non-confidential

If the thesis is confidential, please state the reason:

The contents of the thesis will remain confidential for _____ years.

Remarks on disclosure:

Endorsed by

Signature of Author

Warakas 5 gg. 14 no. 99
Warakas, Tg. Priok
Jakarta 14340
Indonesia

Date: _____

Signature of Supervisor

A.P. Dr. Mohamed Ibrahim Abdul Mutalib

Department of Chemical Engineering
Universiti Teknologi PETRONAS
Bandar Seri Iskandar, Perak
Malaysia

Date: _____

APPROVAL

UNIVERSITI TEKNOLOGI PETRONAS

Approval by Supervisors

The Undersigned certify that they have read, and recommend to The Postgraduate Studies Programme for acceptance, a thesis entitled “**A Study on the Potential of Amino Acid Salt as a Solvent for Acid Gas Removal**” Submitted by **Faisal Harris** for the fulfilment of the requirements for the degree of Master of Science in Chemical Engineering.

Date

Signature : _____

Main supervisor : _____

Date : _____

Signature : _____

Co-Supervisor : _____

Date : _____

UNIVERSITI TEKNOLOGI PETRONAS

A Study on the Potential of Amino Acid Salt as
a Solvent for Acid Gas Removal

By

Faisal Harris

A THESIS

SUBMITTED TO THE POSTGRADUATE STUDIES PROGRAMME
AS A REQUIREMENT FOR THE DEGREE OF MASTER OF SCIENCE
IN CHEMICAL ENGINEERING PROGRAMME

BANDAR SERI ISKANDAR

PERAK

JULY 2009

DECLARATION

I hereby declare that the thesis is based on my original work except for quotations and citations which have been duly acknowledged. I also declare that it has not been previously or concurrently submitted for any other degree at UTP or other institutions.

Signature : _____

Name : FAISAL HARRIS

Date : _____

ABSTRACT

The presence of acid gas impurities has been one of the major problems in natural gas processing, utilization and transportation. Absorption using alkanolamine as reactive solvent is one of the widely used process to remove these impurities. Very recently, it has been observed by various researchers that alkanolamines could be potentially replaced with amino acids salt as alternative solvent for carbon dioxide (CO₂) absorption because of its molecular similarity.

In this study, the potential of sodium glycinate, one of amino acid salt, as absorbent for CO₂ absorption is investigated. Some critical fundamental properties of aqueous sodium glycinate is measured for various concentrations (1, 5, 10, 15, 20, 30 wt. %) at various temperature. Density, kinematic viscosity, refractive index, heat capacity, acidity, conductivity, surface tension and contact angle with stainless steel surface of aqueous sodium glycinate are measured and reported. Absorption test to measure the solubility of carbon dioxide in aqueous sodium glycinate is conducted using SOLTEQ BP-22 High Pressure Solubility Cell. The solubility of CO₂ in aqueous solution of sodium glycinate is measured for the CO₂ partial pressure ranging from 100 to 2500 kPa at temperatures 298.15 and 313.15 K. It is observed that loading capacity increases with an increase in partial pressure of CO₂ but decreases with increase in sodium glycinate concentration and temperature. It is found that sodium glycinate has higher loading capacity compared to monoethanolamine (MEA) for the same solution wt. %. In order to quantify the effect of CO₂ loading on the physical properties of absorbent, the physical properties of CO₂-loaded absorbent are measured. Hence in this present work, the density, kinematic viscosity, heat capacity, acidity, and conductivity of aqueous sodium glycinate after CO₂ absorption are measured and reported.

Case study comparing absorber design of monoethanolamine and sodium glycinate is done to give overview of the overall performance of sodium glycinate in actual acid gas removal system compared to commercial absorbent, MEA. It is observed that the required solution flowrate for sodium glycinate absorber is slightly lower than MEA. The calculated absorber diameter for sodium glycinate is smaller compared to MEA.

These results show that sodium glycinate could be a potential alternative absorbent for acid gas removal.

Keywords: Sodium glycinate, CO₂ absorption, Absorber

ABSTRAK

Kehadiran bendasing di dalam gas asid menjadi penyebab utama kepada permasalahan gas asli. Proses penyerapan dengan menggunakan alkanolamine sebagai bahan pelarut reaktif merupakan satu kaedah yg telah meluas digunapakai untuk menyingkir bendasing tersebut. Pada masa kini para penyelidik telah membuktikan bahawa penggantian alkanolamine kepada larutan garam asid amino sebagai pelarut alternatif bagi penyerapan CO₂ amat berpotensi disebabkan oleh struktur molekul yang sama antara kedua-dua bahan.

Dalam kajian ini, kebolehan salah satu garam asid amino yaitu sodium glycinate digunakan sebagai pelarut bagi penyerapan CO₂ telah diselidik. Seseengah sifat-sifat asas yang kritikal di dalam larutan akueus sodium glycinate telah disukat kepekannya (1, 5, 10, 15, 20, 30 wt. %) pada suhu yang berbeza. Ketumpatan, kelikatan kinematik, index biasan, muatan haba, keasidan, kekonduksian, ketegangan permukaan dan sudut sentuhan dengan permukaan stainless steel larutan akueus sodium glycinate telah disukat dan direkodkan. Ujian penyerapan bagi mengukur kebolehlarutan karbon dioksida di dalam larutan akueus sodium glycinate telah menggunakan alat SOLTEQ BP-22 High Pressure Solubility Cell. Kebolehlarutan CO₂ di dalam larutan akueus sodium glycinate telah disukat bagi tekanan separa CO₂ dari 100 ke 2500 kPa pada suhu 298.15 dan 313.15 K. Keputusan ujikaji menunjukkan pertambahan berlaku kepada tekanan separa CO₂ apabila kapasiti muatan dinaikkan dan sebaliknya apabila ia diturunkan. Ini disebabkan sodium glycinate mempunyai kapasiti muatan yang tinggi berbanding dengan monoethanolamine (MEA) bagi kepekatan yang sama. Bagi mengganggarkan kesan muatan CO₂ terhadap sifat fizikal pelarut, penyukatan dilakukan keatas sifat fizikal pelarut asid amino yang telah menyerap CO₂. Didalam ujikaji ini, ketumpatan, kelikatan kinematik, muatan haba, keasidan, dan kekonduksian larutan akueus sodium glycinate selepas penyerapan CO₂ telah disukat dan direkodkan. Kajian bagi perbandingan rekabentuk penyerap diantara monoethanolamine dengan sodium glycinate telah berjaya memberi gambaran secara menyeluruh kebolehan sodium glycinate di dalam situasi sebenar sistem penyingkiran gas asid berbanding dengan penyerap komersial, MEA. Hasil keputusan pemerhatian menunjukkan yang kadaralir

larutan untuk penyerap menggunakan sodium glycinate sebagai pelarut adalah lebih rendah berbanding penyerap yang menggunakan MEA. Pengiraan diameter penyerap juga menunjukkan diameter yang lebih kecil diperlukan bagi penyerap yang menggunakan sodium glycinate. Keputusan ini telah menunjukkan bahawasanya sodium glycinate berupaya menjadi pelarut alternatif bagi pemisahan gas asid.

Kata kunci: Sodium glycinate, Penyerapan CO₂, Absorber

TABLE OF CONTENT

STATUS OF THESIS	i
APPROVAL	ii
DECLARATION	iv
ABSTRACT	v
ABSTRAK	vii
TABLE OF CONTENT	ix
LIST OF FIGURE	xi
LIST OF TABLE	xiii
CHAPTER 1 INTRODUCTION	1
1.1 Background	1
1.1.1 Natural Gas History	2
1.1.2 Natural Gas Constituents	3
1.2 Problem Statement	4
1.3 Research Objective	5
1.4 Research Scope	6
CHAPTER 2 LITERATURE REVIEW	7
2.1 Natural Gas	7
2.2 Acid Gases	7
2.3 Absorption	8
2.4 Alkaline Salt	9
2.5 Alkanolamines	13
2.6 Amino Acid Salt	16
CHAPTER 3 METHODOLOGY	21
3.1 Amino Acid Salt Preparation	21
3.2 Density	22
3.2.1 Equipment description	22
3.2.2 Measurement method	23
3.3 Kinematic Viscosity	23
3.3.1 Equipment description	23
3.3.2 Measurement method	24
3.3.3 Calculation method	25
3.4 Heat Capacity	25
3.4.1 Equipment description	25
3.4.2 Measurement method	26
3.4.3 Calculation method	26
3.5 Refractive Index	27
3.5.1 Equipment description	27
3.5.2 Measurement method	27
3.6 Acidity	28
3.6.1 Equipment description	28
3.6.2 Measurement method	28
3.7 Conductivity	29
3.7.1 Equipment description	29
3.7.2 Measurement method	29
3.8 Surface Tension and Contact Angle	30
3.8.1 Equipment description	30

3.8.2	Measurement method.....	30
3.9	Absorption Test.....	32
3.9.1	Equipment description.....	32
3.9.2	Experimental method.....	33
3.10	Regenerability test.....	38
CHAPTER 4	RESULT.....	40
4.1	Density.....	40
4.2	Kinematic Viscosity.....	44
4.3	Heat Capacity.....	46
4.4	Refractive Index.....	50
4.5	Acidity.....	51
4.6	Conductivity.....	53
4.7	Surface Tension and Contact Angle.....	55
4.8	Absorption Test.....	56
4.9	Regenerability test.....	65
CHAPTER 5	DESIGN OF ABSORPTION PROCESS.....	67
5.1	Absorber.....	67
5.2	Design of Absorber.....	69
5.3	Material and Energy Balance around Absorber.....	69
5.3.1	Process description.....	69
5.3.2	Calculation method.....	71
5.3.3	Design parameter.....	76
5.4	Diameter of Absorber Calculation.....	76
5.4.1	Calculation method.....	78
5.4.2	Design parameter.....	83
5.5	Absorber Design Result.....	84
CHAPTER 6	CONCLUSION AND RECOMMENDATION.....	86
6.1	Conclusion.....	86
6.2	Recommendation.....	88
REFERENCES	89
PUBLICATION	105
APPENDIX A	106
APPENDIX B	112

LIST OF FIGURE

Figure 1.1 World energy consumption for the year 2007 in Million tonnes oil equivalent.....	1
Figure 2.1 Basic Scheme of absorption-stripping process.....	9
Figure 2.2 Molecular structure of primary, secondary and tertiary amine	14
Figure 2.3 Molecular structure of some alkanolamines.....	16
Figure 2.4 Reaction scheme for carbon dioxide absorption into sodium glycinate.....	18
Figure 3.1 Structure of sodium glycinate.....	22
Figure 3.2 Anton Paar DMA-5000 digital vibrating-tube density meter.....	23
Figure 3.3 Cannon Ubblohde type no 25 B433 viscometer.....	24
Figure 3.4 Perkin Elmer Pyris 1 Digital Scanning Calorimeter.....	26
Figure 3.5 ATAGO RX5000 Refractometer with PORTEGI model 631D water bath	28
Figure 3.6 Mettler Toledo 320 pHmeter	29
Figure 3.7 HACH Sension 7	30
Figure 3.8 Interfacial Tension Meter IFT-700.....	31
Figure 3.9 IFT-700 standard test method.....	31
Figure 3.10 Schematic Diagram of SOLTEQ BP-22 High Pressure Solubility Cell...34	
Figure 3.11 SOLTEQ BP-22 High Pressure Solubility Cell.....	35
Figure 3.12 Typical absorption pressure profile for sodium glycinate-CO ₂ system using SOLTEQ BP-22 High Pressure Solubility Cell.	37
Figure 3.13 ELMA 680DH ultrasonic water bath	39
Figure 4.1 Density as a function of temperature for aqueous sodium glycinate solutions of different concentrations.....	41
Figure 4.2 Heat capacity as a function of temperature for aqueous sodium glycinate solutions of different concentrations.....	47
Figure 4.3 Pressure profile for CO ₂ absorption in aqueous sodium glycinate (SG) at 100 kPa and 313.15 K.....	53
Figure 4.4 Loading capacity of 30 wt. % methyldiethanolamine (MEA) at 313.15K.....	57
Figure 4.5 Loading capacity of aqueous sodium glycinate (SG) at 298.15 K;.....	59
Figure 4.6 Loading capacity of aqueous sodium glycinate (SG) at 313.15 K;.....	59

Figure 4.7 Carbon dioxide solubility in water and aqueous sodium glycinate solution at 313.15 K.....	61
Figure 4.8 Pareto charts for standardized effects of CO ₂ loading factor	63
Figure 4.9 Loading capacity of aqueous sodium glycinate (SG) at 313.15 K.....	64
Figure 4.10 Loading capacity of solution at 313.15 K	65
Figure 4.11 Loading capacity of 10 wt. % aqueous sodium glycinate (SG) at 1000 kPa and 313.15 K.....	66
Figure 5.1 Typical commercial tray.....	68
Figure 5.2 Heat and material balance around absorber.....	70
Figure 5.3 Flow diagram for the material and energy balance around absorber	72
Figure 5.4 Flow diagram for diameter of absorber calculation	77
Figure 5.5 Flooding velocity constant for sieve tray	79
Figure 5.6 Tray layout.....	80

LIST OF TABLE

Table 1.1 Malaysia's oil and gas energy data.....	2
Table 3.1 Experimental parameter for absorption test.....	33
Table 4.1 Densities of aqueous sodium glycinate solutions	41
Table 4.2 Densities of aqueous sodium glycinate solution after CO ₂ absorption.....	43
Table 4.3 Correlation coefficient for Equation 4.4.....	43
Table 4.4 Kinematic viscosities of aqueous sodium glycinate solution	44
Table 4.5 Kinematic viscosities of aqueous sodium glycinate solution after CO ₂ absorption.....	45
Table 4.6 Correlation coefficient for Equation 4.6.....	45
Table 4.7 Heat capacity of water	46
Table 4.8 Heat capacity of aqueous sodium glycinate solution.....	47
Table 4.9 Heat capacity (in kJ.kg ⁻¹ .K ⁻¹) of 1.0 wt. % aqueous sodium glycinate solution after CO ₂ absorption at 298.15 K.....	48
Table 4.10 Heat capacity (in kJ.kg ⁻¹ .K ⁻¹) of 5.0 wt. % aqueous sodium glycinate solution after CO ₂ absorption at 298.15 K.....	48
Table 4.11 Heat capacity (in kJ.kg ⁻¹ .K ⁻¹) of 10 wt. % aqueous sodium glycinate solution after CO ₂ absorption at 298.15 K.....	49
Table 4.12 Heat capacity (in kJ.kg ⁻¹ .K ⁻¹) of 15 wt. % aqueous sodium glycinate solution after CO ₂ absorption at 298.15 K.....	49
Table 4.13 Heat capacity (in kJ.kg ⁻¹ .K ⁻¹) of 20 wt. % aqueous sodium glycinate solution after CO ₂ absorption at 298.15 K.....	49
Table 4.14 Heat capacity (in kJ.kg ⁻¹ .K ⁻¹) of 30 wt. % aqueous sodium glycinate solution after CO ₂ absorption at 298.15 K.....	49
Table 4.15 Correlation coefficient for Equation 4.8.....	50
Table 4.16 Refractive index of aqueous sodium glycinate solutions.....	50
Table 4.17 Acidity of aqueous sodium glycinate solution at various concentrations..	51
Table 4.18 Acidity of aqueous sodium glycinate solution after CO ₂ absorption.....	52
Table 4.19 Conductivity of aqueous sodium glycinate at various concentrations.....	53
Table 4.20 Conductivity of aqueous sodium glycinate solution after CO ₂ absorption	54
Table 4.21 Correlation coefficient for Equation 4.10.....	54

Table 4.22 Surface tension of aqueous sodium glycinate solutions and Contact angle with stainless steel surface at temperature 298.15 K	55
Table 4.23 Solubility of CO ₂ in 30 wt. % MEA Aqueous Solution at 313.15 K.....	56
Table 4.24 Solubilities of CO ₂ ($\alpha = \text{mol CO}_2/\text{mol SG}$)	58
Table 4.25 The correlation constants and R ² for Equation 4.12	60
Table 4.26 Correlation coefficient for Equation 4.13	62
Table 4.27. Solubility of CO ₂ during regenerability test	66
Table 5.1 Coefficient constant for Equation 5.6.....	74
Table 5.2 Feed gas condition and composition.....	76
Table 5.3 Rule of thumb and criterion for absorber design	83
Table 5.4 Absorber design parameter	85

CHAPTER 1

INTRODUCTION

1.1 Background

Natural gas is one of the world's main energy sources beside oil and coal. Natural gas consumption covered around 24 % of world energy consumption during the year 2007 (equal to 2637.7 million ton oil equivalent) [1]. The detailed breakdown of world energy consumption is shown in Figure 1.1. Malaysia's total gas consumption for the year 2006 was 1164.7 billion cubic feet and this ranks Malaysia at the 21st position in the world gas consumer. On the other hand, Malaysia's total gas production for the same year reached 2217.8 billion cubic feet and this placed Malaysia as the 11th largest natural gas producer. The total Malaysia's proven reserved natural gas is 75000 billion cubic feet. Malaysia's oil and gas energy data are shown in Table 1.1 [2].

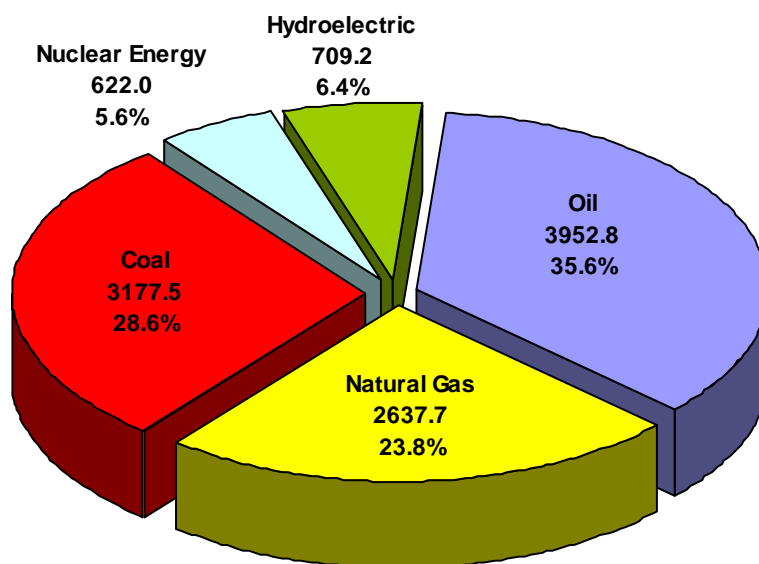


Figure 1.1 World energy consumption for the year 2007 in Million tonnes oil equivalent (Source: BP Report, 2008 [1])

Table 1.1 Malaysia's oil and gas energy data

(Source: EIA Report, 2008 [2])

	Year				
	2003	2004	2005	2006	2007
Petroleum (Thousand Barrels per Day)					
Total Oil Production	841.68	861.81	751.82	729.36	702.97
Crude Oil Production	737.86	755.35	631.07	612.6	588.22
Consumption	480	508	501	501	501*
Net Exports/Imports(-)	362	354	251	228	202*
Proved Reserves	3.10 ⁶	3.10 ⁶	3.10 ⁶	3.10 ⁶	3.10 ⁶
Natural Gas (Billion Cubic Feet)					
Production	2005.9	2204.7	2242.5	2217.8	NA
Consumption	1117	1204.9	1172.5	1164.7	NA
Net Exports/Imports(-)	888.9	999.8	1070	NA	NA
Proved Reserves	75000	75000	75000	75000	75000

* Forecast value

1.1.1 Natural Gas History

Natural gas was initially not recognised as an energy source by itself. It was considered as a nuisance because it was often found during the process of digging well for water or brine in the late 1800's. Some effort was made to utilize this "unwanted" gas in small scale. Natural gas then starts to be known when it was used as a replacement for "coal gas" or also called as "town gas". This "coal gas" is the gas manufactured by heating coal [3]. Difficulties in the transportation coupled with the rapid depletion of gas well due to the small amount of reserve, inefficient processing, leakages during distribution and improper application of natural gas have been some of the factors that hold back the progress of it being used as energy source. The invention of seamless pipe as pipeline material and pipe welding method has overcome the problem in natural gas transportation. Advances in technology for exploration, exploitation and processing of natural gas have also complimented the growth of natural gas usage.

1.1.2 Natural Gas Constituents

Natural gas consists of mainly hydrocarbon gases namely methane, ethane, propane, butane and some impurities. Water is the primary impurity that occurs along with natural gas. All natural gas reservoirs whether it is an associated or non associated gas reservoir, contain water [4]. Water content in natural gas must be removed in order to improve its heating value. The water removal is also necessary to reduce pipeline corrosion and avoid condensation or hydrate formation during gas transportation. The water content in natural gas could be removed by various means. Absorption using liquid absorbent like glycol or saline brines is widely used for gas dehydration process. The utilization of silica-alumina based adsorbent or zeolite based molecular sieve is also commonly practised in gas processing industries [5].

Natural gas from wet gas reservoir also contains higher chain hydrocarbons, which are also considered as impurities. These higher chain hydrocarbons have to be separated to avoid condensation during transportation and also to recover natural gas liquid (NGL), which forms due to condensation of the higher molecular weight hydrocarbon. Condensation and absorption are the common technique used for the removal of these impurities [5].

Other major impurity of natural gas is acid gas. Hydrogen sulphide (H_2S) and carbon dioxide (CO_2) are the primary acid gas contaminants. Hydrogen sulphide is a toxic and highly acidic gas that is commonly found in natural gas while carbon dioxide is the acid gas with most quantity in natural gas. Beside these two gases there are still other acid gases such as nitrogen oxide (NO_x), sulphur dioxide (SO_2) and carbon monoxide (CO). Acid gas like carbon dioxide (CO_2) and sulphur dioxide (SO_2) has to be removed from natural gas in order to reduce the corrosion in pipes and equipment while also increasing the purity of the natural gas. By increasing the purity, the heating value and commercial value of natural gas will be significantly increased. The general and common techniques used for the removal of acid gas are absorption into liquid, adsorption using solid, permeation through membrane, cryogenic condensation or conversion into another compound [5].

Absorption using alkanolamines is one of the well known and widely used process. Aqueous alkanolamine solvent has been chosen due to its high reactivity and low cost. *Monoethanolamine* (MEA), *diethanolamine* (DEA), *triethanolamine* (TEA), *diglycolamine* (DGA), and *methyldiethanolamine* (MDEA) are some of the commonly used alkanolamines for acid gas removal. The use of mixture of these amines or one of them with some sterically hindered amines has been studied by various researchers [6-11].

1.2 Problem Statement

Aqueous alkanolamine solutions are widely used as a reactive solvent for the removal of acid gas in natural gas processing. Alkanolamine solvents have been chosen due to its high reactivity and low cost. Despite of these advantageous properties, alkanolamines pose some problems. Alkanolamines undergo degradation process under oxygen rich atmosphere and produce highly toxic degradation product [12]. Acidic alkanolamine degradation product that formed in the amine circuit might be a potential source of foaming in the acid gas removal system besides condensed hydrocarbon. Primary amine such as MEA also has a problem of high heat of reaction with acid gases and high vapour pressure. The high heat of reaction leads to higher energy requirements for stripping in MEA systems while the relatively high vapor pressure of *monoethanolamine* causes significant vaporization losses [5].

Besides these operational problems, alkanolamine solutions are toxic in nature [13]. The toxicity of alkanolamines needs special caution during operation [14, 15]. Alkanolamines vapour might endanger operating personnel and contaminate atmosphere around the work place. If the work place is a confined space such as naval submarines this would cause more significant hazard [12].

Very recently, it was observed by many researchers that alkanolamines could potentially be replaced with amino acids salt as alternative solvent for CO₂ absorption because of its molecular similarity. Amino acid has the same amine functional group as alkanolamines [12]. Though amino acids are more expensive than alkanolamines, they have certain unique advantages due to their physical and chemical properties [16,

17]. Amino acids salt has been reported to exhibit superior oxidation stability, favourable toxicity and has less volatility due to its ionic nature [12].

However, the available data on physical properties and performance of amino acid salt as absorbent for acid gas removal are still relatively scanty. Previous works on amino acid salt are mainly done for low pressure system [12, 16-22]. The performance of amino acid salt as acid gas absorbent at higher pressure system is required for natural gas processing application. The effects of the absorbed acid gas to the physical properties of the amino acid salt solution are also needed to be investigated. This data would be needed for the material and energy balance calculation of acid gas absorber with amino acid as solvent. Therefore, the research will be addressed to provide data on critical fundamental properties, especially at higher pressure range, required to supports the design of absorber that employs sodium glycinate as reactive solvent for natural gas processing application. The performance of amino acid salt as acid gas absorbent will be compared with alkanolamines.

1.3 Research Objective

The application of Amino acid salts for acid gas removal started with Alkacid process used by BASF. The Alkacid “M” and Alkacid “dik” used amino acid salts solution as absorbent. Hook [12] studied numerous sterically and non-sterically hindered amino acid salts for application in submarine CO₂ absorption process and concluded that amino acid salt is suitable for CO₂ absorption at high CO₂ concentration. Kumar *et al.* [18] and Yan *et al.* [17] studied the removal of CO₂ using a combination of aqueous solution of amino acid salts and polypropylene (PP) hollow fiber membrane and found that amino acid salt-PP membrane system has high CO₂ removal efficiency and lower membrane wetting. Sodium glycinate, one of amino acid salts, in glycerol was used in an immobilized liquid membrane in a closed loop life support system such as space suit [19-21]. Song *et al.* [22] studied CO₂ removal using sodium glycinate at low pressure and found that amino acid salt has good CO₂ loading.

Based on the mentioned studies, amino acid salts appear to have a good potential as an alternative absorbent for acid gas removal. Hence, in this research the potential of sodium glycinate, one of the amino acid salts, as alternative absorbent for carbon dioxide removal is to be studied. The objectives of this research are as follows:

1. To determine critical fundamental properties of the sodium glycinate solvent i.e., density, viscosity and heat capacity in order to develop additional database to support the design of absorber that employs sodium glycinate as reactive solvent.
2. To perform absorption study of CO₂ on sodium glycinate through equilibrium approach to acquire the vapour-liquid equilibrium (VLE) data of CO₂-sodium glycinate system, particularly at moderate to high pressure condition.
3. To demonstrate absorber design for CO₂ absorption process using sodium glycinate as absorbent.

1.4 Research Scope

The study is focus on investigating the potential of sodium glycinate in aqueous solution as the reactive solvent for acid gas removal. Solution concentrations used in this study are 1.0 %, 5.0 %, 10 %, 15 %, 20 % and 30 wt. % of sodium glycinate. Series of measurements were conducted for density, kinematic viscosity, heat capacity, acidity, conductivity, refractive index, surface tension and contact angle for the purpose of studying the physical properties of aqueous sodium glycinate solution. Absorption experiments to measure the solubility of carbon dioxide in aqueous sodium glycinate solution were conducted using SOLTEQ BP-22 High Pressure Solubility Cell. The absorption test is done for CO₂ partial pressure range from 100 to 2500 kPa at temperature 298.15 K and 313.15 K. The solubility data were expressed as CO₂ loading factor of sodium glycinate at various concentrations as function of pressure and temperature. The data acquired from physical properties and solubility measurement would support the design of tray absorber column for CO₂ absorption process using sodium glycinate as absorbent. This absorber design would be compared with the design of tray absorber using *monoethanolamine* as reactive solvent. The comparison based on heat and mass balance around absorber and required absorber (sieve tray) diameter for the same duty/separation load.

CHAPTER 2

LITERATURE REVIEW

2.1 Natural Gas

Natural gas is a mixture of naturally occurring hydrocarbon and non hydrocarbon gases found in porous geologic formation beneath earth surface [13]. Natural gas consists of hydrocarbon gases like methane, ethane, propane, butane, and small amount of heavier hydrocarbon. Other gases like carbon dioxide, hydrogen sulphide, nitrogen oxide, mercaptan, water vapour and some trace of organic and inorganic compound also present in natural gas [5].

2.2 Acid Gases

Acid gas is one of the major impurity in natural gas. Hydrogen sulphide (H_2S) and carbon dioxide (CO_2) are the primary acid gas contaminants. Besides these two gases there are others such as nitrogen oxide (NO_x), sulphur dioxide (SO_2), and carbon monoxide (CO). Hydrogen sulphide is a toxic and highly acidic gas that is commonly found in natural gas. Hydrogen sulphide could be detected from its ‘rotten egg’ odour. Detection threshold for hydrogen sulphide is 0.0047 ppmv [23]. Due to its high toxicity, the regulation for H_2S content in natural gas has been very strict. The maximum allowable H_2S content is 4 ppmv.

Carbon dioxide is another contaminant of natural gas that forms acidic solution with water. Even though it is categorized as acid gas, carbon dioxide is not toxic. Maximum CO_2 content in pipeline gas is 4 vol. % according to GPSA (Gas Processors Suppliers Association) but common pipeline requirement is 1-2 vol. % [24]. Early natural gas reservoirs that were exploited contain very small amount of acid gas. However, due to the increased demand and depletion of the ‘sweet gas’ reservoirs, exploration and production of natural gas from reservoirs with higher CO_2 content become inevitable. Acid gas like carbon dioxide (CO_2) and sulphur dioxide (SO_2) have to be removed from the natural gas to reduce corrosion in pipe and

equipment while increasing the purity, heating value and commercial value of the natural gas.

There are many methods for removal of acid gas from natural gas but in general there are five main ones, namely [5];

1. Absorption into liquid
2. Adsorption using solid
3. Permeation through membrane
4. Conversion into another compound
5. Cryogenic condensation

2.3 Absorption

Absorption refers to transfer of a component of a gas phase into a liquid phase in which it is soluble [5]. The reverse system that releases a component of a liquid phase into gas phase is called desorption or stripping. Basic absorption-stripping scheme for acid gas removal is shown in Figure 2.1.

Interaction between absorbed gas phase, usually called absorbate, with the liquid phase in which the gas dissolves, also known as absorbent, is an important factor that affect absorption process. Absorption could be classified based on the type of interaction between absorbent and absorbate as follows [5]:

1. Physical absorption, occurs when the gas component that being absorbed into the liquid phase is more soluble in liquid phase compared to other component of the gas phase. The equilibrium concentration of this physical absorption is strongly dependent on partial pressure of the absorbate in gas phase.
2. Chemical absorption, occurs when the gas component that is absorbed into the liquid phase also reacted with a component of liquid phase. The equilibrium concentration of this chemical absorption depends on partial pressure of absorbate in gas phase and reaction nature of absorbate with absorbent.

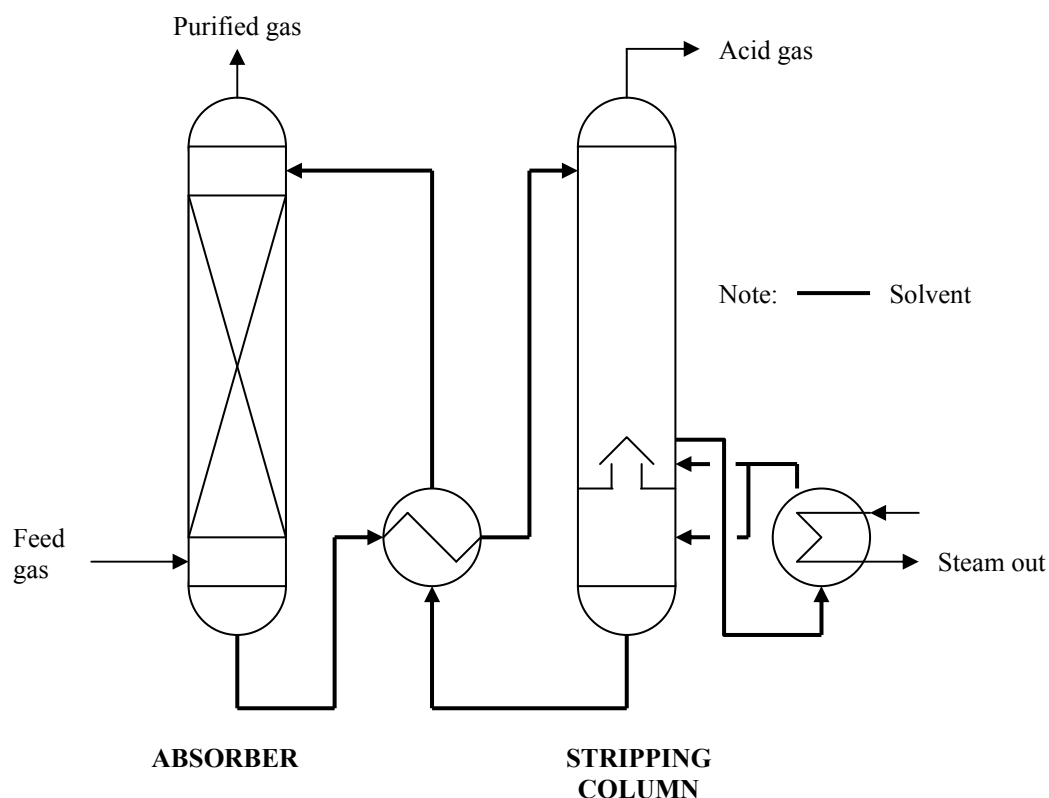


Figure 2.1 Basic Scheme of absorption-stripping process

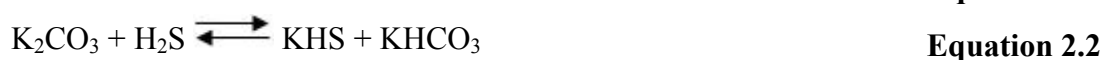
In view of the above, selection of suitable solvent becomes important. The requirements for a good solvent for acid gas removal process are high gas solubility, low volatility, low viscosity, low corrosivity, inexpensive, readily available, non-toxic, non-flammable and chemically stable [25]. Alkaline salt, alkanolamine and amino acid salt are some of the solvent types that are suitable for acid gas removal.

2.4 Alkaline Salt

Alkaline salt solutions usually employ sodium or potassium as cation with carbonate, borate, arsenate, or phenolate as anion. This cation-anion configuration would form buffer solution with pH around 9 to 11. Its alkaline nature allows absorption of H_2S and CO_2 while the buffering effect of the solution would prevent rapid pH changes as the acid gas is absorbed [5].

The early commercial process applying regenerative absorbent are used to purify “town” gas from H_2S . The Seaboard process, employs sodium carbonate (Na_2CO_3),

from ICF Kaiser Engineering (originally licensed by Kopper Company Inc.) was introduced in 1920 [26]. Sodium phenolate process was also proposed by ICF Kaiser Engineering in 1936 [27]. In 1934, Shell Development Company licensed Tripotassium phosphate (K_3PO_4) process for absorption of H_2S [28-29]. The CO_2 and H_2S absorption reaction for alkaline salt system are depending on the solvent used. The CO_2 and H_2S absorption reactions for sodium carbonate system are presented in Equation 2.1 and Equation 2.2 respectively [26]. The reactions for tripotassium phosphate system are presented in Equation 2.3 and Equation 2.4 [28].



Vacuum carbonate process, licensed by ICF Kaiser Engineering, was a further development of seaboard process. Similar to its predecessor, the process utilizes alkaline carbonate solution as absorbent. The use of vacuum distillation for regeneration of spent absorbent is the improvement in this process [30]. Vacuum distillation allows the recovery of H_2S in usable concentrated form. The CO_2 stripping reaction is not completely achieved in this process. Some bicarbonate would accumulate in the solution and reduced CO_2 absorption. The occurrence of *sodium thiocyanate* ($NaSCN$) and *sodium hyposulphite* ($Na_2S_2O_3$) from side reaction with oxygen also degraded the active solution [31-33].

One of the widely used alkaline salt processes for acid gas treating is the Benfield process. Benfield process, licensed by UOP, employs potassium carbonate (K_2CO_3) at elevated temperature as absorbent for acid gas removal. The process was originally invented by Benson and Field at U.S. Bureau of Mines in early 1960's for purification of synthesis gas [34]. The chemical reactions of absorbed CO_2 with potassium carbonate solution are presented by Equation 2.5 to Equation 2.6. At a solution pH greater than 10, carbon dioxide would react with hydroxyl ion to form bicarbonate ion [35]. The low reaction rate of CO_2 in carbonate-bicarbonate solution at room temperature would limit the absorption process; therefore a higher temperature is

needed to increase absorption capability of potassium carbonate [36-37]. Operating temperature from 375.15 to 385.15 K is needed to enhance the absorption reaction rate. This elevated temperature also increase bicarbonate solubility in absorbent solution thus allowing higher concentration of carbonate solution to be utilized. For gas treating application, solution concentration as high as 30 % mass could be used without precipitation problem. But high temperature used in Benfield process also cause high energy consumption. Benfield LoHeat and Benfield Hybrid LoHeat process applied the use of flash recovery, steam ejector and mechanical vapour recompression (MRV) to lower the energy consumption [38-39]. Application of promoter is another method to increase CO₂ reaction rate [40]. Activated Benfield process utilizes *diethanolamine* (DEA) as amine promoter. Addition of DEA resulted in significant improvement of absorption rate (up to 300 %) compared to unpromoted solution. However, the improvement of absorption rate is reduced with CO₂ loading increase [41].



Corrosion is another problem occurs in Benfield process. Severe corrosion was encountered especially where carbonate-bicarbonate conversion are high or where carbon dioxide release due to pressure reduction. In commercial application, potassium metavanadate (KVO₃) is used as corrosion inhibitor [42-44].

The Giammarco-Vetrocoke process is another alkaline process that is widely known for acid gas removal. The original Giammarco-Vetrocoke process, introduced in 1960, uses potassium arsenite at elevated temperature for acid gas absorbent. Formulation of proportionally stoichiometric arsenic trioxide with potassium carbonate resulted in increase in CO₂ absorption and desorption rate [45]. The absorption improvement rate is claimed to be 40 % higher than conventional potassium carbonate for absorption at room temperature.

There are some downsides of this arsenic process. The arsenic is not preferable due to its toxicity and requirement of special handling. Potassium carbonate activated by

arsenite solution is also not suitable for handling oxygen contains gas mixture. The arsenite is oxidized into arsenate thus reducing its absorption capability [46].

To address the setback, Giammarco-Vetrocoke offered a new process which applied glycine instead as the alternate promoter for hot potassium carbonate process. Addition of glycine would increase absorption rate by providing alternative reaction path for CO₂ [46-47]. Glycine promoted potassium carbonate solution is claimed to have more resistant to oxidation compared to *ethanolamine* solution [46].

Giammarco-Vetrocoke also offered dual activator for hot potassium carbonate solution. Combinations between glycine, ethanolamine, As₂O₃ and ammonia as activator have been proposed [48]. The dual activated solution is claimed to have lower CO₂ vapor pressure, higher regenerator efficiency, and higher CO₂ absorption rate than the mono activated solution.

Catacarb process, licensed by Eickmeyer and Associate in 1974, uses catalyzed hot potassium carbonate solution as absorbent. The process was based on the original works by A. G. Eickmeyer [49]. The process employs special formulation of potassium carbonate, potassium borate and amines or amine-borate for specific gas treating application [50]. The used of these formulated potassium carbonate solution is claimed to have low heat of absorption and could increase the CO₂ absorption rate more than 4 times the original solution [51]. This would result in reduction of heat duty and solution circulation rate. Vanadium based corrosion inhibitor is also used in Catacarb process to reduce carbon steel corrosion in the system [52]. The process configuration for Catacarb process is generally similar to Benfield process.

Exxon Research and Engineering Company started the development of series of acid gas treating processes called the FLEXSORB Process in 1983. FLEXSORB SE for removal of hydrogen sulfide, FLEXSORB HP for CO₂ removal, and FLEXSORB PS for removal of both gases [53]. These processes utilize hot potassium carbonate solution activated by proprietary sterically hindered amines. The hindered amines are suitable as promoter because it has low volatility, good stability and low foaming tendency. The reaction mechanism for sterically hindered amine as promoter is similar to other amines. Similar to the other amine promoted potassium carbonate

system, corrosion is a major problem in FLEXSORB process. The use of vanadium based corrosion inhibitor has been recommended for commercial plant.

The recent studies on alkaline salt system mainly related to improvement of absorption capability by addition of promoter. Application of piperazine as promoter for aqueous potassium carbonate has been studied [54-56]. The addition of 0.6 m piperazine to a 20 %wt K_2CO_3 increases the rate of CO_2 absorption by 10 times compared to unpromoted solution at $60^\circ C$ [54].

In general, alkaline salt is widely used as acid gas absorbent due to its reactivity towards acid gas and low solvent cost. The low absorption reaction rate at room temperature and corrosion has been the major problems in alkaline salt system. Absorption at elevated temperature is one of the methods to enhance reaction rate. Another method to improve the reaction rate is the utilisation of alkanolamine, amino acid or hindered amine promoter. The high absorption temperature also increases the solubility of sodium bicarbonate, thus permitting the use of higher solution concentration. This would result in lower solvent circulation rate. The high absorption temperature also has few downsides. High temperature directly means high energy consumption. The high temperature would also promote the corrosion rate. Based on Arrhenius equation, the temperature increase will increase the exchange current depending on the magnitude of activation energy for the corrosion reactions [57]. The use of higher solution concentration at high temperature would need extra precaution since any disturbance leading to temperature loss in the system would cause precipitation and scaling of carbonate which could plug the equipment.

2.5 Alkanolamines

Aqueous alkanolamines solution has been widely use in acid gas removal system. Alkanolamines is a term used to describe chemical compound that has at least one hydroxyl group and one amino group. The hydroxyl group serves to reduce the vapour pressure and water solubility while the amino group give alkalinity in water to cause the absorption of acidic gases [5]. The number of hydrogen that attached to nitrogen in amine group determines the type of alkanolamines and its ability to absorb acid

gas. Alkanolamines which have two hydrogen atoms connected to nitrogen atom is classified as primary amine. Alkanolamines with one and no hydrogen atom attached to the nitrogen atom are called secondary and tertiary amine respectively. The reactivity of primary amine with acid gas is higher than secondary amine while tertiary amine has the lowest reactivity toward acid gas.

The molecular structures for primary, secondary and tertiary amine are shown in Figure 2.2. The CO₂ absorption reactions for alkanolamines are presented in Equation 2.7 to Equation 2.12 [5, 41]. The carbamate formation reaction (Equation 2.9) is the predominant reaction in CO₂ absorption process for primary and secondary alkanolamines. When carbamate formation is the only reaction, the maximum CO₂ loading is limited by stoichiometry to 0.5 mol CO₂/mol of amine. Some of the carbamate would undergo carbamate hydrolysis reaction (Equation 2.11) and generate free amine therefore the CO₂ loading is higher than 0.5 [5]. Tertiary alkanolamines reaction with CO₂ leads to formation of bicarbonate ion as is presented in Equation 2.12. The CO₂ loading based on stoichiometry is 1.0 mol CO₂/mol of amine but the reaction is very slow [5, 41].

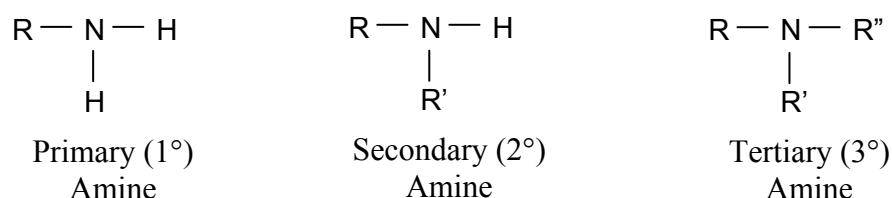
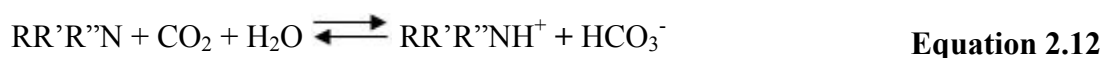
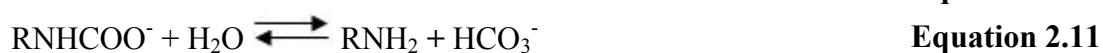
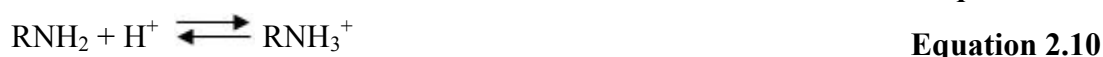


Figure 2.2 Molecular structure of primary, secondary and tertiary amine



The first alkanolamines to be used in commercial acid gas removal system was *triethanolamine* (TEA). The application of TEA in 50 % water solution as acid gas

absorbent was claimed in a 1930 U.S. patent by Bottoms [58]. Some of the disadvantages of TEA are it has low capacity, low reactivity (tertiary amine) and low stability. With the availability of other type of alkanolamines with higher reactivity and higher stability, the application of TEA has been largely reduced.

The high reactivity of *monoethanolamine* (MEA) has made it suitable as acid gas absorbent [59-62]. MEA has shown good acid gas loading even at low acid gas content environment such as submarine atmosphere [12]. High heat of reaction with acid gas, high vapour pressure, corrosive nature at high concentration and decomposition due to side reaction are some of the problems that MEA poses. Application of *diethanolamine* (DEA) for the treatment of natural gas was first disclosed by Bertheir in 1959 for Societe Nationale des Petroles d'Aquitaine (SNPA) of France. DEA is claimed to have higher acid gas loading compared to MEA and more resistance to decomposition due to side reaction with carbonyl sulphide (COS) and carbon disulfide (CS₂) impurities [61-65]. *Methyldiethanolamine* (MDEA) was described by Kohl of Flour Daniel Co. as suitable solvent for selective H₂S absorption in presence of CO₂ in early 1950's. High stability is one of the advantages of this alkanolamine [66-68].

Beside the three alkanolamines previously mention (MEA, DEA, MDEA) there were other alkanolamines that are currently used for acid gas absorption. *Diisopropanolamine* (DIPA) is used as reactive solvent for Sulfinol and Shell Claus Off-gas Treating (SCOT) process [69-71]. *Diglycolamine* (DGA) is also a good absorbent for acid gas because it has the stability and reactivity similar to MEA combined with low vapour pressure and hygroscopicity similar with *diethylene glycol* (DEG) [72-74]. Some sterically hindered amines such as 2-amino-2-methyl-1-propanol (AMP), 2-amino-2-methyl-1,3-propanediol (AMPD), 2-Amino-2-ethyl-1,3-propanediol (AEPD) have also been studied in view of their potential as absorbent for acid gas [8, 11, 75-80]. Solubility of acid gases in mixture of two previously mentioned alkanolamines also has been studied. Combination between primary or secondary amine with tertiary or sterically hindered amines would result in better absorption performance [6, 9, 81-90]. Formulation of few alkanolamines to produce tailored amines mixture for special purpose or to enhance its properties has also been developed. MDEA is usually used as the base for the amine mixture with other amine

such as piperazine or 2-(2-Aminoethylamino)ethanol (AEE) as promoter [91-101]. The molecular structure of some alkanolamines commercially used for acid gas absorption is shown in Figure 2.3.

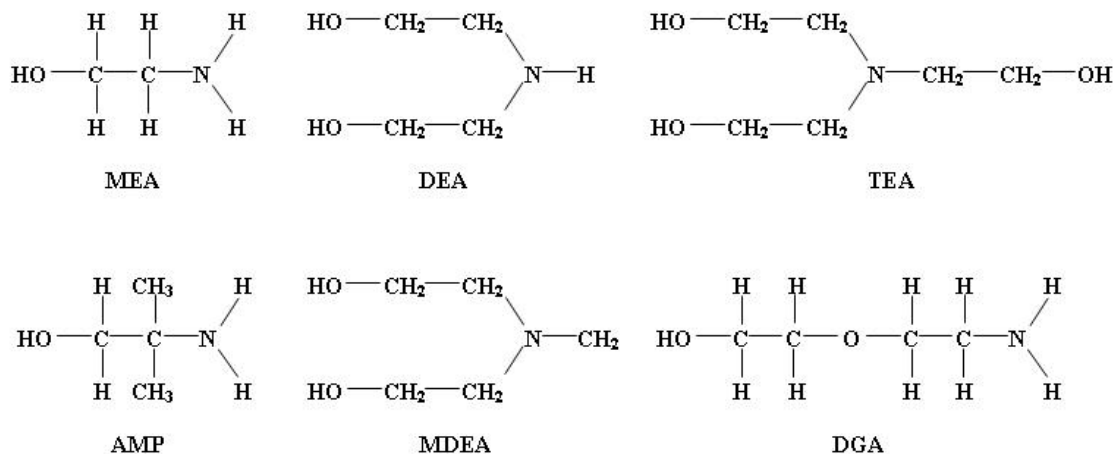


Figure 2.3 Molecular structure of some alkanolamines

The reactivity and stability towards acid gas are the main factors that affect the selection of appropriate alkanolamines as acid gas absorbent. Primary alkanolamine such as MEA would give good reactivity but have poor resistance to unwanted side reaction and high loss during regeneration operation. Tertiary alkanolamine for example MDEA has higher stability but lack off reactivity towards acid gas. Foaming due to the presence of liquid hydrocarbon impurities or operation problem is another main problem in alkanolamine system. Alkanolamine also has toxic nature therefore the handling and disposal of alkanolamine waste would need special precaution.

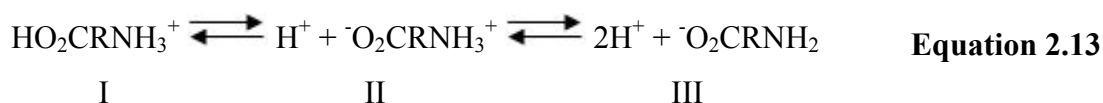
2.6 Amino Acid Salt

The term ‘amino acids’ is generally understood to refer to the aminoalkanoic acids, $\text{H}_3\text{N}^+ - (\text{CR}_1\text{R}_2)_n - \text{CO}_2^-$. However, the term ‘amino acids’ include all structure carrying amine and acid functional groups, including simple aromatic compound and would also cover other types of acidic functional groups such as phosphorus and sulphur oxy-acids [102]. There are 20 amino acids that have important role in human body to construct protein. The first amino acid employed for acid gas removal system

was glycine in Giammarco-Vetrocoke Process. More comprehensive detail of this process has already been described in section 2.4.

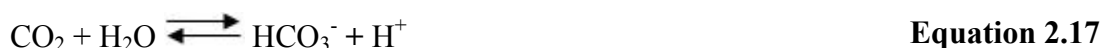
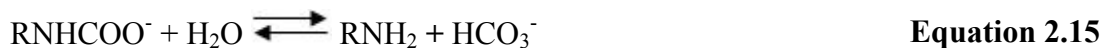
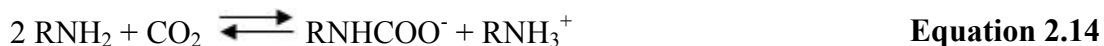
Amino acid salt is a derivative of amino acid with metal ion substitute hydrogen atom in hydroxyl group. One of amino acid salt that has been widely use is *monosodium L-glutamate* (MSG). It is used as meat flavor-enhancer and an enormous quantity of it is now used in various food applications.

Absorption mechanism of carbon dioxide into aqueous amino acid salts solution has been studied by Kumar *et al.* [103]. The amino acid dissolved in water exists as zwitterions (form II). Zwitterion is a chemical compound that is electrically neutral but carries positive and negative charges on different atoms. Addition of OH⁻ would shift the protonated amino group into their deprotonated form (III). This deprotonation step is necessary in order to make the amino group reactive towards CO₂. The ionic equilibrium of the amino acid exists as follows:



A good reference in the determination of the reaction mechanism and kinetic of CO₂ with amino acid is the CO₂ reaction with alkanolamines. Apart from the backbone of the molecule, the functional group of amino acid is basically the same as that of alkanolamines and the reaction mechanism can be expected to be similar [105]. Kumar [104] has shown that the reaction of two amino acids, taurine and glycine, can be described using the same reaction mechanism as used for alkanolamines. Reaction between amino acid salts and carbon dioxide are shown in Equation 2.14 and Equation 2.15. Amino acid salt undergoes reaction with carbon dioxide to form carbamate and protonated amine. The carbamate formed is unstable and could be easily hydrolyzed into its original form and bicarbonate. The instability of carbamate formed from carbon dioxide absorption into amino acid salts was assumed to give significant effect to amino acid salt absorption ability [106]. There is possibility of carbamate side reaction to form acid anhydride but the acid anhydride could be easily hydrolyzed with water. Figure 2.4 shows the reaction scheme for carbon dioxide absorption into sodium glycinate. Beside the two reaction mentioned above, the

reaction of CO₂ with water and OH⁻ to form bicarbonate and carbonic acid are also occurs in CO₂-aqueous amino acid salt system [107]. The reaction for bicarbonate formation and carbonic acid formation are presented in



The application of amino acid salts for acid gas removal has been used by BASF with their Alkacid process. The Alkacid process has three main process variations, Alkacid “M”, Alkacid “dik” and Alkacid “S”. Alkacid “M” uses solution of *sodium alanine* to absorb either H₂S or CO₂. Alkacid “dik” employ *potassium diethylglycine* or *potassium dimethylglycine* solution for selective removal of H₂S from gas containing CO₂ and small amount of CS₂. Alkacid “S” was developed for removal of contaminant other than H₂S and CO₂ such as HCN, ammonia, carbon disulfide, mercaptan, dust and tar. It contains sodium phenolate solution as absorbent.

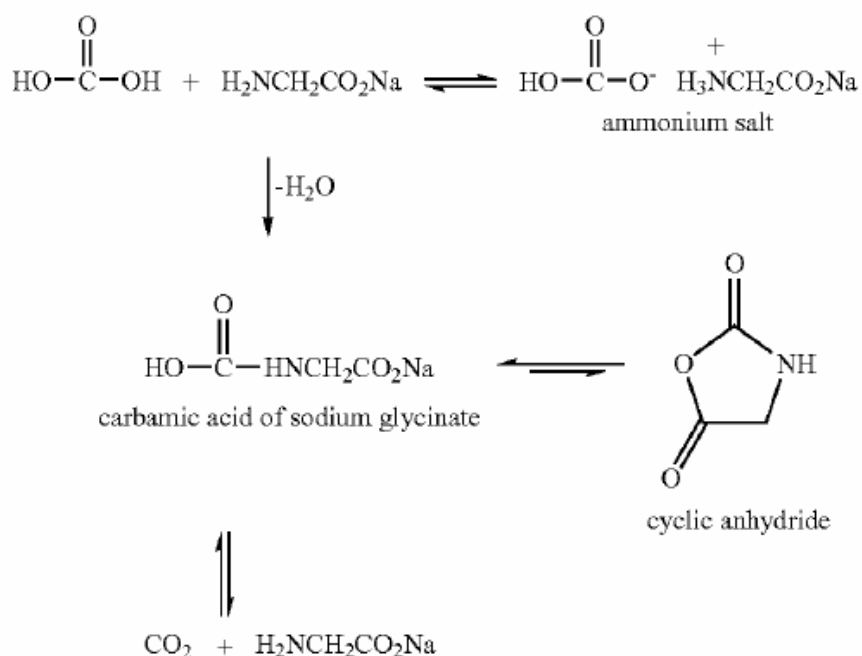


Figure 2.4 Reaction scheme for carbon dioxide absorption into sodium glycinate

Recently, study on numerous sterically and non-sterically hindered amino acid salts for application in submarine CO₂ absorption process has been conducted [12]. Absorption capacity of amino acid salt at high CO₂ concentration was found to be higher than the original MEA solution used for this purpose.

Some extensive studies have been done to design membrane gas absorption process that also utilizes amino acid gas solution as absorbent [104]. The study focuses on modelling and experimental work on application of *potassium taurate* solution as absorbent incorporated with polypropylene (PP) hollow fiber membrane for acid gas removal system.

Potassium glycinate (PG) solution integrated with polypropylene membrane has also been studied for acid gas removal system [17]. It was found that aqueous PG solution has CO₂ removal efficiency above 90 % and mass transfer rate was above 2.0 mol.m⁻²h⁻¹ for 14 % CO₂ in CO₂/N₂/O₂ system with total system pressure of 105 kPa. It is higher compared to MEA and MDEA for the same condition. Aqueous PG solution also has a lower potential of membrane wetting after continuous steady operation for 40 h to maintain CO₂ removal efficiency at around 90 %.

Sodium glycinate, one of amino acid salts, in glycerol was used in an immobilized liquid membrane (ILM) in a closed loop life support system such as space suit [19-21]. The specific application of this ILM hinders the use of alkanolamines as carrier species of ILM due to high volatility and irritative nature of alkanolamines. Glycine-Na is suitable as carrier species because it is environmentally friendly. Glycine-Na-Glycerol ILM system has shown good performance for CO₂/N₂ separation. CO₂/N₂ selectivity as high as 7000 have been observed. The Glycine-Na-Glycerol ILM system also has shown stable and good performance for 25 days testing period [19].

Sodium glycinate has also been tested for CO₂ and N₂O absorption at low pressure [22, 108] for application in CO₂ capture to reduce greenhouse effect. Loading factor of sodium glycinate solution reached 1.075 for 10 wt. % solution at 313.15 K and 199.1 kPa. It was found that 10 wt. % of sodium glycinate solution exhibits greater capacity for CO₂ absorption compared to MEA, AMPD (*2-amino-2-methyl-1,3-*

propanediol), AEPD (*2-amino-2-ethyl-1,3-propanediol*) and TIPA (*triisopropanolamine*) under the same condition. Some physical properties of this amino acid salt solution before absorption are available in literature [109, 110].

Despite the above mentioned good performance of amino acid salts for CO₂ removal, many salts undergo precipitation during the absorption of CO₂ especially for solution of high amino acid salt concentration [12, 103, 104, 111]. This precipitation could trigger the plugging and fouling of the gas-liquid contactor and heat transfer surfaces [103]. The precipitates are identified as the amino acid itself or contain CO₂ species [111]. Kumar [103] pointed out that the concentration of potassium taurate at which the precipitation occurs is not significantly different from the solubility of taurine in water.

Amino acid salt is considered to be a possible alternative to substitute alkanolamines in certain area of acid gas removal due to some reasons. Amino acid salt has the same amino functional group as alkanolamines so it is expected to exhibit same behaviour toward acid gas. Amino acid salt has ionic nature in water solution that makes it more stable against oxidative degradation. Amino acid salt also has other desirable properties such as low volatility and higher surface tension [104]. The previous works on amino acid salt are mainly done for carbon dioxide removal at low pressure application such as CO₂ capture in submarine atmosphere, life support for space suit, and CO₂ capture from fossil fuel emission to reduce greenhouse effect. Acid gas removal from natural gas is another possible application for CO₂ removal using amino acid salt. The application of amino acid salt for acid gas removal from natural gas would require physical properties and vapour-liquid equilibrium data at higher pressure range similar with the actual natural gas condition. Hence potential of sodium glycinate, one of amino acid salts, as absorbent for CO₂ absorbent at higher pressure range is investigated in this study. This study will use sodium glycinate as amino acid salts is safer and environmentally friendly compared to alkanolamines. It is declared to be non hazardous according to Directive 67/548/EEC [112]. This would make the material handling and transportation a lot easier.

CHAPTER 3

METHODOLOGY

Priori knowledge on the critical physical properties is required for a successful design and development of acid gas removal system using amino acid salt as absorbent. This chapter covers the characterisation of amino acid salt and CO₂ absorption process with amino acid salt solution as reactive solvent. The preparation of amino acid salt is presented in section 3.1. Section 3.2 until section 3.8 covers the measurement of some critical fundamental properties of the amino acid salt. The absorption of carbon dioxide into absorbent would change the physical properties of the absorbent. Therefore the physical properties of amino acid salt after CO₂ absorption are also measured in order to quantify the effect of CO₂ loading on the physical properties of amino acid salt solution. Absorption test and regenerability test to measure the CO₂ absorption capability and regenerability of the amino acid salt solution are described in section 3.9 and section 3.10.

3.1 Amino Acid Salt Preparation

The chemical absorbent used in this study was sodium glycinate (C₂H₄NO₂Na). Aqueous sodium glycinate was prepared by neutralization of glycine (C₂H₅NO₂) – Merck, purity ≥ 99.7 %, with an equimolar of sodium hydroxide (NaOH) - R&M Chemicals, purity ≥ 99 %. The amino acid dissolved in water exists as zwitterions. Zwitterion is a chemical compound that is electrically neutral but carries positive and negative charges on different atoms. Addition of OH⁻ would shift the protonated amino group into their deprotonated form. Concentration of the deprotonated amino group (amino acid salt) is estimated by titrating with standard HCl solutions. The endpoint is the isoelectric point of glycine. The concentration of sodium glycinate solution was found to be accurate within 1.0 % of the concentration. Sodium glycinate concentrations from 1.0 % to 30 wt. % were used in the study. This concentration range is chosen to avoid precipitation of amino acid salt. As already mentioned in section 2.6, the concentration of potassium taurate, one of amino acid salt, at which the precipitation occurs is not significantly different from the solubility of taurine in

water [103]. The solubility of glycine in water at 308.15 is 30.17 g/100 g of water (30.16 wt. %) [113].

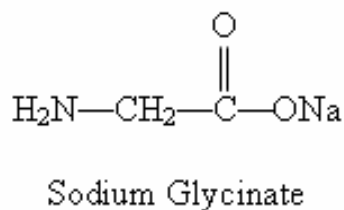


Figure 3.1 Structure of sodium glycinate

3.2 Density

3.2.1 Equipment description

The density, ρ , of aqueous sodium glycinate solution is measured using an Anton Paar DMA-5000 digital vibrating-tube density meter. The Anton Paar DMA 5000 digital vibrating-tube density meter uses U-tube measuring principle with reference oscillator and platinum thermometer. A U-shaped glass tube of known volume and mass is filled with the liquid sample and is electronically excited by a Piezo element. The U-tube is kept oscillating continuously at the characteristic frequency f . Optical pick up record the oscillating period P . This frequency is inversely proportional to the density of the filled in sample. The sample density is calculated using Equation 3.1:

$$\rho = A.P^2 - B \tag{Equation 3.1}$$

where ρ is the density in g.cm^{-3} ; P is the oscillation period in s; A and B are the equation coefficient. The instrument is calibrated with air and water as the sample. The temperature accuracy of the equipment is within $\pm 0.01^\circ\text{C}$.



Figure 3.2 Anton Paar DMA-5000 digital vibrating-tube density meter

3.2.2 Measurement method

The equipment is calibrated with Millipore Ultrapure Water standard and ambient air. The density of aqueous sodium glycinate is measured at temperatures range from 298.15 K to 353.15 K for solution before and after absorption. The precision of the experimental measurements was found to be better than $\pm 0.00002 \text{ g.cm}^{-3}$.

3.3 Kinematic Viscosity

3.3.1 Equipment description

The kinematic viscosity, ν , of aqueous solutions of sodium glycinate is measured using Cannon Ubblohde type no 25 B433 viscometer (CANNON Instrument Company) using ASTM D445 standard test method. The viscosity measurement is based on the time needed for a fixed liquid sample to flow under gravity through the capillary of a calibrated viscometer under a reproducible driving head and at a closely controlled and known temperature. A simple diagram of a capillary viscometer is shown in Figure 3.3.

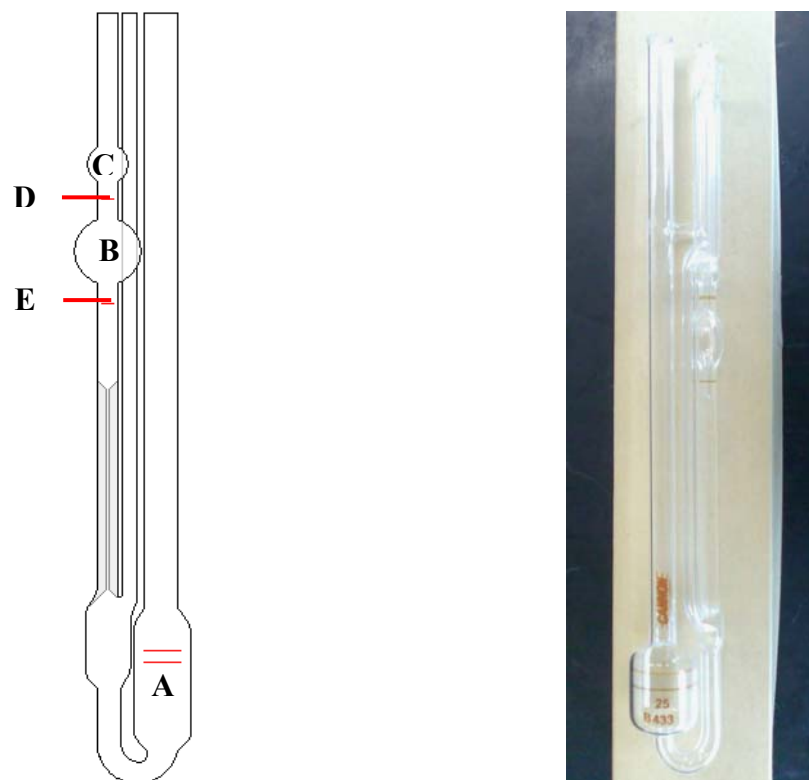


Figure 3.3 Cannon Ubblohde type no 25 B433 viscometer

3.3.2 Measurement method

The schematic diagram of capillary viscometer is shown in Figure 3.3. Liquid sample is charged into bulb A then the apparatus is submerged in vertical position into a water bath. The apparatus must be kept in water bath for 30 minutes prior to viscosity measurement to ensure the sample temperature is equal to the water bath temperature. The water level must be maintained at 20 mm above sample position at all time during measurement. The liquid sample is transferred to bulb B and bulb C by vacuum. The sample is then allowed to flow freely and the required time for liquid meniscus to pass from the first timing mark (point D) to the second timing mark (point E) is recorded [114]. Calibrated Cannon Ubblohde type no 25 B433 viscometer with viscometer constant of $0.001840 \text{ mm}^2/\text{s}^2$ (cSt/s) is used in this experiment. The temperature of the water bath is controlled using Grant type W14 with an uncertainty of $\pm 0.1 \text{ K}$. Time measurements were made with an accuracy of 0.01 second. The kinematic viscosity of the aqueous sodium glycinate solution before absorption is

measured for temperature range from 298.15 K to 333.15 K. The kinematic viscosity of the solution after absorption is measured at 298.15 K.

3.3.3 Calculation method

The kinematic viscosity, ν , of aqueous solutions of sodium glycinate is calculated using Equation 3.2:

$$\nu = tC_{\text{viscometer}} \quad \text{Equation 3.2}$$

where ν is the kinematic viscosity in cSt, $C_{\text{viscometer}}$ is the viscometer constant in cSt.s^{-1} , and t is the measured time interval in second.

3.4 Heat Capacity

3.4.1 Equipment description

Heat capacity, C_p , of the aqueous sodium glycinate solutions is calculated using heat input data measured by Pyris 1 Digital Scanning Calorimeter (DSC) from Perkin Elmer. In Digital Scanning Calorimeter, the measured sample and a reference substance are subjected to a continuously temperature increase. Additional heat is added to the sample or references substance as necessary to maintain the two at identical temperature [115]. The difference in heat flow into the test material and a reference or blank due to energy changes in the material is continually monitored and recorded [116]. The DSC operation range is from -50 to 450°C (223.15 to 723.15 K). The condition of test chamber is maintained by flowing of nitrogen for purge gas with flow rate of $10 \text{ mL}\cdot\text{min}^{-1}$ during heat capacity measurement. The accuracy of the temperature measurement is within $\pm 0.001^\circ\text{C}$. The heat flow calibration for this equipment is done by measuring the T_g (glass transition temperature) for indium (transition point temperature: 156.60°C) and zinc (transition point temperature: 419.47°C) as calibration references.



Figure 3.4 Perkin Elmer Pyris 1 Digital Scanning Calorimeter

3.4.2 Measurement method

The heat capacity measurement method follows the procedure proposed by Chiu *et al.* [117]. The liquid sample is placed within an aluminium hermetic sample pan using sample encapsulating press method. Sample weight of 5 to 10 mg is used for the experiment. The sample and reference is mounted into Digital Scanning Calorimeter (DSC) module and heated with constant temperature increment until desired temperature is attained. The temperature increment applied is 10 K/min. The heat input to compensate temperature difference between sample and reference is recorded with data sampling interval of 1 second. The heat input measurements for solutions before and after absorption is made with temperature range of 25 to 50°C (298.15 to 323.15 K).

3.4.3 Calculation method

The heat capacity of the sample can be calculated using the following equation [117]:

$$C_p = \left[\frac{60E}{H_r} \right] \frac{\Delta H}{m}$$

Equation 3.3

where C_p is heat capacity in $\text{kJ.kg}^{-1}.\text{K}^{-1}$; E is the cell calibration coefficient, H_r is the heating rate in K.min^{-1} , ΔH is the heat flow difference between the sample measurement and baseline measurement in mW and m is the sample mass in mg . The cell calibration coefficient is determined by measuring sample of aluminium oxide standard throughout the temperature range of study. Heat capacity of aluminium oxide standard is taken from data by Ditmars *et al.* [118]. The values of ΔH , C_p , and m are substituted to Equation 3.3 to obtain the E value at temperature of interest.

3.5 Refractive Index

3.5.1 Equipment description

The refractive index, n_D , of aqueous sodium glycinate solutions were measured using ATAGO RX5000 Refractometer. ATAGO RX5000 refractometer is based on optical refraction critical angle detection system. Critical angle is the angle of refraction in a medium when the angle of the incident radiation is 90 deg. The equipment use LED as light source completed with sapphire prism acting as dispersion compensator. The equipment is calibrated against ultra pure water standard.

3.5.2 Measurement method

The refractive index of sodium glycinate solution is measured for temperature range from 298.15 to 333.15 K for solution before absorption. The sample temperature is controlled using PORTEGI model 631D water bath within ± 0.1 K accuracy.



Figure 3.5 ATAGO RX5000 Refractometer with PORTEGI model 631D water bath

3.6 Acidity

3.6.1 Equipment description

Acidity, pH, of aqueous sodium glycinate solutions is measured using Mettler Toledo 320 pHmeter. The pH meter is basically a voltmeter that employs glass calomel electrodes to measure hydrogen ion activity. The small voltage produced by the electrodes is converted into pH unit. The pH meter is required to be calibrated with at least two standard buffer solutions that span throughout the range of pH values to be measured. Calibration should be performed before measurement because the glass electrode does not give a reproducible reading over long period of time.

3.6.2 Measurement method

The pH of the sodium glycinate solution before and after absorption is measured at temperature 298.15 K. The equipment is calibrated using Mettler Toledo 9863 pH buffer 4.01, Mettler Toledo 9865 pH buffer 7.00 and Mettler Toledo 9866 pH buffer 9.21 respectively.



Figure 3.6 Mettler Toledo 320 pHmeter

3.7 Conductivity

3.7.1 Equipment description

Conductivity, σ , of aqueous sodium glycinate solutions were measured by HACH Sension 7. HACH sension 7 employed two electrodes cell (probe) for measuring conductivity of electrolyte solution. Positive and negative ions in solution would move to the oppositely charged electrode when electric charge is applied to the solution, thus conducting current. The conductivity of the solution is the ratio of current to voltage between electrodes.

3.7.2 Measurement method

Conductivity of aqueous sodium glycinate solution is measured at temperature 298.15 K before and after the absorption test. Calibration using HACH sodium chloride standard solution $1000 \pm 10 \mu\text{S}/\text{cm}$ is done prior to usage.



Figure 3.7 HACH Sension 7

3.8 Surface Tension and Contact Angle

3.8.1 Equipment description

Surface tension, γ , and contact angle, θ , of aqueous sodium glycinate solution with stainless steel surface is measured using Interfacial Tension Meter, IFT-700 from VINCI Technologies. The equipment employs Pendant Drop method for measurement of surface tension and Sessile Drop method for contact angle measurement. The image of the droplet shape for both methods is captured by a digital camera. The surface tension and contact angle with solid surface is measured based on the shape of the droplet using Drop Analysis System software. Typical droplet image generated from IFT-700 is shown in Figure 3.9. The operating temperature of the system ranges from ambient temperature up to 453.15 K with uncertainty of $\pm 0.1\text{K}$.

3.8.2 Measurement method

In the pendant drop test, a drop of liquid is positioned in a suspended manner from the end of a tube at mechanical equilibrium. The profile of suspended liquid drop is determined between the gravity and the surface forces [119]. In the sessile drop method, a single drop of liquid is placed on a cleaned and polished solid surface. The droplet would spread on the surface depending on the interaction of the liquid with the

solid surface. The contact angle is defined as the angle made by the intersection of the liquid/solid interface and the liquid/air interface.



Figure 3.8 Interfacial Tension Meter IFT-700

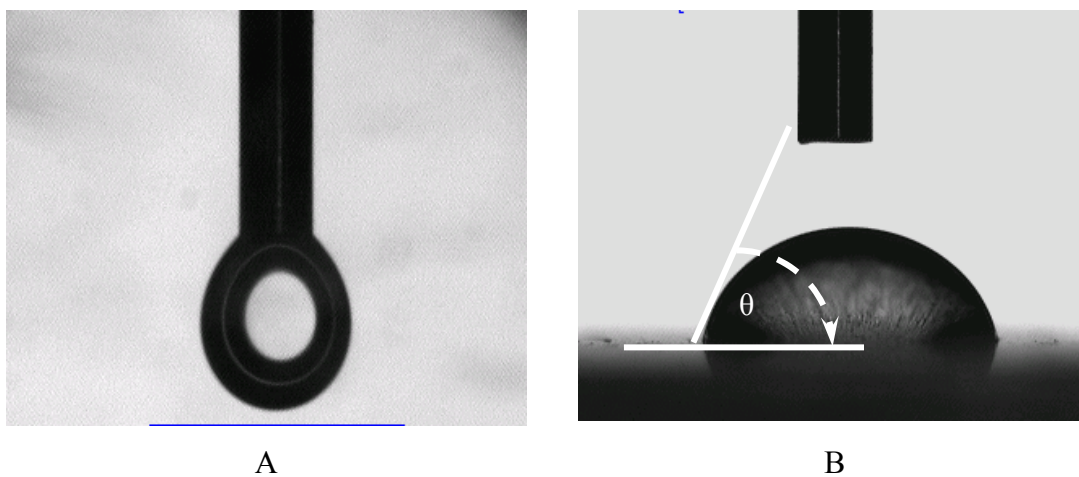


Figure 3.9 IFT-700 standard test method (A) Pendant drop; (B) Sessile drop

Surface tension of aqueous sodium glycinate solution is measured for temperature 298.15 K and pressure 1 atm. The pressure fluid used is air. Contact angle is measured in order to observe the interaction of the absorbent with equipment constructing

material. The equipment constructing material used in the study is stainless steel. The contact angle of aqueous sodium glycinate with steel surface is also measured on the same condition with surface tension measurement.

3.9 Absorption Test

3.9.1 Equipment description

Solubility test for the present study were measured using SOLTEQ BP-22 High Pressure Solubility Cell. The SOLTEQ BP-22 High Pressure Solubility Cell is designed to measure gas solubility in liquid at high pressure and temperature. It is intended to measure the solubility of acid gases e.g. CO₂, H₂S, SO₂, and constituent of natural gases such as methane, ethane, propane and butane in water, amine and alkaline solution. The unit is capable of operating up to a pressure of 65 bar (6500 kPa) and temperature of 300°C (573.15 K). The process parameters are monitored with suitable instrumentations which are linked to a data acquisition system. All the process control, monitoring and data acquisition are done using specialised *LabView*® program.

The schematic diagram of SOLTEQ BP-22 High Pressure Solubility Cell is shown in Figure 3.10. The unit consist of a gas mixing vessel (B1) and equilibrium cell (B2), each immersed in a water-heated jacket vessel (B3 and B4). The temperature of the system is maintained using a thermostatic water circulator (T1, JULABO) with an accuracy of $\pm 0.1^\circ\text{C}$. Prior to operating the unit, both the gas mixing vessel and the equilibrium cell have to be de-gassed using the vacuum pump (P2). Feed gas is then supplied to the mixing vessel and pressurised up to the desired pressure using a gas booster (P1). Liquid absorbent is degassed in liquid degassing unit (B6) before feeding it to the equilibrium cell using liquid feed pump (P3). Magnetic stirrer (M2) is provided to stir liquid absorbent during absorption process. The pressure of the mixing vessel (PI 01) and equilibrium cell (PI 02) is indicated by a digital pressure indicator (Druck DPI 150) with a precision of ± 1.0 kPa for a range of 0 to 10000 kPa. Temperature of the mixing vessel (TI 01), the liquid phase (TI 02) and the gas phase

inside equilibrium cell (TI 03) is measured with a digital thermometer (YOKOGAWA 7653) with a precision of $\pm 0.01^\circ\text{C}$.

3.9.2 Experimental method

The present study is focused on measurement of carbon dioxide solubility in aqueous sodium glycinate solution. Aqueous sodium glycinate concentration from 1.0 to 30 wt. % is used for the absorption test. The partial pressure of CO_2 used is in range of 100 to 2500 kPa to observe the change in CO_2 solubility of the solution at low pressure until higher pressure. The absorption test is done for standard room temperature, 298.15 K, and 313.15 K. The temperature of natural gas exits from reservoir is higher than room temperature [4]. Temperature increase has negative effect to absorption process and therefore cooling process would be needed to reduce the temperature of natural gas prior to acid gas absorption process. Temperature 313.15 K is considered visible to be obtained based on the assumption that the average dry bulb temperature is 303.15 K and 10 K requirement for heat exchanger pinch temperature [24]. The experimental parameters for absorption test are listed in Table 3.1.

Table 3.1 Experimental parameter for absorption test

Experiment Parameter	Value
Absorbent	Aqueous Sodium Glycinate
Concentration (wt. %)	1.0, 5.0, 10, 15, 20 and 30
Testing gas	CO_2
Pressure (kPa)	100, 500, 1000, 1500, 2000 and 2500
Temperature (K)	298.15 and 313.15
Mixing vessel volume (ml)	3000
Equilibrium cell volume (ml)	50
Absorbent volume (ml)	5
Stirrer speed (rpm)	400

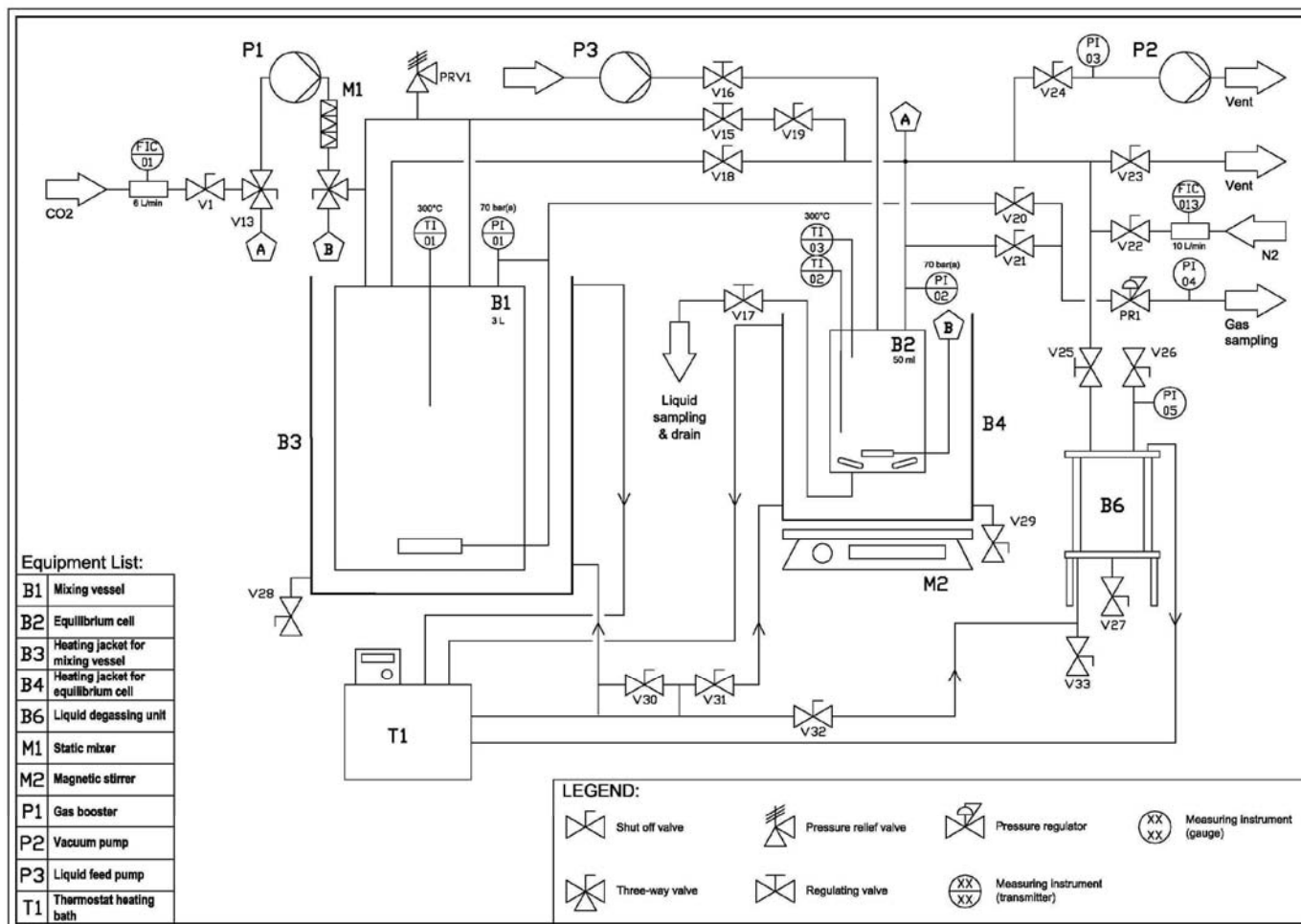


Figure 3.10 Schematic Diagram of SOLTEQ BP-22 High Pressure Solubility Cell



(A)



(B)



(C)



(D)

Figure 3.11 SOLTEQ BP-22 High Pressure Solubility Cell;
(A) Equilibrium Cell, (B) Mixing Vessel, (C) Liquid Feed Pump, (D) Thermostat Heating Bath

Absorption Test Method

Initially, the mixing vessel is pressurised with CO₂ and heated up to the desired pressure and temperature. Approximately 5 ml of aqueous sodium glycinate solution is fed into the equilibrium cell of 50 ml capacity, which was previously purged with nitrogen and vacuumed up to 38 mmHg (-0.95 atm). The apparatus is then brought to a desired temperature and CO₂ is introduced from the mixing vessel to achieve a total system pressure within the range of 100 to 2500 kPa. The solution is continuously stirred with a magnetic stirrer to ensure proper mixing in the system. When the total pressure of the system reaches a constant value and maintained for at least 2 h, the system is considered to have attained equilibrium. Typical absorption pressure profile is shown in Figure 3.12. Liquid sample is withdrawn from the equilibrium cell and analysed using titration method proposed by Shen *et al.* [81] to determine the concentration of CO₂ in the liquid phase. The partial pressure of carbon dioxide at equilibrium is calculated by subtracting the vapour pressure of water from the total system pressure [81]. The pure water vapour pressure is calculated using Equation 3.4 [67].

$$p_{H_2O}^{vap} = 1.35337 \times 10^8 \exp(-5243.04/T) \quad \text{Equation 3.4}$$

where, $p_{H_2O}^{vap}$ is water vapour pressure in kPa and T is temperature in K.

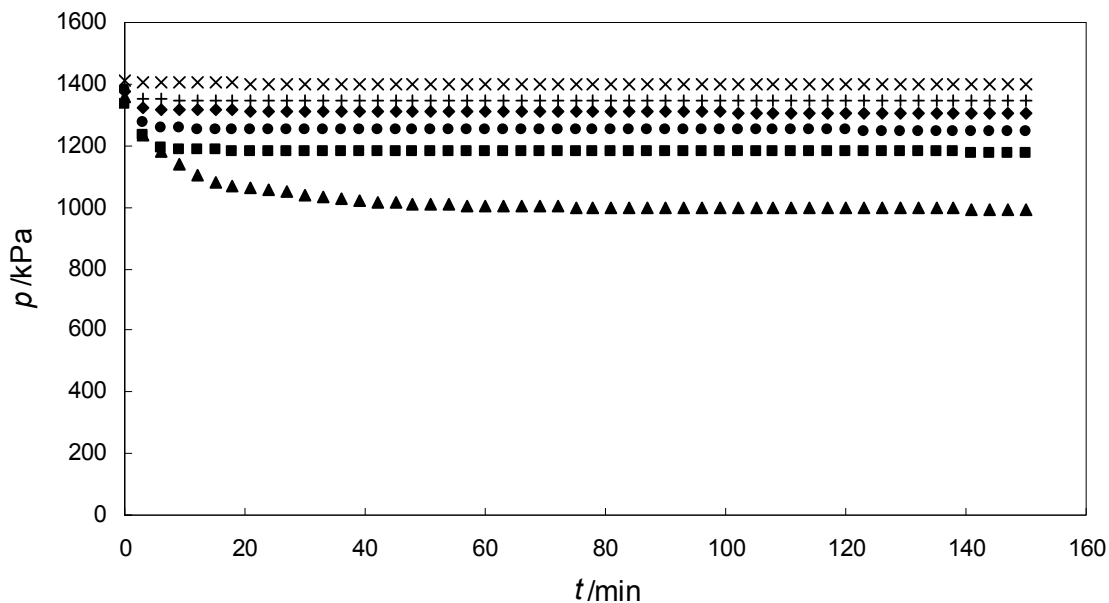


Figure 3.12 Typical absorption pressure profile for sodium glycinate- CO_2 system using SOLTEQ BP-22 High Pressure Solubility Cell.

Titration Method

The titration to determine the concentration of CO_2 in the liquid phase follows the method proposed by Shen *et al.* [81]. The liquid sample withdrawn from the equilibrium cell is transferred into a vessel containing excess 1.0 M *sodium hydroxide* (NaOH) - R&M Chemicals, purity $\geq 99\%$. The sodium hydroxide will react with the free dissolved CO_2 and convert it into Na_2CO_3 . Then an excess amount of 1.0 M *barium chloride* (BaCl_2) – Fluka, purity $> 99\%$ p.a., solution is added to the solution. The addition of BaCl_2 would convert Na_2CO_3 into *barium carbonate* (BaCO_3) that precipitate and *sodium chloride* (NaCl). The solution is titrated with standardised HCl , prepared from HCl – SYSTERM, 36 % p.a., using phenolphthalein as indicator to neutralize the excess NaOH . The amount of total CO_2 absorbed is determined by titration of BaCO_3 with HCl using methyl orange as indicator. The reaction between BaCO_3 and HCl would form BaCl_2 , H_2O and CO_2 . The amount of total CO_2 absorbed can be calculated from the amount of HCl added based on stoichiometry of BaCO_3 and HCl reaction.

3.10 Regenerability test

One of the requisite for an absorbent to be used in continuous acid gas removal system is that the acid gas absorption process must be reversible. The acid gas loaded solution should be regenerable without significant losses in its absorption capability. In this regenerability test, the same sodium glycinate solution undergoes few CO₂ absorption-desorption cycles to check the effect of absorption-desorption process on the solubility of CO₂.

In the actual acid gas absorption process, the absorbent would undergo continuous absorption-desorption cycle. Therefore to imitate this continuous absorption-desorption process, in this regenerability test the same sodium glycinate solution is subjected to several CO₂ absorption-desorption cycles of process. Song [22] pointed out that 10 wt % of aqueous sodium glycinate solution has higher CO₂ loading compared to several alkanolamines. Therefore, this regenerability test is done for 10 wt. % sodium glycinate. Absorption process is conducted at CO partial pressure 1000 kPa and temperature of 298.15 K using SOLTEQ BP-22 High Pressure Solubility Cell. This apparatus and the absorption method have been described in section 3.9. The desorption process is done by degassing the solution using ultrasonic water. This desorption process is done to regenerate the spent solution so it can be used in further absorption process. Figure 3.13 shows the ELMA 680DH ultrasonic water bath. The liquid sample after absorption is placed in a measuring flask and submerged in the ultrasonic water bath. The temperature of water bath is maintained at 333.15 K to avoid water evaporation thus preventing changes in solution concentration. Ultrasonic frequency is used at 40 kHz to enhance the CO₂ desorption process as compensation to the reduced temperature. The desorption process is completed when no visible gas bubble is released from the liquid sample within 1 hour period. There is no visible solution volume reduction after desorption process based on measuring flask reading. The CO₂ concentration in the liquid sample after absorption process and desorption process is determined using titration method proposed by Shen [81]. The titration method has already been described in section 3.9.2. The desorption method and energy requirement in this study is not reflective of the actual method and energy consumption for regeneration process.



Figure 3.13 ELMA 680DH ultrasonic water bath

CHAPTER 4

RESULT

Some critical fundamental properties of aqueous sodium glycinate solution have been successfully measured for a range of concentration (1, 5, 10, 15, 20, 30 wt. %) at various temperature. Density, kinematic viscosity, refractive index, heat capacity, acidity, conductivity, surface tension and contact angle with stainless steel surface of aqueous sodium glycinate are measured and reported. Absorption test and regenerability test to measure the CO₂ absorption capability and regenerability of the aqueous sodium glycinate solution have also been conducted. The absorption of carbon dioxide into absorbent changes the physical properties of the absorbent. Therefore the physical properties of amino acid salt after CO₂ absorption are also measured in order to quantify the effect of CO₂ loading on the physical properties of amino acid salt solution. Some of the measurements results are compared with previous published data while for the others which have no previous data, the result are shown without comparison.

4.1 Density

The experimental data on density of aqueous sodium glycinate solutions before absorption was compared with previously published data [109] and are presented in Table 4.1 and shown in Figure 4.1. It was found that the densities of the aqueous solution of sodium glycinate increases as the concentration increase and decreases with increasing temperature.

Table 4.1 Densities of aqueous sodium glycinate solutions

T/K	$\rho/\text{g}\cdot\text{cm}^{-3}$					
	1 wt. %	5 wt. %	10 wt. %	15 wt. %	20 wt. %	30 wt. %
Present study						
298.15	1.01196	1.01592	1.03452	1.05560	1.08352	1.13040
313.15	1.00200	1.01056	1.02968	1.04832	1.07644	1.11800
323.15	0.99940	1.00512	1.02256	1.04292	1.07100	1.11276
333.15	0.99672	1.00012	1.01756	1.03672	1.06648	1.10748
343.15	0.99016	0.99324	1.01076	1.03008	1.06120	1.10144
353.15	0.98536	0.98720	1.00532	1.02364	1.05448	1.09452
Lee <i>et al.</i> [109]						
303.15	-	-	1.0332	-	1.0800	1.1214
313.15	-	-	1.0296	-	1.0763	1.1176
323.15	-	-	1.0252	-	1.0718	1.1129
333.15	-	-	1.0201	-	1.0665	1.1075
343.15	-	-	1.0145	-	1.0607	1.1015
353.15	-	-	1.0082	-	1.0542	1.0947

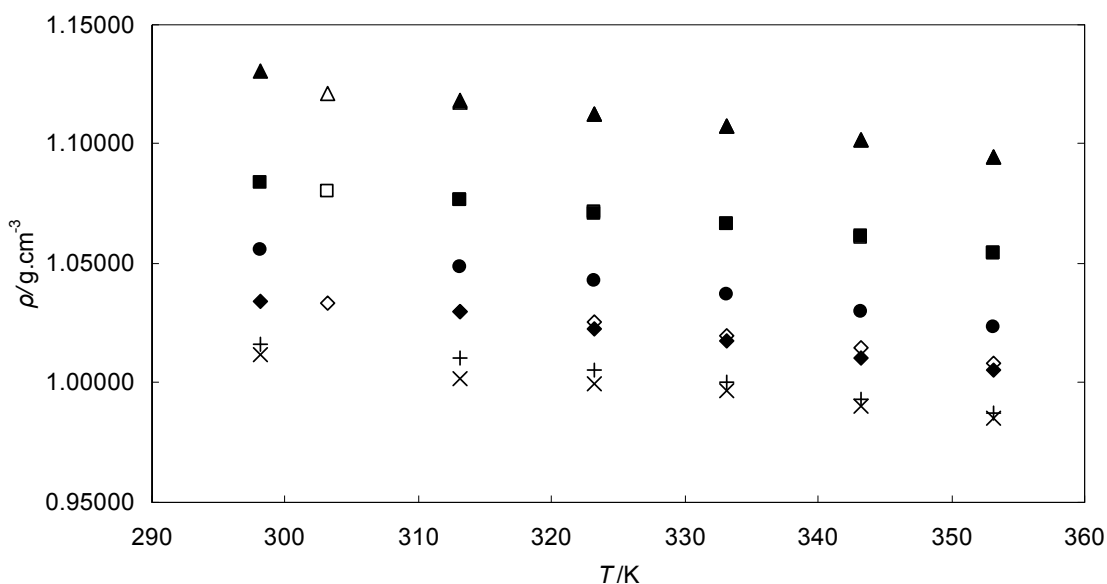


Figure 4.1 Density as a function of temperature for aqueous sodium glycinate solutions of different concentrations; ×, 1 wt. %; +, 5 wt. %; ◆, 10 wt. %; ●, 15 wt. %; ■, 20 wt. %; ▲, 30 wt. %; ◇, 10 wt. % Lee [109]; □, 20 wt. % Lee [109]; △, 30 wt. % Lee [109].

The effect of temperature and solution concentration on the density of aqueous sodium glycinate solutions within the range studied is correlated using the multiple regression method and could be represented by the following equation:

$$\rho = 1.16326 - 5.45608e - 04 T + 4.08441e - 03 C \quad \text{Equation 4.1}$$

where ρ is the density in g.cm^{-3} ; T is the temperature in K; C is the solution concentration in wt. %. The calculation error (ε) and root mean square error (RMSE) of the data is calculated using the following equations [120]:

$$\varepsilon = |X_{\text{exp}} - X_{\text{cal}}| \quad \text{Equation 4.2}$$

$$RMSE = \left(\frac{\sum_1^n (X_{\text{exp}} - X_{\text{cal}})^2}{n} \right)^{0.5} \quad \text{Equation 4.3}$$

where X_{exp} , X_{cal} and n are the measured experimental values, calculated values using the equations and the number of measurements made respectively. The minimum and maximum absolute errors of the data within the range of study are found to be 0.00125 and 0.01115 respectively. The RMSE of the solution density between experimental data and calculated from Equation 4.1 is 0.00560.

Similarly, the measurement for density of the aqueous sodium glycinate solution after absorption of CO_2 was performed and the result are shown in Table 4.2. The densities of aqueous sodium glycinate after CO_2 absorption gave higher values compared to the solution prior to absorption and increases with an increase in pressure. The multiple regression method is applied to the density data after absorption to quantify the effect of absorption pressure and solution concentration at constant temperature. The correlation between density, absorption pressure and concentration is represented by the equation below.

$$\rho' = A_0 + A_1 p + A_2 C \quad \text{Equation 4.4}$$

where ρ' is the density after absorption in g.cm^{-3} ; p is the pressure in kPa; C is the solution concentration in wt. %; A_0 , A_1 and A_2 are the equation constant. The

calculation error (ε) and the root mean square error (RMSE) of the data are calculated using Equation 4.2 and Equation 4.3. The equation constant, error and RSME is presented in Table 4.3.

Table 4.2 Densities of aqueous sodium glycinate solution after CO₂ absorption

p/kPa	$\rho/\text{g.cm}^{-3}$					
	1 wt. %	5 wt. %	10 wt. %	15 wt. %	20 wt. %	30 wt. %
$T/\text{K} = 298.15$						
100	1.33538	1.34013	1.34695	1.35005	1.35220	1.37842
500	1.33610	1.34370	1.34854	1.35799	1.35609	1.38046
1000	1.33714	1.34420	1.34994	1.35800	1.36843	1.38128
1500	1.33769	1.34469	1.35340	1.35820	1.36853	1.38267
2000	1.33774	1.34517	1.35351	1.35856	1.37229	1.38407
2500	1.33853	1.34529	1.35732	1.35975	1.37498	1.38733
$T/\text{K} = 313.15$						
100	1.33649	1.34136	1.34831	1.35605	1.35969	1.37670
500	1.33864	1.34263	1.34972	1.35646	1.36520	1.37959
1000	1.33894	1.34518	1.35222	1.35829	1.36945	1.38072
1500	1.33895	1.34574	1.35430	1.35941	1.37061	1.38437
2000	1.33918	1.34605	1.35448	1.35955	1.37446	1.38488
2500	1.33967	1.34665	1.35759	1.36023	1.37626	1.38819

Table 4.3 Correlation coefficient for Equation 4.4

	$T/\text{K} = 298.15$	$T/\text{K} = 313.15$
A_0	1.33076	1.33290
$10^6 A_1$	3.81241	3.29270
$10^3 A_2$	1.52972	1.52587
Minimum ε	0.00007	0.00007
Maximum ε	0.00954	0.00461
RSME	0.00285	0.00198
Pressure range	100 to 2500 kPa	
Concentration range	1.0 to 30 wt. %	

The small value of errors and RSME proves that Equation 4.4 could be used to represent the effect of absorption pressure and solution concentration to the density of CO₂-loaded aqueous sodium glycinate within the range studied.

4.2 Kinematic Viscosity

The kinematic viscosities of aqueous sodium glycinate before absorption are presented in Table 4.4. It was found that the kinematic viscosity of aqueous sodium glycinate solution increases as the concentration increase and decreases with increasing temperature. The effect of temperature and solution concentration to kinematic viscosity of aqueous solution of sodium glycinate is represented by Equation 4.5.

$$\ln v = \frac{1955.92}{T} + 2.99479e - 02 C - 6.61722 \quad \text{Equation 4.5}$$

where v is the kinematics viscosity in cSt; T is the temperature in K; C is the solution concentration in wt. %. The calculation error (ϵ) and root mean square error (RMSE) of the data are calculated using Equation 4.2 and Equation 4.3. The values of the minimum absolute error, maximum absolute error and RMSE are 0.00285, 0.08373, and 0.04263 respectively.

Table 4.4 Kinematic viscosities of aqueous sodium glycinate solution

T/K	v/cSt					
	1 wt. %	5 wt. %	10 wt. %	15 wt. %	20 wt. %	30 wt. %
298.15	0.9930	1.1453	1.2780	1.4194	1.6173	2.5105
313.15	0.7282	0.7596	0.8812	1.0613	1.3166	1.6711
323.15	0.6043	0.6365	0.7366	0.8717	1.1254	1.3527
333.15	0.5148	0.5473	0.6278	0.7334	0.9169	1.1288

Similarly, the kinematic viscosity of the aqueous sodium glycinate solution is measured for the solution after absorption of CO₂ and the result are shown in Table 4.5. The kinematic viscosity of the solution after CO₂ absorption is found to be lower than before absorption. The effect of absorption pressure and solution concentration on the solution kinematic viscosity within the range of study is correlated using the multiple regression method and shown in Equation 4.6.

$$\ln v' = B_0 p + B_1 C + B_2 \quad \text{Equation 4.6}$$

where ν' is the kinematic viscosity after absorption in cSt; p is the pressure in kPa; C is the solution concentration in wt. %; B_0 , B_1 and B_2 are the equation constant. The calculation error (ε) and the root mean square error (RMSE) of the data are calculated using Equation 4.2 and Equation 4.3. The equation constant, error and RSME are tabulated in Table 4.6.

Table 4.5 Kinematic viscosities of aqueous sodium glycinate solution after CO₂ absorption

p/kPa	ν/cSt					
	1%-wt	5%-wt	10%-wt	15%-wt	20%-wt	30%-wt
T = 298.15 K						
100	0.8396	0.9353	1.2168	1.4155	1.6099	2.4827
500	0.8212	0.9261	1.1506	1.3382	1.5768	2.4514
1000	0.8083	0.9003	1.1193	1.3290	1.5271	2.4459
1500	0.8065	0.8985	1.0733	1.3051	1.5014	2.3981
2000	0.8028	0.8801	1.0696	1.2757	1.4866	2.2159
2500	0.7991	0.8617	1.0420	1.2334	1.3971	2.2086
T = 313.15 K						
100	0.5177	0.5432	0.6831	0.8268	1.1689	1.3108
500	0.4662	0.5103	0.6721	0.7992	1.1634	1.2360
1000	0.4478	0.4974	0.5930	0.7550	1.0346	1.1127
1500	0.4312	0.4827	0.5525	0.7348	1.0199	1.0980
2000	0.4294	0.4606	0.5473	0.6189	0.7273	0.9895
2500	0.4257	0.4404	0.4792	0.4993	0.6464	0.7638

Table 4.6 Correlation coefficient for Equation 4.6

	$T/\text{K} = 298.15$	$T/\text{K} = 313.15$
$10^4 \cdot B_0$	-0.44768	-1.59204
B_1	0.03664	0.03238
B_2	-0.21437	-0.63742
Minimum ε	0.00023	0.00153
Maximum ε	0.07219	0.24840
RSME	0.03175	0.09640
Pressure range	100 to 2500 kPa	
Concentration range	1.0 to 30 wt. %	

Based on the correlation result in Table 4.6, Equation 4.6 is appropriate to represent the effect of absorption pressure and concentration to the kinematic viscosity of aqueous sodium glycinate solution within studied range.

4.3 Heat Capacity

Heat capacity of water is measured to verify the accuracy of Pyris 1 Digital Scanning Calorimeter (DSC). The measured water heat capacity is compared with published data from Osborne *et al.* [121] and presented in Table 4.7. Heat capacity of water is found to be in good agreement with published data.

Table 4.7 Heat capacity of water

<i>T/K</i>	<i>C_p/kJ.kg⁻¹.K⁻¹</i>				
	Osborne <i>et al.</i>	this study			Average value
		Run 1	Run 2	Run 3	
303.15	4.1785	4.185	4.181	4.172	4.179
308.15	4.1782	4.187	4.184	4.177	4.183
313.15	4.1786	4.186	4.186	4.181	4.184
318.15	4.1795	4.185	4.187	4.183	4.185
323.15	4.1807	4.183	4.188	4.186	4.185
328.15	4.1824	4.181	4.188	4.188	4.185
333.15	4.1844	4.179	4.188	4.190	4.186
338.15	4.1868	4.177	4.189	4.192	4.186
343.15	4.1896	4.176	4.190	4.195	4.187
348.15	4.1928	4.176	4.192	4.198	4.188
353.15	4.1964	4.175	4.193	4.201	4.190

The experimental data on heat capacity of aqueous sodium glycinate solutions before CO₂ absorption are presented in Table 4.8. It was found that heat capacity of aqueous solutions of sodium glycinate decreases as the concentration increase and increases with an increase in temperature. The heat capacities data for 30 wt. % sodium glycinate was compared with published data and is shown in Figure 4.2. Heat capacity of 30 wt. % sodium glycinate is found to be in good agreement with the published data by Song *et al.* [122]. The effect of temperature and solution concentration on the heat capacity of aqueous sodium glycinate solutions within the range of study could be represented by the following equation:

$$C_p = 3.45989 + 2.36286e - 03 T - 2.41933e - 02 C \quad \text{Equation 4.7}$$

where C_p is the heat capacity in kJ.kg.K⁻¹; T is temperature in K; C is the solution concentration in wt. %. The calculation error (ϵ) and root mean square error (RMSE) of the data is calculated using Equation 4.2 and Equation 4.3. The calculated

minimum absolute error, maximum absolute error and RMSE of the data are 0.00019, 0.04758, and 0.02542 respectively.

Table 4.8 Heat capacity of aqueous sodium glycinate solution

T/K	$C_p/kJ.kg^{-1}.K^{-1}$						Song [122] 30 wt. %
	Present study						
	1 wt. %	5 wt. %	10 wt. %	15 wt. %	20 wt. %	30 wt. %	
298.15	4.140	4.084	3.946	3.840	3.635	3.391	3.441
303.15	4.141	4.085	3.947	3.842	3.661	3.417	3.445
308.15	4.143	4.088	3.950	3.845	3.692	3.444	3.450
313.15	4.147	4.092	3.953	3.849	3.723	3.471	3.454
318.15	4.151	4.096	3.956	3.853	3.753	3.500	3.459
323.15	4.152	4.103	3.960	3.859	3.786	3.528	3.463

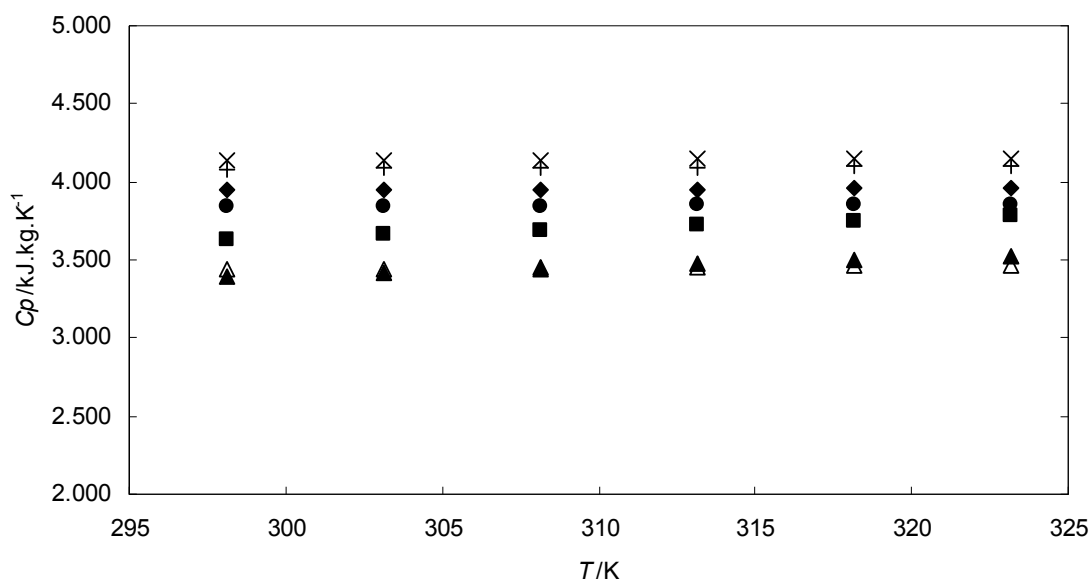


Figure 4.2 Heat capacity as a function of temperature for aqueous sodium glycinate solutions of different concentrations; \times , 1 wt. %; $+$, 5 wt. %; \blacklozenge , 10 wt. %; \bullet , 15 wt. %; \blacksquare , 20 wt. %; \blacktriangle , 30 wt. %; \triangle , 30 wt. % Song [122].

Similarly, the measurement was done for solution after CO_2 absorption at 298.15 K to avoid the effect of temperature change to the CO_2 loading of the initial sample [123]. Heat capacity of the solution after CO_2 absorption at 298.15 K is expressed as a function of CO_2 loading factor (α). The data are tabulated in Table 4.9 up to Table 4.14. The heat capacity of aqueous sodium glycinate solution is also included in Table

4.9 up to Table 4.14 as heat capacity for unloaded solution or α equal to 0. As observed from the result, the heat capacity of the CO₂ loaded solution increases with temperature but decreases with the CO₂ loading. Therefore the heat capacity of the CO₂-loaded aqueous sodium glycinate solution was found to be lower than unloaded solution. The effect of CO₂ loading to the heat capacity of CO₂ loaded solution at constant solution concentration could be expressed as a function of heat capacity of unloaded solution and CO₂ loading factor as follows:

$$Cp' = C_0 + C_1 Cp + C_2 \alpha \quad \text{Equation 4.8}$$

where Cp' is the heat capacity of CO₂ loaded solution in kJ.kg.K⁻¹; Cp is the heat capacity in kJ.kg.K⁻¹; α is the CO₂ loading factor; C_0 , C_1 and C_2 are the equation constants. The calculation error (ϵ) and root mean square error (RMSE) of the data is calculated using Equation 4.2 and Equation 4.3. The equation constant, error and RSME are presented in Table 4.15.

Table 4.9 Heat capacity (in kJ.kg⁻¹.K⁻¹) of 1.0 wt. % aqueous sodium glycinate solution after CO₂ absorption at 298.15 K

<i>T/K</i>	<i>α (mol CO₂/mol SG)</i>						
	0.000	2.313	2.688	3.188	3.375	3.563	4.063
298.15	4.140	4.028	3.983	3.938	3.907	3.897	3.832
303.15	4.141	4.048	4.007	3.968	3.941	3.933	3.872
308.15	4.143	4.068	4.032	4.005	3.977	3.975	3.917
313.15	4.147	4.088	4.061	4.039	4.013	4.014	3.964
318.15	4.151	4.108	4.091	4.068	4.051	4.048	4.013
323.15	4.152	4.128	4.112	4.100	4.090	4.087	4.068

Table 4.10 Heat capacity (in kJ.kg⁻¹.K⁻¹) of 5.0 wt. % aqueous sodium glycinate solution after CO₂ absorption at 298.15 K

<i>T/K</i>	<i>α (mol CO₂/mol SG)</i>						
	0.000	1.238	1.363	1.375	1.438	1.413	1.525
298.15	4.084	3.953	3.859	3.836	3.790	3.792	3.713
303.15	4.085	3.979	3.876	3.881	3.841	3.841	3.765
308.15	4.088	4.005	3.913	3.932	3.901	3.892	3.822
313.15	4.092	4.031	3.958	3.978	3.958	3.945	3.885
318.15	4.096	4.058	4.010	4.019	4.004	4.002	3.950
323.15	4.103	4.084	4.079	4.064	4.041	4.060	4.010

Table 4.11 Heat capacity (in $\text{kJ}\cdot\text{kg}^{-1}\cdot\text{K}^{-1}$) of 10 wt. % aqueous sodium glycinate solution after CO_2 absorption at 298.15 K

T/K	α (mol CO_2 /mol SG)						
	0.000	0.969	1.156	1.281	1.319	1.363	1.431
298.15	3.946	3.741	3.720	3.632	3.597	3.568	3.515
303.15	3.947	3.775	3.765	3.672	3.621	3.609	3.560
308.15	3.950	3.817	3.814	3.716	3.652	3.649	3.609
313.15	3.953	3.855	3.860	3.766	3.701	3.699	3.666
318.15	3.956	3.885	3.891	3.822	3.778	3.771	3.743
323.15	3.960	3.911	3.896	3.882	3.895	3.883	3.863

Table 4.12 Heat capacity (in $\text{kJ}\cdot\text{kg}^{-1}\cdot\text{K}^{-1}$) of 15 wt. % aqueous sodium glycinate solution after CO_2 absorption at 298.15 K

T/K	α (mol CO_2 /mol SG)						
	0.000	0.929	1.013	1.046	1.054	1.113	1.138
298.15	3.840	3.620	3.552	3.489	3.468	3.420	3.384
303.15	3.842	3.640	3.601	3.547	3.528	3.486	3.453
308.15	3.845	3.674	3.649	3.610	3.601	3.553	3.525
313.15	3.849	3.713	3.697	3.672	3.690	3.632	3.601
318.15	3.853	3.754	3.746	3.732	3.770	3.716	3.679
323.15	3.859	3.812	3.794	3.793	3.792	3.777	3.758

Table 4.13 Heat capacity (in $\text{kJ}\cdot\text{kg}^{-1}\cdot\text{K}^{-1}$) of 20 wt. % aqueous sodium glycinate solution after CO_2 absorption at 298.15 K

T/K	α (mol CO_2 /mol SG)						
	0.000	0.703	0.941	0.991	1.022	1.116	1.134
298.15	3.635	3.490	3.298	3.253	3.232	3.154	3.143
303.15	3.661	3.526	3.367	3.325	3.303	3.247	3.223
308.15	3.692	3.571	3.451	3.400	3.376	3.324	3.311
313.15	3.723	3.618	3.524	3.477	3.454	3.393	3.401
318.15	3.753	3.664	3.581	3.555	3.537	3.473	3.492
323.15	3.786	3.714	3.643	3.633	3.627	3.589	3.587

Table 4.14 Heat capacity (in $\text{kJ}\cdot\text{kg}^{-1}\cdot\text{K}^{-1}$) of 30 wt. % aqueous sodium glycinate solution after CO_2 absorption at 298.15 K

T/K	α (mol CO_2 /mol SG)						
	0.000	0.623	0.906	0.958	0.967	0.985	1.031
298.15	3.391	3.173	3.016	2.861	2.833	2.820	2.775
303.15	3.417	3.207	3.080	2.946	2.912	2.877	2.859
308.15	3.444	3.241	3.156	3.032	2.998	2.966	2.952
313.15	3.471	3.278	3.226	3.121	3.091	3.062	3.055
318.15	3.500	3.316	3.283	3.213	3.193	3.167	3.169
323.15	3.528	3.356	3.334	3.307	3.307	3.303	3.295

Table 4.15 Correlation coefficient for Equation 4.8

	1 wt. %	5 wt. %	10 wt. %	15 wt. %	20 wt. %	30 wt. %
C_0	-45.53972	-43.69715	-66.07009	-56.17693	-5.01023	-6.53932
C_1	12.01015	11.82890	17.79110	15.72005	2.42875	2.94783
C_2	-0.07419	-0.54739	-0.39572	-0.64542	-0.56186	-0.60412
Min. ϵ	0.00001	0.00031	0.00112	0.00260	0.00010	0.00091
Max. ϵ	0.04888	0.07516	0.08820	0.07515	0.07602	0.12826
RSME	0.01895	0.02610	0.03448	0.03079	0.02538	0.05352

It is observed from Table 4.15 that the errors and RMSE between the experimental data and calculated data from Equation 4.8 are small therefore it can be concluded that Equation 4.8 is suitable to represent the effect of the absorbed CO₂ to the heat capacity of aqueous sodium glycinate solution within the range of study.

4.4 Refractive Index

The experimental data on refractive index of aqueous sodium glycinate solution is presented in Table 4.16. The refractive index of aqueous sodium glycinate solution is found to increase with concentration and decreases with temperature. Temperature influences on the refractive index primarily because of the accompanying change in density [115]. Calibration plot between refractive index of a solution against the solution concentration could be used to determine the unknown concentration of the same solution based on its refractive index.

Table 4.16 Refractive index of aqueous sodium glycinate solutions

T/K	n_D					
	1 wt. %	5 wt. %	10 wt. %	15 wt. %	20 wt. %	30 wt. %
303.15	1.336240	1.344137	1.350003	1.355967	1.362627	1.374727
313.15	1.334847	1.342673	1.348607	1.354520	1.361337	1.373883
323.15	1.333207	1.341170	1.347330	1.353490	1.360363	1.372973
333.15	1.330777	1.339080	1.345670	1.352610	1.358210	1.370843

The temperature and solution concentration effects on solution refractive index could be represented by the following equation:

$$n_D = -1.44778e - 04 T + 1.32169e - 03 C + 1.38011 \quad \text{Equation 4.9}$$

where n_D is the refractive index; T is the temperature in K ; C is the solution concentration in wt. %. The minimum and maximum absolute errors calculated from Equation 4.2 are $1.89055e-06$ and 0.00242 respectively. The root mean square error (RMSE) of the data is 0.00095 calculated using Equation 4.3. Therefore Equation 4.9 could be used to estimate the concentration of unknown sodium glycinate solution based on its refractive index and temperature for concentration range from 1 to 30 wt. % and temperature range from 303.15 to 333.15 K

4.5 Acidity

The pH of the aqueous solution of sodium glycinate before absorption is presented in Table 4.17. Sodium glycinate in water would form electrolyte with sodium as cation and glycinate as anion. This cation-anion configuration would form buffer solution. From the measurement result, it is found that the pH of sodium glycinate solution is around 11 to 12. The alkaline nature of the solution would allow the absorption of H_2S and CO_2 while the buffering effect of the solution would prevent rapid pH changes as the acid gas is absorbed. Similar principle is also applied in alkaline salt system [5].

Table 4.17 Acidity of aqueous sodium glycinate solution at various concentrations

wt. %	<i>pH</i>
1	11.35
5	11.67
10	11.72
15	11.75
20	11.78
30	11.79

The pH of the aqueous solution of sodium glycinate after CO_2 absorption is presented in Table 4.18. It can be observed that the pH of aqueous sodium glycinate after absorption is lower than before absorption. This is due to the formation of carbonic acid from CO_2 absorbed into the solution. The acidity of the solution after CO_2 absorption would be close to neutral condition with pH around 7 to 8.

Some exceptions are observed for absorption result at 100 kPa. The acidity of solution at high concentration is still at base condition with pH more than 9. This indicates that there is a factor that limits the CO₂ absorption. From the observation of the system pressure profile during absorption process, it is found that amount of available CO₂ is the factor that limits the absorption for high solution concentration at 100 kPa. Figure 4.3 shows the pressure profile for CO₂ absorption at 100 kPa and 313.15 K. It can be observed from Figure 4.3 that the system pressure is limited at a certain value. The absorption process is halted at this condition thus resulted in lower amount of CO₂ absorbed and higher pH.

Table 4.18 Acidity of aqueous sodium glycinate solution after CO₂ absorption

<i>p</i> /kPa	<i>pH</i>					
	1%-wt	5%-wt	10%-wt	15%-wt	20%-wt	30%-wt
T = 298.15 K						
100	8.36	8.21	8.62	9.72	9.51	10.49
500	8.33	8.21	8.23	8.12	8.22	8.41
1000	8.20	8.14	8.13	8.02	8.06	8.05
1500	8.29	8.17	8.26	8.01	8.13	8.05
2000	8.33	8.20	8.22	8.06	8.06	8.00
2500	8.29	8.18	8.12	8.08	8.22	7.85
T = 313.15 K						
100	7.50	8.01	8.82	9.60	9.75	10.49
500	7.76	7.95	8.02	8.01	8.16	8.62
1000	8.22	8.19	8.10	8.10	8.10	8.01
1500	7.97	7.80	7.84	7.76	7.81	7.84
2000	7.84	7.85	7.81	7.74	7.79	7.92
2500	7.61	7.90	7.68	7.74	7.75	7.81

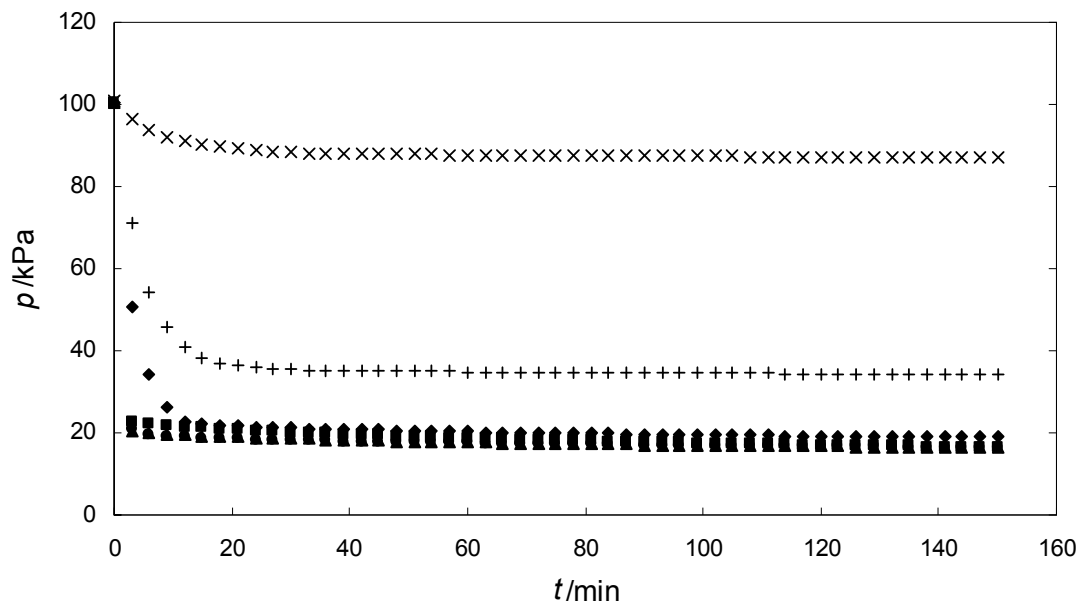


Figure 4.3 Pressure profile for CO₂ absorption in aqueous sodium glycinate (SG) at 100 kPa and 313.15 K; ×, 1 wt. %; +, 5 wt. %; ◆, 10 wt. %; ●, 15 wt. %; ■, 20 wt. %; ▲, 30 wt. %.

4.6 Conductivity

The measured conductivity data for aqueous sodium glycinate before absorption is tabulated in Table 4.19. It was found that the conductivity of the solution increases with an increase in concentration. This occurs due to the fact that sodium glycinate in water would form ions. Solution concentration would directly affect the number of ions available in solution.

Table 4.19 Conductivity of aqueous sodium glycinate at various concentrations

wt. %	$\sigma/\text{mS}\cdot\text{cm}^{-1}$	T/K
1	6.86	295.55
5	27.00	294.95
10	44.20	294.85
15	55.90	294.75
20	62.40	294.75
30	66.30	294.55

The measured conductivity data after CO₂ absorption is presented in Table 4.20. The measured solution conductivity after CO₂ absorption is lower than before absorption

and decreases with the pressure increase. The effect of CO₂ absorbed to the solution conductivity at constant temperature is expressed in Equation 4.10 as a function of the solution conductivity before absorption and absorption pressure using multiple regression method.

$$\sigma' = D_0 + D_1 p + D_2 \sigma \quad \text{Equation 4.10}$$

where σ' is the conductivity after CO₂ absorption in mS.cm⁻¹; σ is the conductivity before CO₂ absorption in mS.cm⁻¹; p is the pressure in kPa; D_0 , D_1 and D_2 are the equation constant. The calculation error (ε) and root mean square error (RMSE) of the data is calculated using Equation 4.2 and Equation 4.3. The equation constant, errors and RMSE for the equation are presented in Table 4.21.

Table 4.20 Conductivity of aqueous sodium glycinate solution after CO₂ absorption

p/kPa	$\sigma/\text{mS.cm}^{-1}$					
	1%-wt	5%-wt	10%-wt	15%-wt	20%-wt	30%-wt
T = 298.15 K						
100	7.58	27.55	44.05	54.2	61.00	65.45
500	7.98	26.85	43.90	52.75	59.25	61.4
1000	7.56	25.20	43.45	52.05	57.05	61.25
1500	7.38	25.15	43.15	51.85	56.85	61.15
2000	6.50	23.85	41.50	51.05	56.70	60.2
2500	6.20	22.60	40.40	49.50	54.45	56.2
T = 313.15 K						
100	6.97	27.35	43.65	53.9	59.75	60.15
500	6.70	25.90	42.3	51.7	55.7	58.9
1000	6.59	25.65	41.8	51.25	55.25	57.5
1500	6.70	22.40	37	48.7	54.75	56.5
2000	5.69	21.65	36.9	48.5	54.65	55.4
2500	6.16	21.00	36.35	47.15	52.1	54.9

Table 4.21 Correlation coefficient for Equation 4.10

	$T/\text{K} = 298.15$	$T/\text{K} = 313.15$
	D_0	3.51623
D_1	-0.00186	-0.00232
D_2	0.90835	0.87093
Minimum ε	0.01614	0.02398
Maximum ε	2.88487	2.40572
RSME	1.07671	1.22157

The errors and RSME of the data is still within acceptable limit therefore Equation 4.10 could be used to estimate the effect of CO₂ absorbed to the conductivity of sodium glycinate solution at different system pressure for the range studied.

4.7 Surface Tension and Contact Angle

The experimental data on surface tension of sodium glycinate solution is compared with published data and presented in Table 4.22. The result is shown good agreement with published data from Lee *et al.* [109]. The liquid surface tension is found to increase almost linearly with increasing sodium glycinate concentration. Similar result was also reported by Lee *et al.* [109]. The effect of sodium glycinate concentration to surface tension could be represented in following equation:

$$\gamma = 0.32967 C + 34.39948 \quad \text{Equation 4.11}$$

where γ is the surface tension in dyne.cm⁻¹ and C is the solution concentration in wt. %. The R² and RMSE for the equation are 0.9885 and 0.3427 respectively.

Contact angle of the solutions with stainless steel surface are also presented in Table 4.22. The contact angle between aqueous sodium glycinate solutions with stainless steel surface is found to be lower than 90°. Thus, it could be considered that the solution has a tendency to wet the stainless steel surface [124].

Table 4.22 Surface tension of aqueous sodium glycinate solutions and Contact angle with stainless steel surface at temperature 298.15 K

wt. %	$\gamma/\text{dyne.cm}^{-1}$		$\theta/^\circ$
	This study	Lee [109]	
1	35.04	-	54.18
5	35.36	-	62.30
10	37.91	38.49	65.79
15	39.46	-	70.75
20	41.21	40.72	75.72
30	44.12	43.98	76.61

4.8 Absorption Test

In order to verify and confirm the reliability and reproducibility of the SOLTEQ BP-22 High Pressure Solubility Cell, the equipment is used to measure the solubility of CO₂ in 30 %wt MEA solution and the results are compared with the available published data on the same pressure range [81, 125], which are shown in Figure 4.4. The measured loading capacity (mol CO₂/mol MEA) result is in good agreement with published data reported by Shen *et al.* [81] with an exception for result at low pressure. The measured loading capacity at low pressure is found to be lower than the published data. This minor deviation could be caused by the difference in the type of measurements. The present study involves the high pressure solubility cell. In this system, the acid gas and absorbent is placed in a closed vessel until its equilibrium condition reached. Shen *et al.* [81] have used two types of equipments namely low pressure (<) and high pressure (> 200 kPa). The low pressure equipment employs vapour recirculation equilibrium cell. The acid gas partial pressure in the vapour recirculation equilibrium cell is maintained by addition of feed gas. The high pressure equipment employs batch equilibrium cell. The operation principle of the batch equilibrium cell is similar with the high pressure solubility cell. For better comparison, the data are shown in Table 4.23. This result verifies that the SOLTEQ BP-22 High Pressure Solubility Cell is suitable as an instrument for the measurement of acid gas solubility in absorbent.

Table 4.23 Solubility of CO₂ in 30 wt. % MEA Aqueous Solution at 313.15 K

Present work		Shen and Li [81]	
p/kPa	α	p/kPa	α
		2.2	0.471
		5	0.496
		12.8	0.512
		28.7	0.538
		58.4	0.57
92	0.526	101.3	0.594
		140.1	0.62
504	0.653	552	0.676
1001	0.734	883	0.728
		1256	0.763
1504	0.784	1580	0.772
2007	0.830	1973	0.806
2512	0.842		

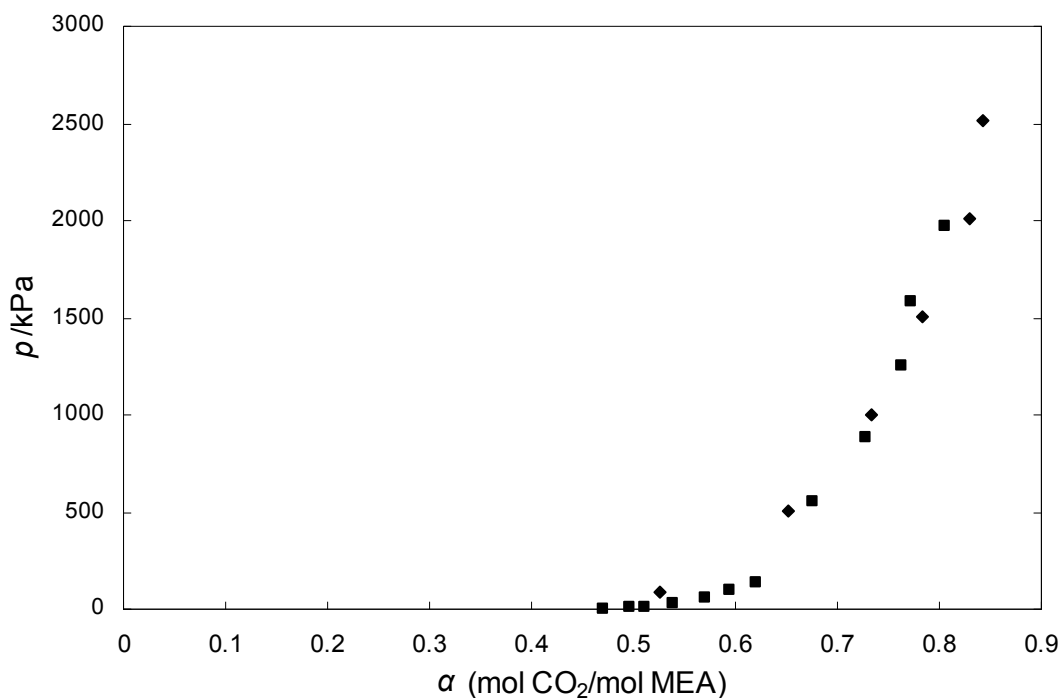


Figure 4.4 Loading capacity of 30 wt. % methyldiethanolamine (MEA) at 313.15K;
 ◆, current work; ■, Shen and Li [81]

The solubility of carbon dioxide in aqueous solutions of sodium glycinate is expressed as CO₂ loading factor ($\alpha = \text{mol CO}_2/\text{mol SG}$). The measured values of carbon dioxide solubility in aqueous sodium glycinate solutions for temperatures of 298.15 K and 313.15 K are presented in Table 4.24. The data are shown in Figure 4.5 and Figure 4.6 for temperatures of 298.15 and 313.15 K respectively. It is observed that for the same temperature, the CO₂ loading factor increases with the increase in CO₂ partial pressure but decreases with the increase in sodium glycinate concentration. CO₂ absorption using amino acid salt is categorized as exothermic chemical reaction. According to Le Chatelier principle, increase in temperature would lead to the decrease in the extent of reaction for this absorption. The results agree with this theory, the CO₂ loading factor of aqueous sodium glycinate solution at temperature 313.15 K is lower than at temperature 298.15 K within the pressure range studied.

Table 4.24 Solubilities of CO₂ ($\alpha = \text{mol CO}_2/\text{mol SG}$)

T = 298.15 K		T = 313.15 K	
p/kPa	α	p/kPa	α
1 wt. % sodium glycinate			
98	2.313	92	2.063
515	2.688	528	2.438
1031	3.188	995	2.750
1527	3.375	1510	2.938
2017	3.563	2030	3.125
2535	4.063	2483	3.313
5 wt. % sodium glycinate			
98	1.238	92	1.188
547	1.363	514	1.238
1022	1.375	1029	1.288
1511	1.438	1503	1.338
2020	1.413	2007	1.410
2500	1.525	2503	1.488
10 wt. % sodium glycinate			
98	0.969	91	0.888
522	1.156	512	1.050
1009	1.281	1018	1.150
1517	1.319	1515	1.231
2024	1.363	2022	1.256
2498	1.431	2505	1.275
15 wt. % sodium glycinate			
98	0.929	91	0.842
526	1.013	520	1.029
1002	1.046	1017	1.067
1536	1.054	1504	1.083
2035	1.113	2038	1.142
2521	1.138	2499	1.175
20 wt. % sodium glycinate			
98	0.703	90	0.681
528	0.941	508	0.913
1010	0.991	1009	1.000
1541	1.022	1516	1.031
2038	1.116	2019	1.075
2531	1.134	2513	1.131
30 wt. % sodium glycinate			
98	0.623	91	0.575
516	0.906	508	0.867
1026	0.958	1011	0.954
1526	0.967	1525	0.975
2049	0.985	2003	0.979
2534	1.031	2501	0.988

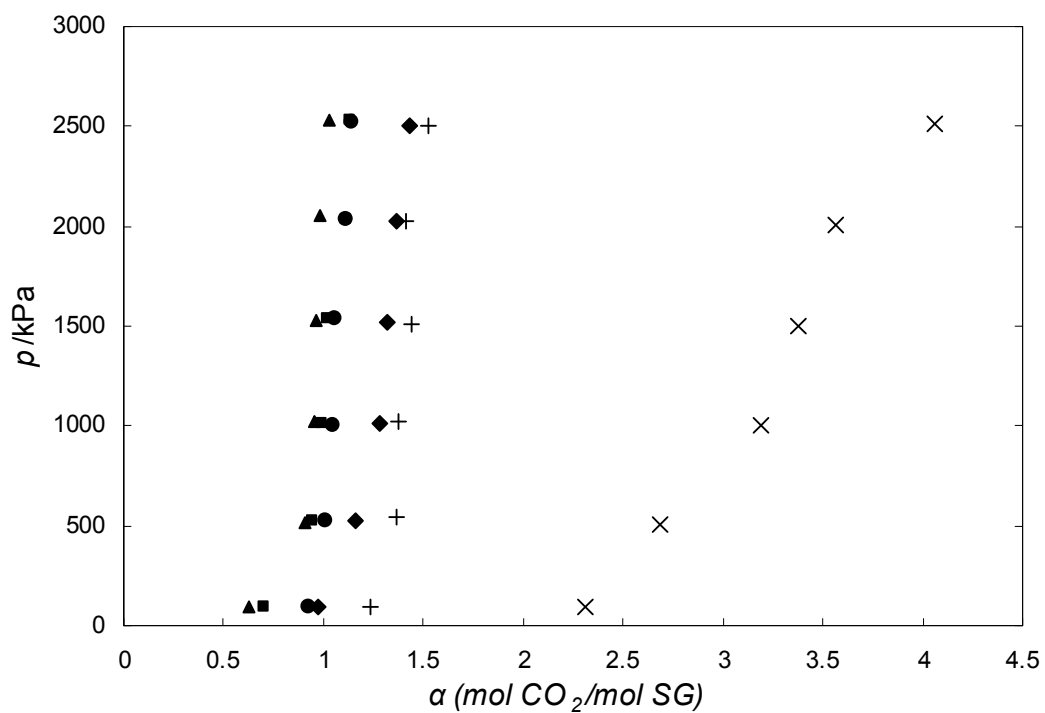


Figure 4.5 Loading capacity of aqueous sodium glycinate (SG) at 298.15 K; \times , 1 wt. %; +, 5 wt. %; \blacklozenge , 10 wt. %; \bullet , 15 wt. %; \blacksquare , 20 wt. %; \blacktriangle , 30 wt. %.

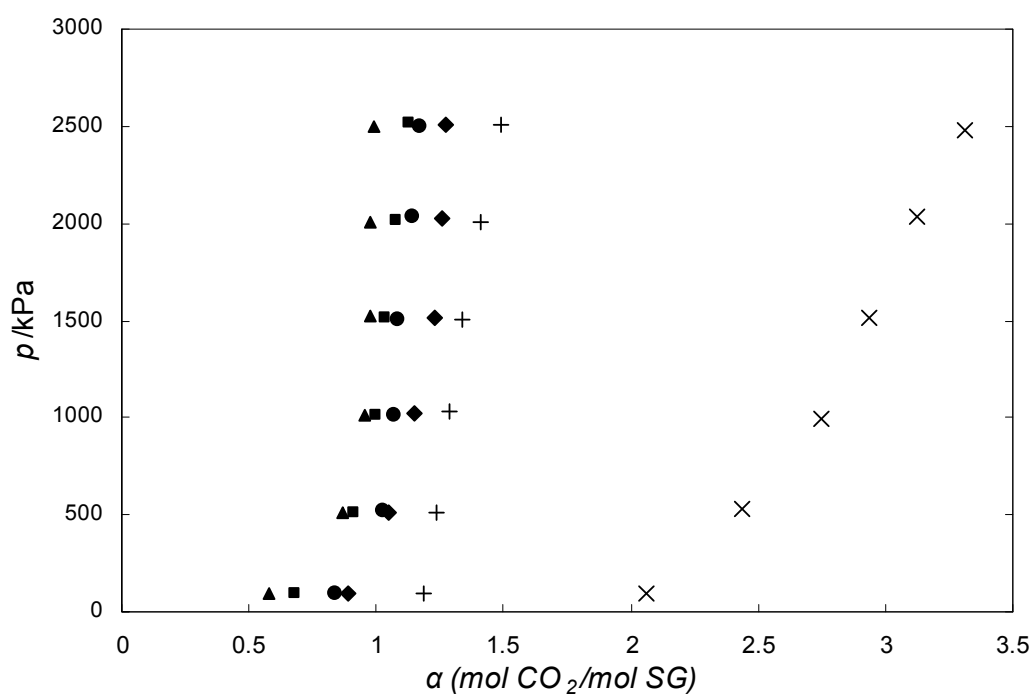


Figure 4.6 Loading capacity of aqueous sodium glycinate (SG) at 313.15 K; \times , 1 wt. %; +, 5 wt. %; \blacklozenge , 10 wt. %; \bullet , 15 wt. %; \blacksquare , 20 wt. %; \blacktriangle , 30 wt. %.

The CO₂ loading factor is plotted against CO₂ partial pressure at equilibrium condition using the following equation:

$$p = D_0 \exp(D_1 \alpha) \quad \text{Equation 4.12}$$

where p is the CO₂ partial pressure in kPa; α is the CO₂ loading factor; D_0 and D_1 are the correlation constants. The correlation constants and R^2 for Equation 4.12 is presented in Table 4.25.

Table 4.25 The correlation constants and R^2 for Equation 4.12

wt. %	D_0	D_1	R^2
$T/K = 298.15$			
1	2.38754	1.83335	0.8780
5	6.807e-05	11.75369	0.8740
10	0.11153	7.13906	0.9837
15	6.648e-05	1.56171	0.9309
20	0.47870	7.61694	0.9795
30	0.60099	7.97165	0.9469
$T/K = 313.15$			
1	0.70118	2.56102	0.9360
5	0.00223	9.69949	0.7759
10	0.07927	8.12417	0.9837
15	0.01568	10.31710	0.9791
20	0.49020	7.66376	0.9941
30	1.10346	7.46072	0.9489

The total absorbed CO₂ per volume of solution increases with an increase in solution concentration. But the increase in CO₂ absorbed is not as high as the concentration increment. This can be observed from Figure 4.6, for CO₂ partial pressure 1000 kPa and temperature 313.15K, the loading factor for 1, 5 and 10 wt. % of sodium glycinate solution are 2.750, 1.288 and 1.150 respectively. The net CO₂ absorbed in these solutions are 0.282, 0.662 and 1.181 mol/dm³ as shown in Figure 4.7. Based on the CO₂ absorption mechanism explained in section 2.6, one mole of CO₂ will react with 2 mole of amino acid salt therefore the increment in the amount of CO₂ absorbed would be lower than the concentration increment. It also observed from Figure 4.7 that CO₂ solubility for 1 wt. % sodium glycinate is almost similar with CO₂ solubility

in water. This indicates at low sodium glycinate concentration the water reaction with CO_2 effect is dominant compared to the sodium glycinate reaction with CO_2 .

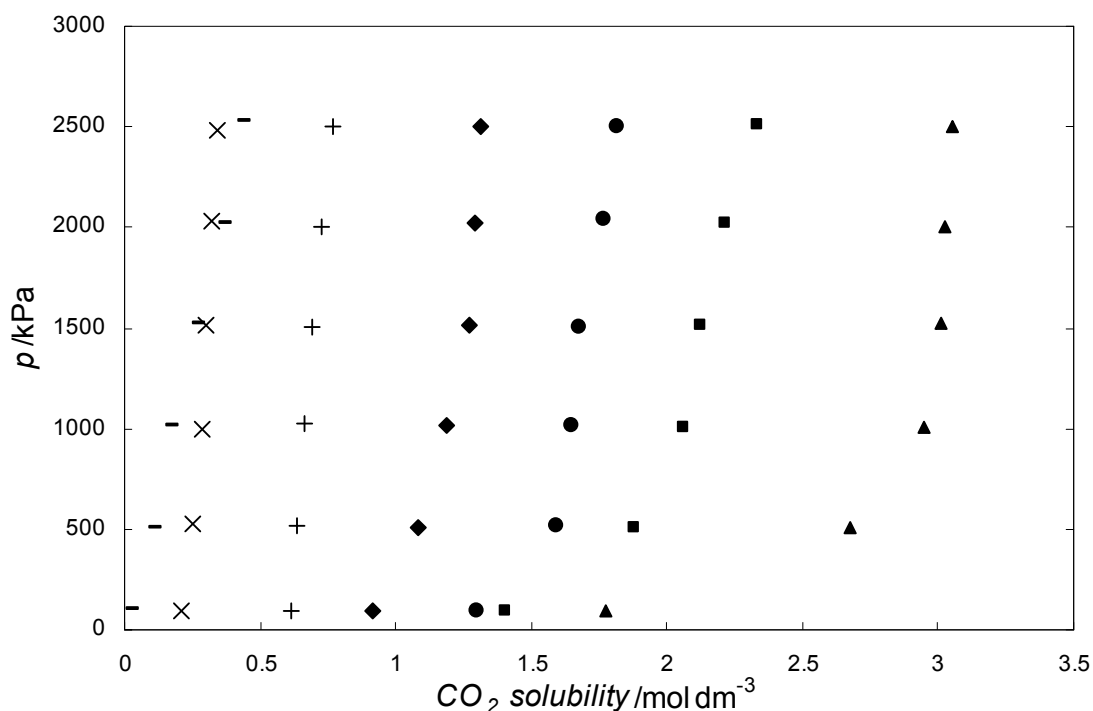


Figure 4.7 Carbon dioxide solubility in water and aqueous sodium glycinate solution at 313.15 K; -, water [5]; ×, 1 wt. %; +, 5 wt. %; ◆, 10 wt. %; ●, 15 wt. %; ■, 20 wt. %; ▲, 30 wt. %.

Statistical Analysis for Full Factorial Design

Statistical analyses for full factorial design estimates the effect of the interaction strength of pressure and concentration on the solution CO_2 loading factor. The full factorial design requires constant interval in parameter value therefore some result points are excluded from this design. The full factorial design is evaluated for pressure range 500 to 2500 kPa and concentration range 5 wt. % to 20 wt. % at temperature 298.15 K and 313.15 K. Pareto charts describe the relative importance of the factor and also the effect of factor setting adjustment, by displaying the most influencing factor followed by the least one. Regression analysis data of the loading capacity is expressed as second-order polynomial equation and shown in Equation 4.13.

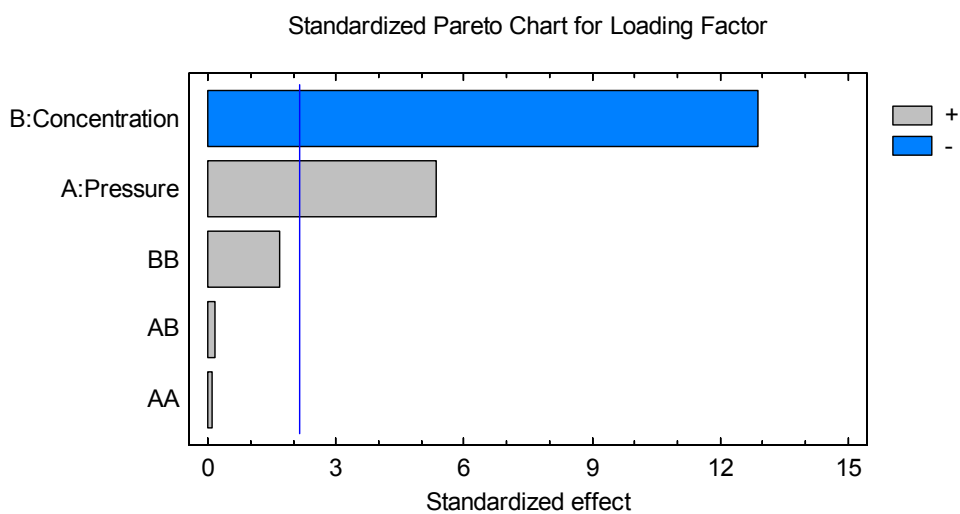
$$\alpha = E_0 + E_1p + E_2C + E_3p^2 + E_4p \cdot C + E_5C^2 \quad \text{Equation 4.13}$$

where α is the CO₂ loading factor; p is the CO₂ partial pressure in kPa; C is the solution concentration in wt. %; E_0 , E_1 , E_2 , E_3 , E_4 , and E_5 are the correlation constants. The equation constant, R^2 and mean absolute error for the equation are presented in Table 4.26. The Pareto charts of the standardized effects of the interaction between each factor affecting loading capacity at temperature 298.15 and 313.15 K are shown in Figure 4.8.

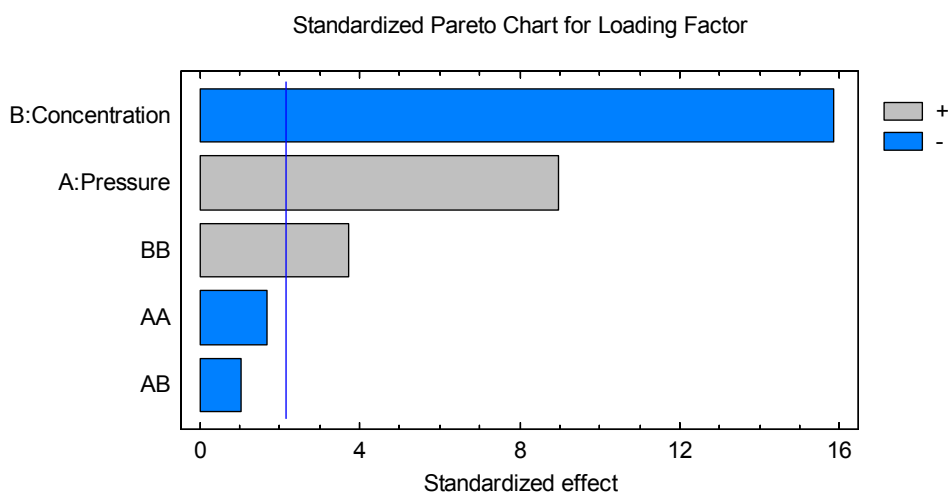
Table 4.26 Correlation coefficient for Equation 4.13

	$T/K = 298.15$	$T/K = 313.15$
E_0	1.5364	1.36425
$10^5 \cdot E_1$	7.63571	22.6614
$10^2 \cdot E_2$	-4.8656	-5.0076
$10^9 \cdot E_3$	2.71429	-32.5714
$10^7 \cdot E_4$	5.28	-20.88
$10^4 \cdot E_5$	8.08	12.08
R^2	93.3731	96.1421
Mean absolute ε	0.03563	0.02191

It can be observed from Figure 4.8 that concentration has the highest effect to CO₂ loading factor. Another factor that has significant effect to CO₂ loading factor is pressure. For temperature 313.15 K, the square of concentration also has significant effect to CO₂ loading factor. It is observed that for the same temperature, the CO₂ loading factor increases with the increase in CO₂ partial pressure but decreases with the increase in sodium glycinate concentration.



(A)



(B)

Figure 4.8 Pareto charts for standardized effects of CO₂ loading factor; (A) 298.15 K; (B) 313.15 K

The loading capacity of aqueous sodium glycinate at 313.15 K is compared with those of Song *et al.* [22] in Figure 4.9. Song *et al.* has studied the solubility of CO₂ in aqueous sodium glycinate solution at low CO₂ partial pressure (up to 200 kPa), while the present study is intended for high pressure CO₂. The present data shows a fair degree of comparison with those of published data.

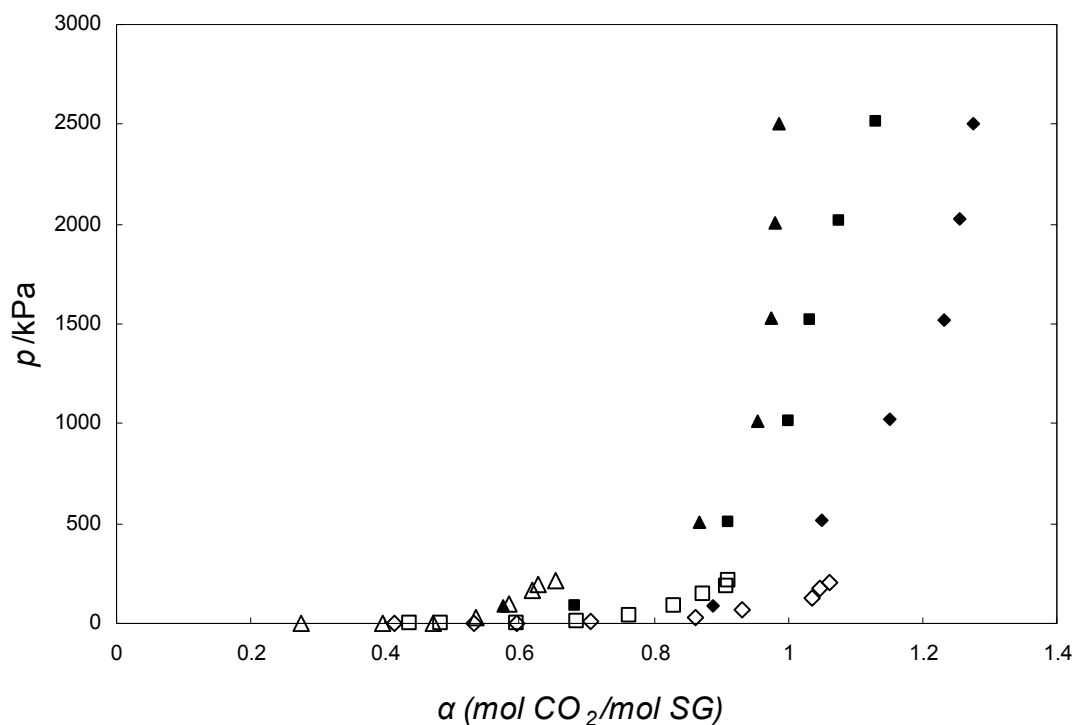


Figure 4.9 Loading capacity of aqueous sodium glycinate (SG) at 313.15 K; ◆, 10 wt. %; ◇, 10 wt. % Song [22]; ■, 20 wt. %; □, 20 wt. % Song [22]; ▲, 30 wt. %; △, 30 wt. % Song [22].

Comparison of loading factor of aqueous sodium glycinate solution with published data for MEA [81] is presented in Figure 4.10. It is found that sodium glycinate has higher loading capacity compared to MEA for the same solution wt. %. This result indicates that aqueous sodium glycinate solution has a good potential as an alternative absorbent for acid gas removal.

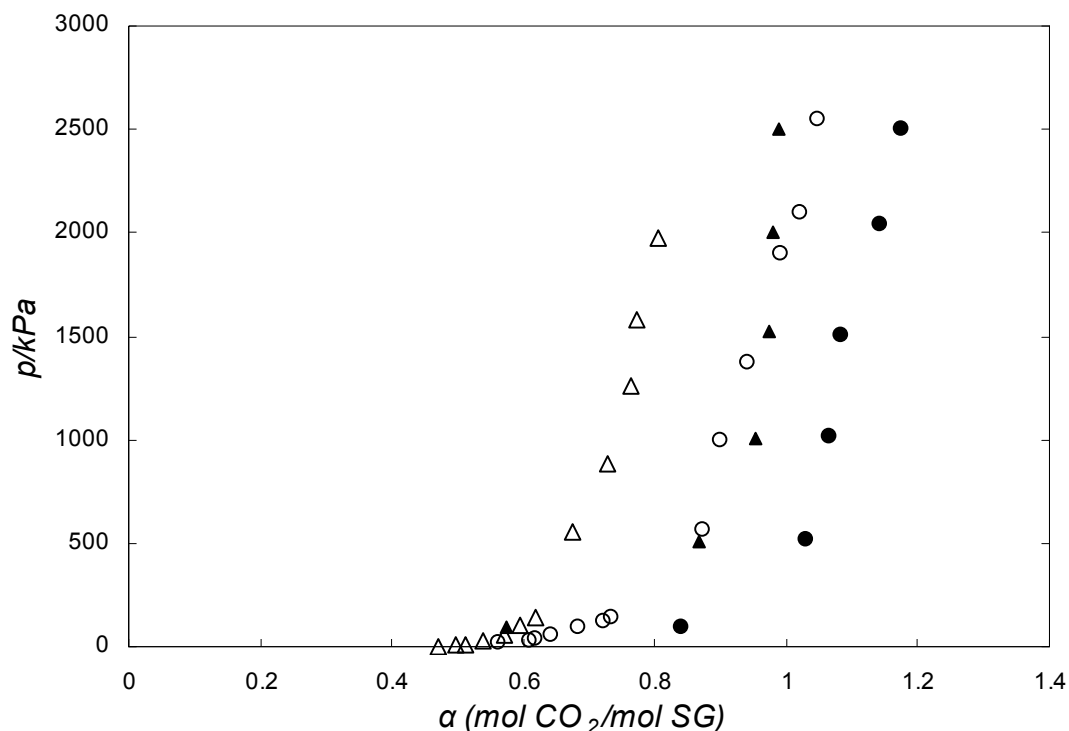


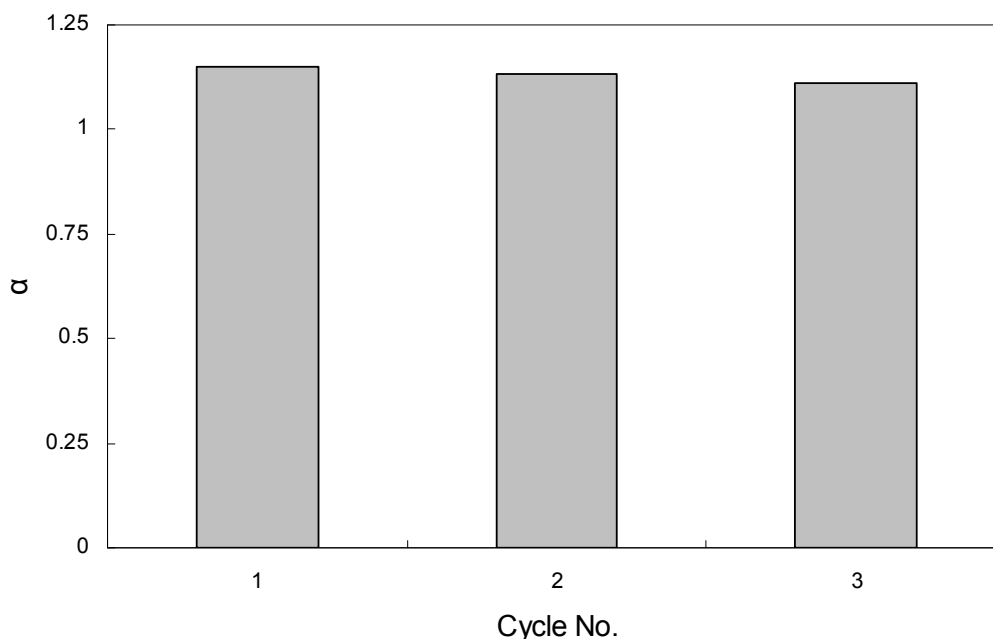
Figure 4.10 Loading capacity of solution at 313.15 K; ●, SG 15 wt. %; ▲, SG 30 wt. %; ○, MEA 15.3 wt. % Shen [81]; △, MEA 30 wt. % Shen [81]

4.9 Regenerability test

Regeneration test result for 10 wt. % sodium glycinate solution is shown in Table 4.27. There is slight reduction in CO₂ loading factor observed during regenerability test. Figure 4.11 shows that the CO₂ loading factor at 1000 kPa and 313.15 K is reduced by 1.65 % and 3.22 % for the second and third cycle respectively. This small loading capacity reduction indicates that aqueous sodium glycinate has a potency to be suitable absorbent for continuous acid gas removal system. However, further investigation should be carried out for various solution concentrations at condition near the actual acid gas removal process condition to get better understanding of aqueous sodium glycinate solution regenerability.

Table 4.27. Solubility of CO₂ during regenerability test

Cycle No.	α (mol CO ₂ /mol SG)	
	Absorption	Desorption
1	1.150	0.675
2	1.131	0.675
3	1.113	-

**Figure 4.11** Loading capacity of 10 wt. % aqueous sodium glycinate (SG) at 1000 kPa and 313.15 K

Some critical fundamental properties of aqueous sodium glycinate solution have been successfully measured. Several correlations have been proposed to quantify the effects of temperature and solution concentration to the solution physical properties. Absorption test and regenerability test results shown that aqueous sodium glycinate solution has a good potential as an alternative absorbent for acid gas removal. Several correlations have also been proposed to quantify the CO₂ loading effect to sodium glycinate physical properties as the function of the unloaded solution physical properties and absorption condition. Some of the results are compared with previous published data and they are in good agreement with the published data. These results will be a valuable addition to the information database that required to supports the absorber design with sodium glycinate as absorbent.

CHAPTER 5

DESIGN OF ABSORPTION PROCESS

5.1 Absorber

Absorber is a term used to identify gas-liquid contactor in which absorption process takes place. Stripping column is another gas-liquid contactor used in natural gas processing for absorbent regeneration purpose. Primary function of gas-liquid contactor is to provide large contact area for the liquid and gas phase under condition that facilitates mass transfer between the two phases.

Tray absorber is a column that utilizes multiple plates to provide gas-liquid contact. Tray absorber is suitable for large installation; clean, non corrosive, non foaming liquids; and low-medium liquid flow application. Figure 5.1 is shows the types of tray that are commonly used in tray absorber. Sieve tray or perforated tray application as gas-liquid contactor has been used since early 1900 [126]. The gas phase would pass through tray perforation and goes into direct contact with the liquid phase that flow across the tray. Several modifications were proposed to increase the performance of the sieve tray such as the change in tray configuration, the use of liquid recirculator and non-circular perforation [127-130]. Bubble cap tray is another type of tray for gas-liquid contactor introduced in 1920's [131]. Bell shape cap is provided to cover perforation hole. The gas goes through the hole into the space inside the cap then bubbling through the slot in the lower edge of the cap. Valve tray, invented by I.E. Nutter in 1955, apply valve mechanism for controlling gas flow with the gas itself being the actuator [132-134]. The valve will rise to provide larger opening for larger gas flow to counter the pressure from liquid above the valve. The valve leg is hooked to the tray to limit the maximum valve opening. Valve trays have been widely used due to its ability to tolerate wider vapour flow range than sieve or bubble cap tray.

Packed absorber applies the use of packing to provide gas-liquid contact area for mass transfer. Packed absorber is suitable for system that needs high mass transfer efficiency and low pressure drop [135]. The early packed absorber column employs random packing which could be easily filled into column. Later, structured packing design has been invented by some manufacturer which is suitable for large scale application. Packed column is generally preferred for small installation, corrosive service, liquid with tendency to foam, very high liquid to gas ratio and application in which a low pressure drop is desired.

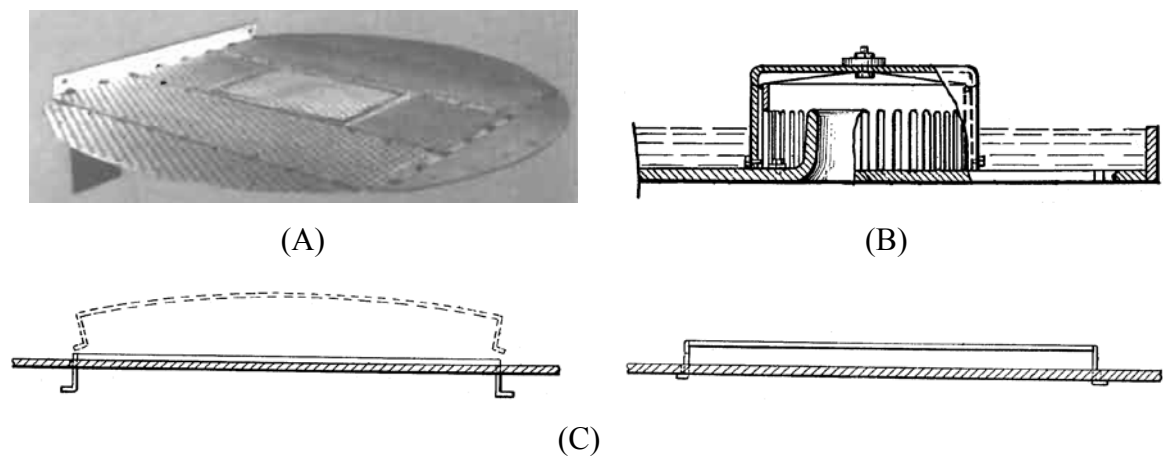


Figure 5.1 Typical commercial tray; (A) Sieve tray (Source: Kohl [5]); (B) Bubble cap tray (Source: Millard [131]); (C) Valve tray (Source: Nutter [133])

Physical properties data of the solvent, such as density, viscosity, heat capacity, and surface tension, and hydraulic behaviour of the column internals are needed in designing an absorber column. Vast amount of literature data are available for flow hydraulic and mechanical design of sieve tray. Chan and Fair [136, 137], Barnicki [138], and Sinnott [139] have outlined design methods for sieve tray absorber. However, available data for valve and packing are limited and are made proprietary by the manufacturer. These types of absorber are designed in consultation with the manufacturer.

5.2 Design of Absorber

The purpose of the design conducted in the work is to indicate on the overall performance of sodium glycinate in actual acid gas removal system compared to commercial absorbent, MEA. The design of the absorber consists of two main parts, the material and energy balance around the absorber and the calculation and provision of absorber diameter and tray geometry. The material and energy balance around absorber is solved to obtain all the flow rate, condition and composition of all streams entering and leaving the absorber. These data is then used to calculate the required absorber diameter and geometry. The material and energy balance calculation around absorber was done based on the simplified design procedure as proposed by Kohl [5]. The calculation for absorber diameter and geometry is done for plate absorber according to method proposed by R.K. Sinnott [139]. The design of the absorber is performed for two different absorbent, *monoetanolamine* (MEA) and sodium glycinate (SG), with the same inlet gas flow rate and composition.

5.3 Material and Energy Balance around Absorber

The material and energy balance calculation around absorber was done based on the simplified design procedure as proposed by Kohl [5]. The procedure was originally meant for calculation of amine system absorber. The calculation for sodium glycinate absorber is done using the same procedure due to the fact that acid gas absorption using both absorbents is categorised as chemical absorption. The data for physical properties of gases, water and *monoetanolamine* are compiled from various sources [5, 24, 121, 141]. The vapour-liquid equilibrium for MEA absorber system is calculated from previously published data [81, 125, 142]. Physical properties and vapour-liquid equilibrium data for sodium glycinate are acquired from the experiment conducted in this work and also from previously published data [22, 108, 110].

5.3.1 Process description

Schematic diagram of heat and material balance for absorber is presented in Figure 5.2. The feed gas is fed to the bottom part of the absorber column. The feed gas could

be hydrocarbon gas, synthesis gas, or flue gas that contains acid gas impurities. Regenerated absorbent or often called 'lean solution' from stripping column enters from the top part of the absorber. The feed gas then contacted with the absorbent in the absorber. The configuration and method of contact between the feed gas and absorbent is dependant on the type of column internal applied in the absorber, whether it is tray or packing. During this contact, the acid gas will be transferred from the feed gas into the absorbent. The exit gas after the absorption process exits from top of the absorber to the next process. This gas is called 'product gas' or 'sweet gas'. The spent solution would leaves from the bottom part of the absorber and sent to the stripping column. This stream is known as 'rich solution'.

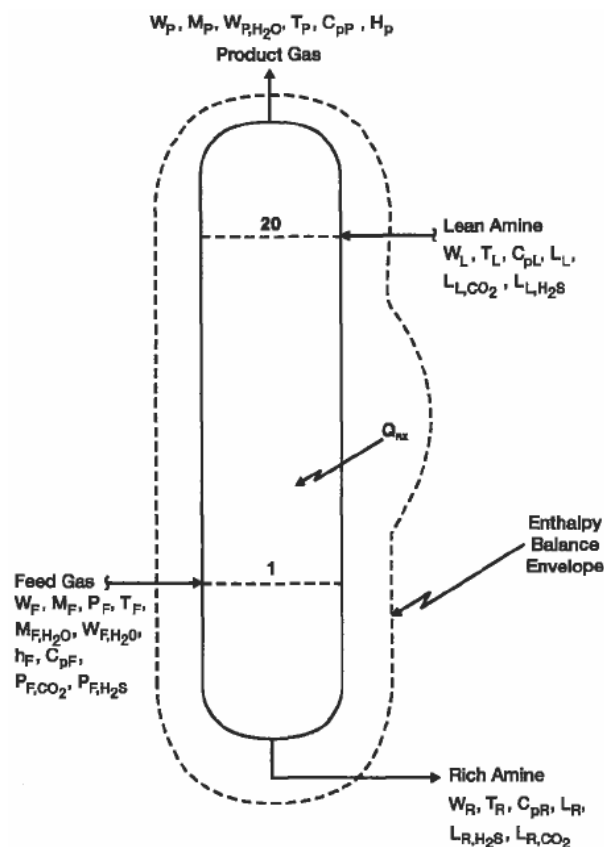


Figure 5.2 Heat and material balance around absorber (source: Kohl [5])

The absorption of acid gas in the process follows few steps [140]. These are as below:

1. Dissolving of acid gas from gas phase into liquid phase
2. Mixing of acid gas with component of liquid phase
3. Reaction of acid gas with component of liquid phase.

During the absorption process, heat is generated and it is known as heat of absorption. Under most circumstances, the heat of absorption would leave the absorber with rich solution except if the feed gas contains low acid gas and/or the concentration of lean solution is high [5].

5.3.2 Calculation method

The material and energy balance calculation around absorber was done based on the simplified design procedure as proposed by Kohl [5]. The basic principle of this approach is maximum acid gas loading occurs on equilibrium of absorbent with feed gas at the bottom of absorber column. Total acid gas removal is another assumption used in this method. The flow diagram showing the calculation method for the material and energy balance around absorber is shown in Figure 5.3. Calculation steps to determine the heat and mass balance around absorber are as follows:

1. Define the inlet regenerated absorbent condition. The required data are absorbent composition, temperature and acid gas loading (mol acid gas/mol absorbent).
2. Specify the feed gas condition. The basic information of feed gas data needed are gas flow rate, temperature, pressure, composition, water vapor content and latent heat of water vapour in feed gas. The feed gas consists of hydrocarbon gas, acid gas and water vapour for natural gas feed. The latent heat of water is determined using the following equation [143]:

$$\Delta H_v = 5.2053 \times 10^7 (1 - T_r)^{0.3199 - 0.212T_r + 0.25795T_r^2} \quad \text{Equation 5.1}$$

$$T_r = \frac{T}{T_c} \quad \text{Equation 5.2}$$

where ΔH_v is latent heat of evaporation in J.kmol^{-1} ; T_r is the reduced temperature; T is the temperature in K; T_c is the critical temperature in K. The critical temperature for water is 647.3 K.

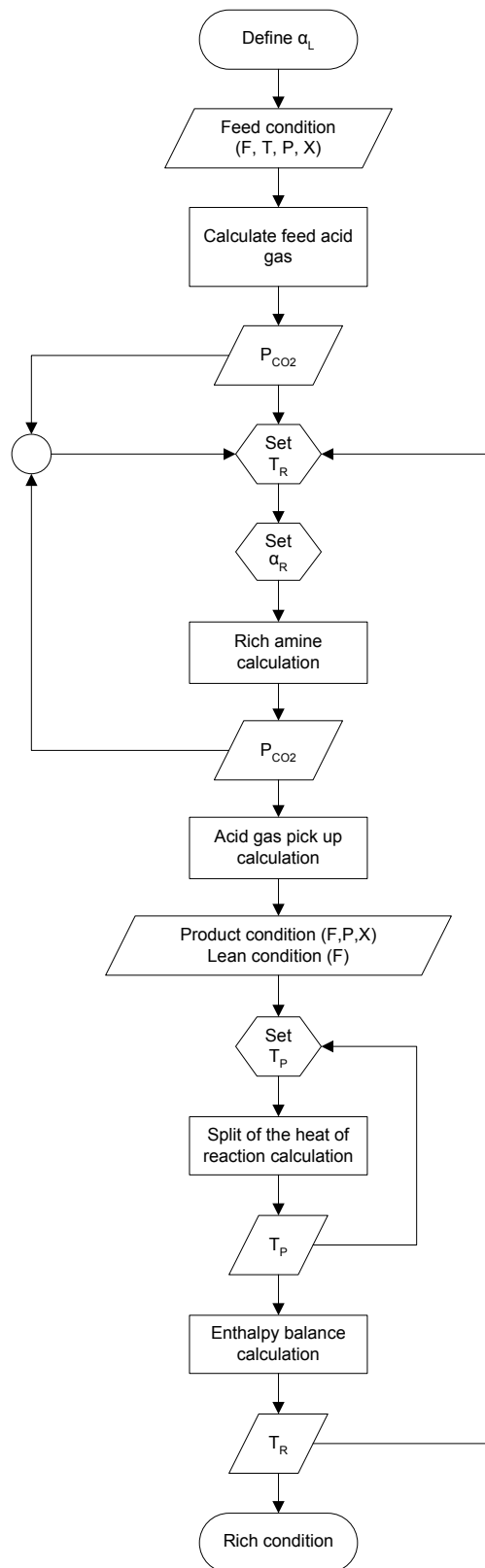


Figure 5.3 Flow diagram for the material and energy balance around absorber

3. Calculate total acid gas content and partial pressure of acid gas in feed gas. Partial pressure of acid gas is a function of feed gas composition and total pressure as shown in Equation 5.3.

$$p_{CO_2} = y_{CO_2} P \quad \text{Equation 5.3}$$

where p_{CO_2} is the partial pressure of carbon dioxide in kPa; y_{CO_2} is the mole fraction of carbon dioxide; P is the total system pressure in kPa.

4. Set initial value for spent solution temperature.
5. Assume acid gas loading of the spent solution. Then calculate the acid gas vapor pressure at spent solution temperature for the assumed acid gas loading. The acid gas vapor pressure at spent solution temperature could be obtained from vapor-liquid equilibrium (VLE) data of the absorbent with acid gas. Due to limitation in available published VLE data, the acid gas vapor pressure at temperature other than temperature of published data could be estimated using the following equation [5]:

$$\ln P_R^o = \ln P_1^o + \left[\frac{\frac{1}{T_1} - \frac{1}{T_R}}{\frac{1}{T_1} - \frac{1}{T_2}} \right] \ln \left(\frac{P_2^o}{P_1^o} \right) \quad \text{Equation 5.4}$$

where P_R^o is the acid gas vapour pressure at spent solution temperature; P_1^o and P_2^o are the acid gas vapour pressure for published data at T_1 and T_2 respectively; T_1 and T_2 are the temperature of published VLE data; T_R is the spent solution temperature. Adjust the acid gas loading until the acid gas vapor pressure is equal to the acid gas partial pressure in the feed gas.

6. Calculate the required inlet flow rate of the regenerated absorbent based on the total acid gas pick up (AGPU) of the absorbent. The total acid gas pick up

(AGPU) is the difference between acid gas loadings of the spent solution and the inlet absorbent.

7. Determine the product gas condition. Since total acid gas removal is assumed in this method, the product gas will consist of only hydrocarbon gases and water vapour. The water content of the product gas is calculated using Raoult's law. This is based on the fact that the product gas is in equilibrium with the inlet absorbent. The water saturation pressure is estimated using Daubert and Danner correlation shown in Equation 5.6 [140].

$$y_i P = x_i P_i^{sat} \quad \text{Equation 5.5}$$

$$\ln P_w^{sat} = D1 + \frac{D2}{T} + D3 \ln T + D4 T^{D5} \quad \text{Equation 5.6}$$

where x is the mole fraction in liquid phase; y is the mole fraction in gas phase; P is the total pressure in Pa; P^{sat} is the saturation pressure in Pa; T is the temperature in K; D1, D2, D3, D4, and D5 are the equation coefficients. Coefficient constant for Equation 5.6 is tabulated in Table 5.1.

Table 5.1 Coefficient constant for Equation 5.6 [140]

	Water
D1	72.55
D2	-7206.7
D3	-7.1385
D4	4.046e-6
D5	2.0

8. Calculate the heat of absorption, Q_{abs} . The heat of absorption is calculated by multiplying the enthalpy of absorption, ΔH_{abs} , with the amount of acid gas absorbed. The enthalpy of absorption could be estimated from the vapour-liquid equilibrium (VLE) data using Classius-Clapeyron correlation.

$$\left[\frac{\partial \ln p}{\partial (1/T)} \right]_{\alpha} = \frac{\Delta H_{abs}}{R} \quad \text{Equation 5.7}$$

where p is the acid gas partial pressure in kPa; T is the temperature in K; ΔH_{abs} is the heat of absorption in $\text{J}\cdot\text{mol}^{-1}$; R is the ideal gas constant. Heat of absorption data for MEA system is available in the literature [5, 144].

9. Calculate the latent heat of vaporisation for water. The amount of water evaporated or condensed depends on the difference in water content of feed gas and product gas.
10. Calculate the actual spent solution temperature based on enthalpy balance around absorber. Enthalpy balance around absorber could be expressed using the following equation:

$$m_F cp_F (T_F - T_{\text{ref}}) + m_L cp_L (T_L - T_{\text{ref}}) + Q_{\text{abs}} + Q_{H_2O} = m_R cp_R (T_R - T_{\text{ref}}) + m_P cp_P (T_P - T_{\text{ref}}) \quad \text{Equation 5.8}$$

where m_F is the feed gas flowrate; m_L is the inlet absorbent flowrate; m_R is the spent solution flowrate; m_P is the product gas flowrate; cp_F is the feed gas heat capacity; cp_L is the inlet absorbent heat capacity; cp_R is the spent solution heat capacity; cp_P is the product gas heat capacity; T_F is the feed gas temperature; T_L is the inlet absorbent temperature; T_R is the spent solution temperature; T_P is the product gas temperature; T_{ref} is the reference temperature; Q_{abs} is the heat of absorption; Q_{H_2O} is the heat of water evaporation or condensation. Equation 5.8 could be simplified by specify reference temperature equal with feed gas temperature. The actual temperature of the spent solution could be calculated from Equation 5.9.

$$T_R = \frac{m_L cp_L (T_L - T_F) - m_P cp_P (T_P - T_F) + Q_{\text{abs}} + Q_{H_2O}}{m_R cp_R} + T_F \quad \text{Equation 5.9}$$

11. Compare the actual temperature of the spent solution with initial value from step 4. Perform iterated calculation to adjust the actual temperature to be equal to the initial value.

5.3.3 Design parameter

The case study is performed for two different absorbents, *monoethanolamine* (MEA) and sodium glycinate (SG), with the same inlet gas flow rate and composition. The condition and composition of the feed gas is presented in Table 5.2. The feed gas for the absorber column is assumed to be mixture of methane, carbon dioxide and water at saturated condition. The absorbents used for this case study are monoethanolamine with concentration of 15.3 wt. % and sodium glycinate with concentration of 15 wt. %. The CO₂ loading of regenerated MEA is 0.12 mol CO₂/mol MEA, based on data by Fitzgerald and Richardson [5]. There are no available data on CO₂ loading of regenerated absorbent for sodium glycinate. Therefore for calculation purpose it is assumed to be equal with CO₂ loading of regenerated MEA.

Table 5.2 Feed gas condition and composition

Feed gas condition	Value
Pressure	2000 kPa
Temperature	313.15 K
Molar Flowrate	1000 kmol.h ⁻¹
Mass Flowrate	21644 kg.h ⁻¹
Molecular weight	21.644 kg.kmol ⁻¹
Composition/ % mol	
CH ₄	79.59
CO ₂	20.00
H ₂ O	0.41

5.4 Diameter of Absorber Calculation

The absorber type used for this study is sieve tray absorber. Sieve tray absorber was chosen because tray absorber is widely used for acid gas removal process and the availability of data and methods for its design. The available data for design of packed absorber is limited and usually proprietary to the manufacturer. The calculation for absorber diameter and geometry is done for plate absorber according to method proposed by R.K. Sinnott [139]. The calculation is based on trial and error approach

using empirical correlation and some rule of thumb. All stream flow rate and properties used is calculated in previous section. Flow diagram for diameter of absorber calculation is shown in Figure 5.4.

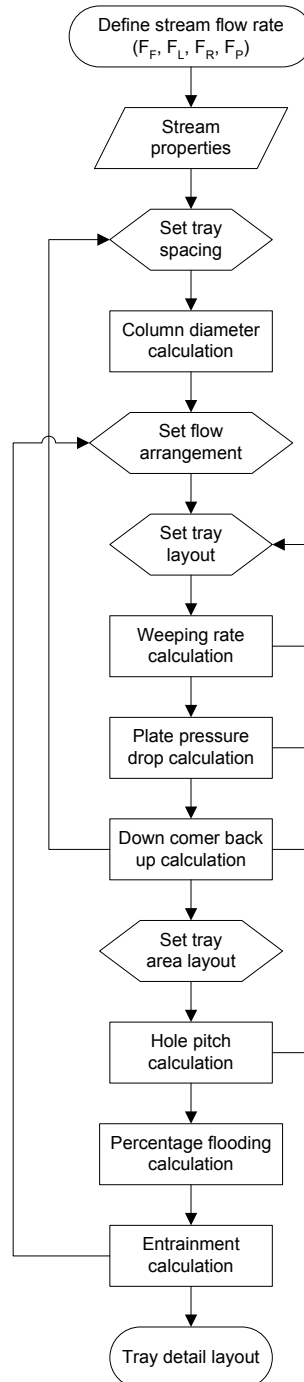


Figure 5.4 Flow diagram for diameter of absorber calculation

5.4.1 Calculation method

Typical design procedure for tray design is as follows [139]:

1. Calculate the maximum and minimum vapour and liquid flow rate for turn down ratio. Turndown ratio is the ratio of minimum or maximum allowable flowrate to the design flowrate, in which the process could operate without affecting its performance.

2. Collect or estimate the system physical properties.

3. Select trial plate spacing.

Tray spacing is the distance between two consecutive trays. Tray spacing will depend on column diameter, operating condition, tray arrangement and maintenance access.

4. Estimate the column diameter based on flooding consideration.

Flooding consideration is depends on the minimum vapour velocity where flooding started to occur or usually called flooding velocity. Vapour velocity ranged from 70 to 90 % flooding velocity would be normally used. Flooding velocity can be estimated from correlation by Fair [145]:

$$u_f = K_1 \left(\frac{\rho_L - \rho_G}{\rho_G} \right)^{0.5} \quad \text{Equation 5.10}$$

where u_f is the flooding velocity in m.s^{-1} ; ρ_L is the liquid density in kg.m^{-3} ; ρ_G is the gas density in kg.m^{-3} ; K_1 is the equation constant. The value of K_1 could be obtained from Figure 5.5 for liquid with surface tension, σ , 0.02 N/m.

5. Decide the liquid flow arrangement.

The liquid flow on tray would depend on the column diameter and liquid flow rate. Double pass, single pass and reverse flow are the typical liquid flow arrangement for tray contactor. Single pass flow is used in this study.

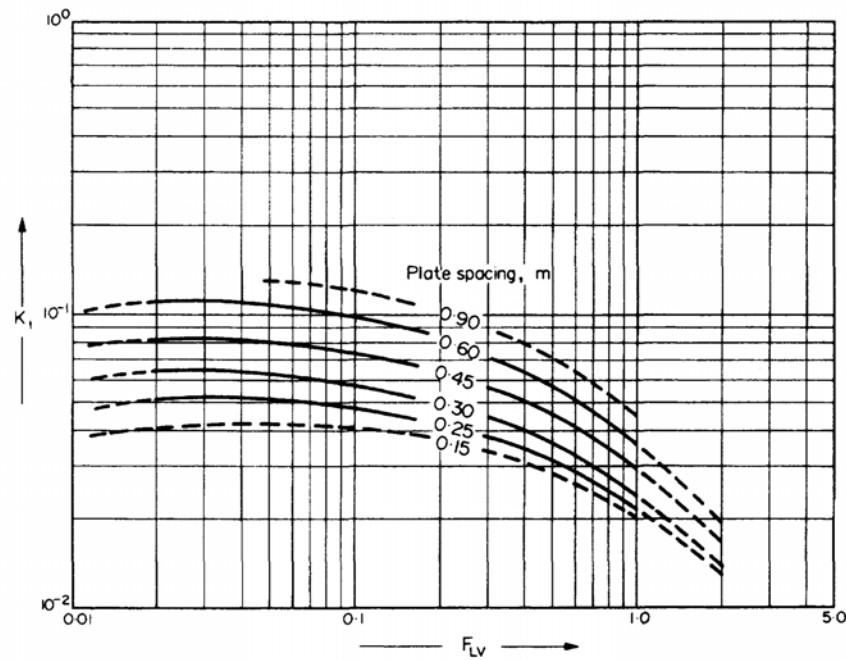


Figure 5.5 Flooding velocity constant for sieve tray [145]

6. Make trial plate layout. The layout include downcomer area, active area, hole area, hole size, and weir height.

Several terms are used to describe the areas in a tray. Typical tray layout is shown in Figure 5.6. Column area, A_c , is area of column based on column diameter, D_c . Downcomer area, A_d , is the area of downcomer which depend on the weir length. Downcomer area could be calculated from ratio of downcomer width, l_d , to column diameter using empirical correlation for cylindrical height and area conversion [146]. Correlation between column diameter, downcomer wide, column area and downcomer area is shown in Equation 5.11.

$$\frac{A_d}{A_c} = \frac{-4.75593 \times 10^{-5} + 0.174875 \left(\frac{l_d}{D_c} \right) + 5.668973 \left(\frac{l_d}{D_c} \right)^2 - 4.916441 \left(\frac{l_d}{D_c} \right)^3 - 0.145348 \left(\frac{l_d}{D_c} \right)^4}{1.0 + 3.924091 \left(\frac{l_d}{D_c} \right) - 6.358805 \left(\frac{l_d}{D_c} \right)^2 + 4.018448 \left(\frac{l_d}{D_c} \right)^3 - 1.801705 \left(\frac{l_d}{D_c} \right)^4}$$

Equation 5.11

where A_d , is the downcomer area in m; A_c , is the column area in m; l_d is the downcomer width in m; D_c is the column diameter in m. Net area, A_n , is the column area minus by downcomer area. Active area, A_a , is the net area minus inlet

downcomer area or equal with column are minus two downcomer areas. Downcomer subtended angle, θ_c , and weir length could be determined geometrically from downcomer width and column diameter. The weir height normally around 40 to 90 mm for column operated above atmospheric pressure.

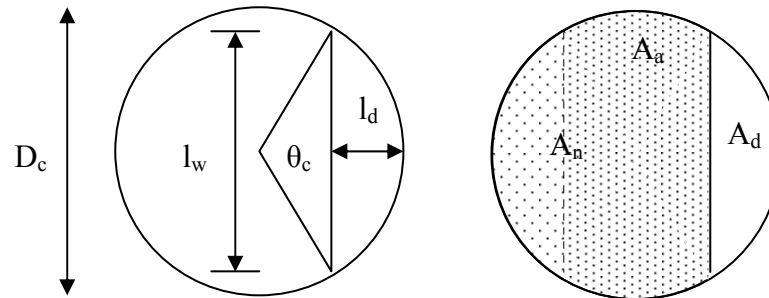


Figure 5.6 Tray layout

7. Check weeping rate, if unsatisfactory return to step 6.

Lockett [147] proposed method to find the position of weep point based weep flux data. Effect of the hole gas velocity is expressed as Froude number. Correlation between weep flux and Froude number is shown in Equation 5.12. Weep point occurs at weep flux equal to zero.

$$WF = 0.020Fr^{-1} - 0.030 \quad \text{Equation 5.12}$$

$$Fr = u_h \left(\frac{\rho_G}{gh_{cl}\rho_L} \right)^{0.5} \quad \text{Equation 5.13}$$

where WF is the weep flux in $\text{m}^3 \cdot \text{m}^{-2} \cdot \text{s}^{-1}$; Fr is the Froude number; u_h is the hole gas velocity in $\text{m} \cdot \text{s}^{-1}$; ρ_L is the liquid density in $\text{kg} \cdot \text{m}^{-3}$; ρ_G is the gas density in $\text{kg} \cdot \text{m}^{-3}$; g is the gravity acceleration in $\text{m} \cdot \text{s}^{-2}$; h_{cl} is the clear liquid head in m.

8. Check plate pressure drop, if unsatisfactory return to step 6.

Tray pressure drop, h_t , has been modelled as the sum of three component parts, the dry tray pressure drop, the clear liquid head and the residual head loss. The dry tray pressure drop could be calculated from Equation 5.15. Equation 5.16 is shown the correlation for residual head. The value for effective open area, β , and orifice coefficient, ϵ , for normal tray is proposed to be 0.079 and 1.86 [130]. The

height of liquid crest over the weir is calculated from Francis weir equation shown in Equation 5.17 [139].

$$h_t = h_{dry} + h_{cl} + h_{residual} \quad \text{Equation 5.14}$$

$$h_{dry} = \frac{\epsilon \rho_G u_s^2}{2 \rho_L g} \left(\frac{1}{\beta^2} - 1 \right) \quad \text{Equation 5.15}$$

$$h_{residual} = \frac{4\sigma}{d_h \rho_L g} \quad \text{Equation 5.16}$$

$$h_{ow} = 750 \left[\frac{L_w}{\rho_L l_w} \right] \quad \text{Equation 5.17}$$

where h_t is the tray pressure drop in m; h_{dry} is the dry tray pressure drop in m; h_{cl} is the clear liquid head in m; $h_{residual}$ is the residual head pressure drop in m; u_s is the superficial gas velocity in m.s^{-1} ; ϵ is the orifice coefficient; ρ_G is the gas density in kg.m^{-3} ; β is the effective open area; g is the gravity acceleration in m.s^{-2} ; ρ_L is the liquid density in kg.m^{-3} ; σ is the liquid surface tension in N.m^{-1} ; d_h is the hole diameter in m; L_w is the liquid flowrate in kg.s^{-1} ; l_w is the weir height in m.

9. Check downcomer back up, if too high return to step 6 or step 3.

Downcomer back up could be calculated using Equation 5.18. The head loss in downcomer, h_{dc} , could be estimated using correlation by Cicalese shown in Equation 5.19 [139]. The clearance area under downcomer, A_{ap} , is calculated using Equation 5.20. The height of the bottom edge of the apron above the tray, h_{ap} , is normally set at 5 to 10 mm below weir height.

$$h_b = h_w + h_{ow} + h_t + h_{dc} \quad \text{Equation 5.18}$$

$$h_{dc} = 166 \left(\frac{L_{wd}}{\rho_L A_m} \right)^2 \quad \text{Equation 5.19}$$

$$A_{ap} = h_{ap} l_w \quad \text{Equation 5.20}$$

where h_b is the downcomer backup in m; h_w is the weir height in m; h_{ow} is the liquid crest over the weir in m; h_t is the tray pressure drop in m; h_{dc} is the head loss in the downcomer in m; L_{wd} is the liquid flow rate in downcomer in $\text{kg}\cdot\text{s}^{-1}$; ρ_L is the liquid density in $\text{kg}\cdot\text{m}^{-3}$; A_m is minimum value between downcomer area or clearance area under downcomer in m^2 ; A_{ap} is the clearance area under downcomer in m^2 ; h_{ap} is the height of the bottom edge of the apron above the tray in m.

10. Decide plate layout detail. Detail plate layout includes calming zone and unperforated areas. Check hole pitch, if unsatisfactory return to step 6.

The available active area calculated from plate design above could not fully utilize as perforation area due to some obstruction caused by structural components, such as tray support rings and beams, and due to the need of calming zone. Hole pitch is the centre to centre distance between to holes in the sieve tray based on hole configuration. Equilateral triangular pattern is preferred to be used. Correlation between hole area with perforated area for equilateral triangular pitch is presented in Equation 5.21.

$$\frac{A_h}{A_p} = 0.9 \left[\frac{d_h}{l_p} \right]^2 \quad \text{Equation 5.21}$$

where A_h is the hole area; A_p is the perforated area; d_h is the hole diameter; l_p is the hole pitch.

11. Recalculate the percentage of flooding based on chosen column diameter.
12. Check entrainment, if too high return to step 4.

Commercial sieve tray for non foaming system usually operated between froth regime and spray regime. Basic correlation by Hunt for calculating uniform froth regime entrainment is provided in Equation 5.22 [148].

$$E = 3.08 \times 10^5 \left(\frac{u_s}{S - 2.5h_c} \right)^{3.2} \left(\frac{73}{\sigma} \right) \quad \text{Equation 5.22}$$

where u_s is the superficial gas velocity in m.s^{-1} ; S is the tray spacing in mm; h_c is the froth regime clear liquid height in mm; σ is the liquid surface tension in dyne.cm^{-1} .

13. Optimize design. Repeat steps 3 to 12 to obtain acceptable smallest diameter and tray spacing.

14. Finalize design. Sketch plate layout and state tray specification.

5.4.2 Design parameter

The absorber diameter calculation is based on empirical correlation and some rule of thumb. Rule of thumb is principle with broad application that is not intended to be strictly accurate or reliable for every situation. Therefore trial and error approach is applied in conjunction with boundary criterion to achieve satisfactory result. Some rule of thumb and criterion applied in the absorber diameter calculation for both MEA and sodium glycinate systems are listed in Table 5.3.

Table 5.3 Rule of thumb and criterion for absorber design

Feed gas condition	Value
Tray Spacing	0.9 m
Flooding design factor	0.85
Liquid flow arrangement	single
Hole area design factor	0.08
Hole pitch type	Equilateral Triangular
Hole size	0.005 m
Weir height	0.05 m
Entrainment regime	Froth

5.5 Absorber Design Result

The result for absorber design is presented in Table 5.4. Detail calculation for the design of absorber is explained in Appendix A. The required inlet absorbent for sodium glycinate absorber is slightly lower compared to MEA due to the higher loading capacity of sodium glycinate. This higher acid gas loading is caused by two factors, the solubility of carbon dioxide and spent solution temperature. As previously mentioned in section 4.8, sodium glycinate has higher loading capacity compared to MEA for the same solution wt. % at the same temperature. It is also found that loading capacity decreases as the temperature increases. The calculation result shows that the temperature of MEA spent solution is higher than sodium glycinate therefore the loading capacity of MEA is lower than sodium glycinate.

The temperature of spent solution is dependant on the heat of absorption and its heat capacity. From the calculation, it is found that the heat of absorption for MEA system is higher than sodium glycinate. The heat of absorption of MEA system is 1.7×10^7 kJ.h⁻¹ compared to 3.2×10^6 kJ.h⁻¹ for sodium glycinate. The heat capacity of spent solution of MEA is lower than sodium glycinate but due to its high heat of absorption, the spent solution temperature for MEA system is higher compared to sodium glycinate.

The required absorber column diameter using sodium glycinate as the solvent is found to be slightly smaller than the one using MEA as solvent. This is highly affected by the lower required solution for absorption in sodium glycinate system. The required inlet absorbent for sodium glycinate absorber is 152768.1 kg.h⁻¹ while MEA inlet flowrate is 155035.2 kg.h⁻¹. Some physical properties, such as density and surface tension, also affect the absorber diameter size. The density of MEA is lower than sodium glycinate. It means the volumetric flowrate of MEA is higher than sodium glycinate for the same solution mass and this will increase the required absorber diameter. The surface tension of MEA is higher than sodium glycinate. Surface tension of the solution will affect the pressure drop of the tray. Higher surface tension would result in higher tray pressure drop. High tray pressure drop is undesirable to the

process therefore a larger absorber diameter is needed to reduce the tray pressure drop. Based on the study case it could be concluded that overall performance of aqueous sodium glycinate as absorbent for acid gas removal system is comparable with commercial absorbent, MEA. This result is only serves as estimation and there are other parameters that required to be accommodated for the design of actual absorber such as feed quality, other impurities that exist in the system, stability of the solution system, etc. Nevertheless, these results show that sodium glycinate could be a potential alternative absorbent for acid gas removal.

Table 5.4 Absorber design parameter

Absorber Parameter	Value	
	Monoethanolamine	Sodium glycinate
Inlet absorbent		
Mass flowrate (kg.h ⁻¹)	155035.2	152768.1
Temperature (K)	318.71	318.71
Composition		
Absorbent (wt. %)	15.30	15.00
H ₂ O (wt. %)	84.70	85.00
Product gas		
Mass flowrate (kg.h ⁻¹)	12768.6	12768.6
Temperature (K)	318.71	318.71
Spent solution		
Mass flowrate (kg.h ⁻¹)	163911.1	161644.0
Temperature (K)	346.00	323.71
Composition		
Absorbent (wt. %)	14.47	14.18
H ₂ O (wt. %)	80.16	80.38
Acid gas (wt. %)	5.37	5.45
Absorber diameter (m)	1.17	1.14

CHAPTER 6

CONCLUSION AND RECOMMENDATION

6.1 Conclusion

The potential of sodium glycinate as absorbent for acid gas absorption has been investigated in this study. Some critical fundamental properties of aqueous sodium glycinate are measured for a range of concentration namely 1, 5, 10, 15, 20 and 30 wt. % at various temperatures. Density, kinematic viscosity, heat capacity, refractive index, acidity, conductivity, surface tension and contact angle with stainless steel surface of aqueous sodium glycinate are measured and reported. Density, of aqueous sodium glycinate solution is found to increase with concentration and decrease with temperature. Similar trend also found for the measured data on solution kinematic viscosity. The heat capacity of aqueous sodium glycinate is found to decrease with concentration but increases with temperature. The solution refractive index increases with concentration but decrease with temperature. Concentration increment gives positive effect to acidity and conductivity of sodium glycinate solution. Surface tension of aqueous sodium glycinate solution is found to increase with concentration. The contact angle between aqueous sodium glycinate solutions with stainless steel surface is found to be lower than 90°. Thus, it could be considered that the solution has a tendency to wet the stainless steel surface.

Absorption test to measure the solubility of carbon dioxide in aqueous sodium glycinate is conducted using SOLTEQ BP-22 High Pressure Solubility Cell. The solubility of CO₂ in aqueous solution of sodium glycinate is measured for the CO₂ partial pressure ranging from 100 to 2500 kPa at temperatures of 298.15 and 313.15 K. It was observed that loading capacity increases with an increase in partial pressure of CO₂ but decreases with increase in sodium glycinate concentration and temperature. Sodium glycinate is found to has higher loading capacity compared to *monoethanolamine* (MEA) for the same solution wt. %.

Regenerability test to investigate the regenerability of sodium glycinate has also been conducted using the same equipment. In the actual acid gas absorption process, the

absorbent would undergo continuous absorption-desorption cycle. Therefore to imitate this continuous absorption-desorption process, in the regenerability test the same sodium glycinate solution is subjected to several CO₂ absorption-desorption cycle of process. The test result shows slight reduction in CO₂ loading capacity of regenerated sodium glycinate solution. This result indicates that aqueous sodium glycinate is suitable as absorbent for continuous acid gas removal system.

In order to quantify the effect of CO₂ loading on the physical properties of absorbent, the physical properties of CO₂-loaded absorbent are measured. Hence in this present work, the density, kinematic viscosity, heat capacity, acidity, and conductivity of aqueous sodium glycinate after CO₂ absorption are measured and reported. Several correlations have been proposed to quantify the CO₂ loading effect to sodium glycinate physical properties as the function of the unloaded solution physical properties and absorption condition. In general, the CO₂ loading increases the density and kinematic viscosity of aqueous sodium glycinate solution. Heat capacity, acidity and conductivity of aqueous sodium glycinate solution are found to decrease with CO₂ loading.

Case study comparing absorber design of *monoethanolamine* and sodium glycinate is done to give overview of the overall performance of sodium glycinate in actual acid gas removal system compared to commercial absorbent, MEA. It is observed that the required solution flowrate for sodium glycinate absorber is slightly lower than MEA. The calculated absorber diameter for sodium glycinate is smaller compared to MEA. The result only serves as estimation and there are other parameters that required to be accommodated for the design of actual absorber such as feed quality, other impurities that exist in the system, stability of the solution system, etc. Nevertheless, these results show that sodium glycinate could be a potential alternative absorbent for acid gas removal.

6.2 Recommendation

Based on the outcome of the study, sodium glycinate has shown great potential alternative absorbent for acid gas removal. Some future studies are needed to give further insight of the actual capability of sodium glycinate as acid gas absorbent. Solubility of other gases, especially gases that present in natural gas, in sodium glycinate solution is requires to be investigated. The effects of these gases to the physical properties of sodium glycinate solution after absorption are also need to be studied. Solubility of those gases at higher solution concentration, in which precipitation might occurs, also needed to be studied. The effect of amino acid precipitation phenomena to the performance of sodium glycinate solution is another interesting subject to be explored. The absorption kinetic and mechanism at condition near actual natural gas condition are another major problem that needs to be investigated. Comprehensive knowledge on these data would give better understanding of the potential of sodium glycinate solution as acid gas absorbent for natural gas. Regeneration system for acid gas contained sodium glycinate solution is another matter that needs further investigation. With the knowledge on the regeneration system, the actual solution flowrate and energy consumption of the system could be estimated. Thus the application of sodium glycinate solution in continuous acid gas removal system could be realized.

REFERENCES

1. British Petroleum, Statistical Review of World Energy 2008, www.bp.com/productlanding.do?categoryId=6929&contentId=7044622
2. Energy Information Administration, U.S. Department of Energy, Malaysia Energy Data, http://tonto.eia.doe.gov/country/country_energy_data.cfm?fips=MY
3. Busby, R. L. *Natural Gas in Non Technical Language*; PennWell: Oklahoma, 1999.
4. McCain, W.D. Jr. *Properties of Petroleum Fluids*, 2nd ed.; Pennwell: Oklahoma, 1990.
5. Kohl, A.; Nielsen, R. *Gas Purification*, 5th ed.; Gulf Publishing Company: Texas, 1997.
6. Li, M.H.; Shen, K.P. Calculation of Equilibrium Solubility of Carbon Dioxide in Aqueous Mixtures of Monoethanolamine with Methyldiethanolamine. *Fluid Phase Equilibria* **1993**, *85*, 129-140.
7. Posey, M.L.; Tapperson, K.G.; Rochelle, G.T. A Simple Model for Prediction of Acid Gas Solubilities in Alkanolamines. *Gas. Sep. Purif.* **1996**, *vol. 10 no.3*, 181-186.
8. Dallos, A; Altsach, T; Kotsis, L. Enthalpies of Absorption and Solubilities of Carbon Dioxide in Aqueous Polyamines Solution. *Journal of Thermal Analysis and Calorimetry* **2001**, *65*, 419-423.
9. Liao, H.L.; Li, M.H. Kinetics of Absorption of Carbon Dioxide into Aqueous Solutions of Monoethanolamine + N-methyldiethanolamine. *Chemical Engineering Science* **2002**, *57*, 4569-4582.

10. Sun, W. C.; Yong, C. B.; Li, M. H. Kinetics of the Absorption of Carbon Dioxide into Mixed Aqueous Solutions of 2-amino-2-methyl-1-propanol and Piperazine. *Chemical Engineering Science* **2005**, *60*, 503-516.
11. Arcis, H.; Rodier, L.; Coxam, J. Y. Enthalpy of Solution of CO₂ in Aqueous Solutions of 2-amino-2-methyl-1-propanol. *J. Chem Thermodynamics* **2007**, *39*, 878-887.
12. Hook, R. J. An Investigation of Some Sterically Hindered Amines as Potential Carbon Dioxide Scrubbing Compounds. *Ind. Eng. Chem. Res.* **1997**, *36*, 1779-1790.
13. Kirk, O. *Kirk-Othmer Encyclopedia of Chemical Technology*, 5th ed.; John Wiley & Sons: 2001.
14. Cheremisinoff, N. P. *Handbook of Hazardous Chemical Properties*; Butterworth-Heinemann: Boston 2000.
15. Martin, W. F.; Lippit, J. M.; Webb, P. J. *Hazardous Waste Handbook for Health and Safety*, 3rd ed.; Butterworth-Heinemann: Boston 2000.
16. Kumar, P. S.; Hongendoorn, J. A.; Versteeg, G. F.; Veron, P. H. M. Density, Viscosity, Solubility and Diffusivity of N₂O in Aqueous Amino Acid Salt Solutions. *J. Chem. Eng. Data* **2001**, *46*, 1357-1361.
17. Yan, S. P.; Fang, M. X.; Zhang, W. F.; Wang, S. Y.; Xu, Z. K.; Luo, Z. Y.; Cen, K. F. Experimental Study on the Separation of CO₂ from Flue Gas using Hollow Fiber Membrane Contactor without Wetting. *Fuel Processing Technology* **2007**, *88*, 501-511.
18. Kumar, P.S.; Hongendoorn, J.A.; Versteeg, G.F.; Veron, P.H.M. New Absorption Liquid for the Removal of CO₂ from Dilute Gas Streams using Membrane Contactors. *Chem. Eng. Science* **2002**, *57*, 1639-1651.

19. Chen, H.; Kovvali, A. S.; Sirkar, K. K. Selective CO₂ Separation from CO₂-N₂ Mixtures by Immobilized Glycine-Na-Glycerol Membranes. *Ind. Eng. Chem. Res.* **2000**, *39*, 2447-2458.
20. Chen, H.; Obuskovic, G.; Majumdar, S.; Sirkar, K. K. Immobilized Glycerol-based Liquid Membrane in Hollow Fibers for Selective CO₂ Separation from CO₂-N₂ mixtures. *Journal of Membrane Science* **2001**, *183*, 75-88.
21. Murdoch, K.; Thibaud-Erkey, C.; Sirkar, K. K. Membrane based CO₂ removal from Spacesuit.
<http://www.dsls.usra.edu/meeting/bio2001/pdf/session/abstracts/138p.pdf>
22. Song, H. J.; Lee, S.; Maken, S.; Park, J. J.; Park, J. W. Solubilities of Carbon Dioxide in Aqueous Solutions of Sodium Glycinate. *Fluid Phase Equilibria* **2006**, *246*, 1-5.
23. Aller, M. *Environmental Engineers' Handbook*; CRC Press: Florida, 1999.
24. Gas Processors Suppliers Association. *GPSA Engineering Data Book*, 11th edition; Gas Processors Association: Oklahoma, 1998.
25. SM's e-Home, Solvent Selection.
http://www.separationprocesses.com/Absorption/GA_Chp03d.htm.
26. Speer, F.W., Jr. Gas Purification Process. U.S. Patent No. 1,533,773, 1925.
27. Shaw, J.A. Separation and Purification of Gaseous Mixture. U.S. Patent No. 2,028,124, 1936.
28. Rosenstein, L. Process for Recovering the Sulphur Content of Gases. U.S. Patent No. 1,945,163, 1934.

29. Rosenstein, L. Recovery and Conversion of the Sulphur Content of Industrial Gases. U.S. Patent No. 2,107,907, 1938.
30. Speer, F.W., Jr. Process of Producing Alkali Metal Solution. U.S. Patent No. 1,542,971, 1925.
31. Speer, F.W., Jr. Gas Purification process. U.S. Patent No. 1,653,933, 1927.
32. Speer, F.W., Jr. Gas Purification process. U.S. Patent No. 1,806,370, 1931.
33. Speer, F.W., Jr. Apparatus for Treating Gases. U.S. Patent No. 1,809,646, 1931.
34. Benson, H.E. Method for Separating CO₂ and H₂S from Gas Mixtures, U.S. Patent No. 2,886,405, 1959.
35. Astarita, G.; Savage, D.W.; Longo, J.M. Promotion of CO₂ Mass Transfer in Carbonate Solutions. *Chemical Engineering Science* **1981**, *36*, 581-588.
36. Williamson R.V.; Mathews, J.H. Rate of Absorption and Equilibrium of Carbon Dioxide in Alkaline Solutions. *Ind. Eng. Chem.* **1924**, *16*, 1157-1161.
37. Bresler, S.A.; Francis, A.W. Process for Removal of Acid Gas from Gas Streams. U.S. Patent No. 3,101,996, 1963.
38. Benson, H. E. Separation of CO₂ and H₂S from Gas Mixtures. U.S. Patent No. 3,563,695, 1971.
39. Benson, H. E. Separation of CO₂ and H₂S from Gas Mixtures. U.S. Patent No. 3,563,696, 1971.
40. Shrier, A.L.; Danckwert, P.V. Carbon Dioxide Absorption into Amine-Promoted Potash Solutions. *Ind. Eng. Chem. Fundam.* **1969**, *8*, 415-423.

41. Sartori, G.; Savage, D.W. Sterically Hindered Amines for Carbon Dioxide Removal from Gases. *Ind. Eng. Chem. Fundam.* **1983**, *22*, 239-249.
42. Field, J.H; Bienstock, D. Method of Inhibiting Corrosion in Purifying Gases. U.S. Patent No. 3,181,929, 1965.
43. Field, J.H. Separation of CO₂ from gas mixtures. U.S. Patent No. 3,907,969, 1975.
44. Mago, B.F. Corrosion Inhibition of Aqueous Potassium Carbonate Gas Treating System. U.S. Patent No. 3,951,844, 1976.
45. Giammarco, G. Method of Removing Hydrogen Sulfide from Gaseous Mixtures. U.S. Patent No. 2,943,910, 1960.
46. Giammarco, G. Process for the Removal of Carbon Dioxide and/or Hydrogen Sulphide and Other Acidic Gases from Gas Mixtures. U.S. Patent No. 3,897,227, 1975.
47. Giammarco, G.; Giammarco, P. Process for Regenerating Absorbent Solutions Used for Removing Gaseous Impurities from Gaseous Mixtures by Stripping with Steam. U.S. Patent No. 3,962,404, 1976.
48. Giammarco, G. Absorption of CO₂ and/or H₂S Utilizing Solutions Containing Two Different Activators. U.S. Patent No. 4,434,144, 1984.
49. Eickmeyer, A.G. Method for Removing Acid Gases from Gaseous Mixture. U.S. Patent No. 3,851,041, 1974.
50. Eickmeyer, A.G. Method and Compositions for Removing Acid Gases from Gaseous Mixtures. U.S. Patent No. 4,271,132, 1981.

51. Eickmeyer, A.G. Method and Compositions for Removing Acid Gases from Gaseous Mixtures and Reducing Corrosion of Ferrous Surface Areas in Gas Purification Systems. U.S. Patent No. 3,896,212, 1975.
52. Eickmeyer, A.G. Removal of CO₂ from Gas Mixtures. U.S. Patent No. 4,430,312, 1984.
53. Comyns, A.E. *Encyclopedic Dictionary of Named Processes in Chemical Technology*, 3rd ed.; CRC Press: Boca Raton 2007.
54. Cullinane, J.T.; Rochelle, G.T. Carbon Dioxide Absorption with Aqueous Potassium Carbonate Promoted by Piperazine, *Chem. Eng. Sci.* **2004**, *59*, 3619-3630.
55. Oyenekan, B.A.; Rochelle, G.T. Energy Performance of Stripper Configurations for CO₂ Capture by Aqueous Amines. *Ind. Eng. Chem. Res.* **2006**, *45*, 2457-2464.
56. Cullinane, J.T.; Rochelle, G.T. Kinetics of Carbon Dioxide Absorption into Aqueous Potassium Carbonate and Piperazine. *Ind. Eng. Chem. Res.* **2006**, *45*, 2531-2545.
57. Shrier, L.L.; Jarman, R.A.; Burstein, G.T. *Corrosion: Metal/Environment Reaction*, 3rd ed.; Butterworth Heinemann: Oxford 2000.
58. Bottoms, R.R. Process for Separating Acidic Gases. U.S. Patent No. 1,783,901, 1930.
59. Clarke, J.K.A. Kinetics of Absorption of Carbon Dioxide in Monoethanolamine Solutions at Short Contact Times. *Ind. Eng. Chem. Fundamen.* **1964**, *3*, 239-245.

60. Gioia, F.; Astarita, G. General Solution to the Problem of Hydrogen Sulfide Absorption in Alkaline Solutions. *Ind. Eng. Chem. Fundamen.* **1967**, *6*, 370-375.
61. Lawson, J.D.; Garst, A.W. Gas sweetening data: equilibrium solubility of hydrogen sulfide and carbon dioxide in aqueous monoethanolamine and aqueous diethanolamine solutions. *J. Chem. Eng. Data* **1976**, *21*, 20-30.
62. Lawson, J.D.; Garst, A.W. Hydrocarbon Gas Solubility in Sweetening Solutions: Methane and Ethane in Aqueous Monoethanolamine and Diethanolamine. *J. Chem. Eng. Data* **1976**, *21*, 30-32.
63. Lee, J.I.; Otto, F.D.; Mather, A.E. Solubility of Carbon Dioxide in Aqueous Diethanolamine Solutions at High Pressures. *J. Chem. Eng. Data* **1972**, *17*, 465-468.
64. Lee, J.I.; Otto, F.D.; Mather, A.E. Solubility of Hydrogen Sulfide in Aqueous Diethanolamine Solutions at High Pressures. *J. Chem. Eng. Data* **1973**, *18*, 71-73.
65. Kennard, M.L.; Misen, A. Mechanisms and kinetics of diethanolamine degradation, *Ind. Eng. Chem. Fundamen.* **1985**, *24*, 129-140.
66. Al-Ghawas, H.A.; Hagewiesche, D.P.; Ruiz-Ibanez, G.; Sandall, O.C. Physicochemical Properties Important for Carbon Dioxide Absorption in Aqueous Methyldiethanolamine. *J. Chem. Eng. Data* **1989**, *34*, 385-391.
67. Kuranov, G.; Rumpf, B.; Smirnova, M.A.; Maurer, G. Solubility of Single Gases Carbon Dioxide and Hydrogen Sulfide in Aqueous Solutions of N-Methyldiethanolamine in the Temperature Range 313–413 K at Pressures up to 5 MPa, *Ind. Eng. Chem. Res.* **1996**, *35*, 1959-1966.

68. Li, Y.; Mather, A.E. Correlation and Prediction of the Solubility of CO₂ and H₂S in Aqueous Solutions of Methyldiethanolamine, *Ind. Eng. Chem. Res.* **1997**, *36*, 2760-2765.
69. Isaacs, E.E.; Otto, F.D.; Mather, A.E. Solubility of Hydrogen Sulfide and Carbon Dioxide in an Aqueous Diisopropanolamine Solution, *J.Chem. Eng. Data* **1977**, *22*, 71-73.
70. Isaacs, E.E.; Otto, F.D.; Mather, A.E. Solubility of Hydrogen Sulfide and Carbon Dioxide in a Sulfinol Solution, *J.Chem. Eng. Data* **1977**, *22*, 317-319.
71. Sanchez, F.C. (2005) Absorption of Carbon Dioxide at High Partial Pressures in Aqueous Solutions of Di-isopropanolamine, *Ind. Eng. Chem. Res.* **2005**, *44*, 7451-7457.
72. Martin, J.L.; Otto, F.D.; Mather, A.E. Solubility of hydrogen sulfide and carbon dioxide in a diglycolamine solution, *J.Chem. Eng. Data* **1978**, *23*, 163-164.
73. Al-Juained, M.; Rochelle, G.T. Absorption of CO₂ in Aqueous Diglycolamine, *Ind. Eng. Chem. Res.* **2006**, *45*, 2473-2482.
74. Al-Juained, M.; Rochelle, G.T. Thermodynamics and Equilibrium Solubility of Carbon Dioxide in Diglycolamine/Morpholine/Water, *J. Chem. Eng. Data* **2006**, *51*, 708-717.
75. Alper, E. Reaction Mechanism and Kinetics of Aqueous Solutions of 2-amino-2-methyl-1-propanol and Carbon Dioxide, *Ind. Eng. Chem. Res.* **1990**, *29*, 1725-1728.
76. Yih, S.M; Shen, K.P. Kinetics of carbon dioxide reaction with sterically hindered 2-amino-2-methyl-1-propanol aqueous solutions, *Ind. Eng. Chem. Res.* **1988**, *27*, 2237-2241.

77. Aroonwilas, A.; Tontiwachwuthikul, P. Mass Transfer Coefficients and Correlation for CO₂ Absorption into 2-Amino-2-methyl-1-propanol (AMP) Using Structured Packing, *Ind. Eng. Chem. Res.* **1998**, *37*, 569-575.
78. Choi, W.J.; Min, B.M.; Seo, J.B.; Park, S.W.; Oh, K.J. Effect of Ammonia on the Absorption Kinetics of Carbon Dioxide into Aqueous 2-Amino-2-methyl-1-propanol Solutions, *Ind. Eng. Chem. Res.* **2009**, *48*, 4022-4029.
79. Baek, J.; Yoon, J.H. Solubility of Carbon Dioxide in Aqueous Solutions of 2-Amino-2-methyl-1,3-propanediol, *J. Chem. Eng. Data* **1998**, *43*, 635-637.
80. Yoon, S.J.; Lee, H.; Yoon, J.H.; Shim, J.G.; Lee, J.K.; Min, B.Y.; Eum, H.M. Kinetics of Absorption of Carbon Dioxide into Aqueous 2-Amino-2-ethyl-1,3-propanediol Solutions, *Ind. Eng. Chem. Res.* **2002**, *41*, 3651-3656.
81. Shen, K.P.; Li, M.H. Solubility of Carbon Dioxide in Aqueous Mixtures of Monoethanolamine and Methyldiethanolamine. *J. Chem. Eng. Data* **1992**, *37*, 96-100.
82. Seo, D.J.; Hong, W.H. Solubilities of Carbon Dioxide in Aqueous Mixtures of Diethanolamine and 2-Amino-2-methyl-1-Propanol. *J. Chem. Eng. Data* **1996**, *41*, 258-260.
83. Silkenbaumer, D.; Rumpf, B.; Lichtenthaler, R.N. Solubility of Carbon Dioxide in Aqueous Solutions of 2-Amino-2-methyl-1-propanol and N-Methyldiethanolamine and Their Mixtures in the Temperature Range from 313 to 353 K and Pressures up to 2.7 MPa. *Ind. Eng. Chem. Res.* **1998**, *37*, 3133-3141.
84. Xiao, J.; Li, C.W.; Li, M.H. Kinetics of Absorption of Carbon Dioxide into Aqueous Solutions of 2-amino-2-methyl-1-propanol + Monoethanolamines. *Chemical Engineering Science* **2000**, *55*, 161-175.

85. Rinker, E.B.; Ashour, S.S.; Sandall, O.C. Absorption of Carbon Dioxide into Aqueous Blends of Diethanolamine and Methyldiethanolamine. *Ind. Eng. Chem. Res.* **2000**, *39*, 4346-4356.
86. Zhang, X.; Zhang, C.F.; Liu, Y. Kinetics of Absorption of CO₂ into Aqueous Solution of MDEA Blended with DEA. *Ind. Eng. Chem. Res.* **2002**, *41*, 1135-1141.
87. Park, S.H.; Lee, K.B.; Hyun, J.C.; Kim, S.H. Correlation and Prediction of the Solubility of Carbon Dioxide in Aqueous Alkanolamine and Mixed Alkanolamine Solutions. *Ind. Eng. Chem. Res.* **2002**, *41*, 1658-1665.
88. Mandal, B.P.; Kundu, M.; Padhiyar, N.U.; Bandyopadhyay, S.S. Physical Solubility and Diffusivity of N₂O and CO₂ into Aqueous Solutions of (2-Amino-2-methyl-1-propanol + Diethanolamine) and (N-Methyldiethanolamine + Diethanolamine). *J. Chem. Eng. Data* **2004**, *49*, 264-270.
89. Mandal, B.P.; Kundu, M.; Padhiyar, N.U.; Bandyopadhyay, S.S. Physical Solubility and Diffusivity of N₂O and CO₂ into Aqueous Solutions of (2-Amino-2-methyl-1-propanol + Monoethanolamine) and (N-Methyldiethanolamine + Monoethanolamine). *J. Chem. Eng. Data* **2005**, *50*, 352-358.
90. Kundu, M.; Bandyopadhyay, S.S. Solubility of CO₂ in Water + Diethanolamine + 2-Amino-2-methyl-1-propanol. *J. Chem. Eng. Data* **2006**, *51*, 398-405.
91. Xu, G.; Zhang, C.; Qin, S.; Wang, Y. Kinetics Study on Absorption of Carbon Dioxide into Solutions of Activated Methyldiethanolamine. *Ind. Eng. Chem. Res.* **1992**, *31*, 921-927.
92. Xu, G.W.; Zhang, C.F.; Qin, S.J.; Zhu, B.C. Desorption of CO₂ from MDEA and Activated MDEA Solutions. *Ind. Eng. Chem. Res.* **1995**, *34*, 874-880.

93. Xu, G.W.; Zhang, C.F.; Qin, S.J.; Gao, W.H.; Liu, H.B. Gas-Liquid Equilibrium in a CO₂-MDEA-H₂O System and the Effect of Piperazine on It. *Ind. Eng. Chem. Res.* **1998**, *37*, 1473-1477.
94. Liu, H.B.; Zhang, C.F.; Xu, G.W. A Study on Equilibrium Solubility for Carbon Dioxide in Methyldiethanolamine-Piperazine-Water Solution. *Ind. Eng. Chem. Res.* **1999**, *38*, 4032-4036.
95. Zhang, X.; Zhang, C.F.; Xu, G.W.; Gao, W.H.; Wu, Y.Q. An Experimental Apparatus to Mimic CO₂ Removal and Optimum Concentration of MDEA Aqueous Solution. *Ind. Eng. Chem. Res.* **2001**, *40*, 808-901.
96. Bishnoi, S.; Rochelle, G.T. Thermodynamics of Piperazine-Methyldiethanolamine-Water-Carbon Dioxide. *Ind. Eng. Chem. Res.* **2002**, *41*, 604-612.
97. Xu, H.J.; Zhang, C.F.; Zheng, Z.S. Solubility of Hydrogen Sulfide and Carbon Dioxide in a Solution of Methyldiethanolamine Mixed with Ethylene Glycol. *Ind. Eng. Chem. Res.* **2002**, *41*, 6175-6180.
98. Zhang, X.; Wang, J.; Zhang, C.F.; Yang, Y.H.; Xu, J.J. Absorption Rate into a MDEA Aqueous Solution Blended with Piperazine under a High CO₂ Partial Pressure. *Ind. Eng. Chem. Res.* **2003**, *42*, 118-122.
99. Bonenfant, D.; Mimeault, M.; Hausler, R. Comparative Analysis of the Carbon Dioxide Absorption and Recuperation Capacities in Aqueous 2-(2-Aminoethylamino)ethanol (AEE) and Blends of Aqueous AEE and N-Methyldiethanolamine Solutions. *Ind. Eng. Chem. Res.* **2005**, *44*, 3720-3725.
100. Samanta, A.; Roy, S.; Bandyopadhyay, S.S. Physical Solubility and Diffusivity of N₂O and CO₂ in Aqueous Solutions of Piperazine and (N-Methyldiethanolamine + Piperazine). *J. Chem. Eng. Data* **2007**, *52*, 1381-1385.

101. Bonenfant, D.; Mimeault, M.; Hausler, R. Estimation of the CO₂ Absorption Capacities in Aqueous 2-(2-Aminoethylamino)ethanol and Its Blends with MDEA and TEA in the Presence of SO₂. *Ind. Eng. Chem. Res.* **2007**, *46*, 8968-8971.
102. Barrett, G.C.; Elmore, D.T. *Amino Acids and Peptide*; Cambridge University Press: Cambridge 1998.
103. Kumar, P. S.; Hangendoorn, J. A.; Feron, P. H. M.; Versteeg, G. F. Equilibrium Solubility of CO₂ in Aqueous Potassium Taurate Solutions: Part 1. Crystallization in Carbon Dioxide Loaded Aqueous Salts Solutions of Amino Acids. *Ind. Eng. Chem. Res.* **2003**, *42*, 2832-2840.
104. Kumar, P.S. Development and Design of Membrane Gas Absorption Processes. Ph.D. Thesis, University of Twente, Enschede, The Netherlands, 2002.
105. Holst, J.; Versteeg, G. F.; Brilman, D.W.F.; Hangendoorn, J. A. Kinetic study of CO₂ with various amino acid salts in aqueous solution. *Chem. Eng. Sci.* **2009**, *64*, 59.68.
106. Jang, R.J.; Eum, H.M.; Kim, D.W.; Kim, J.H.; Min, B.M.; Lee, S.C. Absorbent and Method for Separating Acid Gases from Gas Mixture. U.S Patent No. US2006/0270551 A1, 2006.
107. Lee, S.; Song, H.J.; Maken, S. Park, J.W. Kinetics of CO₂ Absorption in Aqueous Sodium Glycinate Solutions. *Ind. Eng. Chem. Res.* **2007**, *46*, 1578-1583.
108. Lee, S; Song, H. J.; Maken, S.; Shin, H. C.; Song, H. C.; Park, J. W. Physical Solubility and Diffusivity of N₂O and CO₂ in Aqueous Sodium Glycinate Solutions. *J. Chem. Eng. Data* **2006**, *51*, 504-509.
109. Lee, S.; Choi, S. I.; Maken, S.; Song, H. J.; Shin, H. C.; Park, J. W.; Jang, K. R.; Kim, J. H. Physical Properties of Aqueous Sodium Glycinate Solution as an

- Absorbent for Carbon Dioxide Removal. *J. Chem. Eng. Data* **2005**, *50*, 1773-1776.
110. Park, S.J.; Jang, K.R.; Park, I.H. Determination and Calculation of Physical Properties for Sodium Glycinate as a CO₂ Absorbent. *Korean Chem. Eng. Res.* **2006**, *44*, 277-283.
111. Majchrowicz, M.; Niederer, J.P.M.; Velders, A.H.; Versteeg, G.F. Precipitation in Amino Acid Salt CO₂ Absorption System. www.co2-cato.nl/doc.php?lid=129
112. Sigma Aldrich, Material Safety Data Sheet Sodium Glycinate.
113. Ramasami, P. Solubilities of Amino Acids in Water and Aqueous Sodium Sulfate and Related Apparent Transfer Properties. *J. Chem. Eng. Data* **2002**, *47*, 1164-1166.
114. ASTM International, D 445-04 "Standard Test Method for Kinematic Viscosity of Transparent and Opaque Liquids (and the Calculation of Dynamic Viscosity)". ASTM International: Pennsylvania. 2004.
115. Skoog, D.A.; West, D.M. *Principles of Instrumental Analysis*, 2nd ed.; Saunders College: Philadelphia. 1980.
116. ASTM International, E 1269-01 "Standard Test Method for Determining Specific Heat Capacity by Differential Scanning Calorimetry". ASTM International: Pennsylvania. 2001.
117. Chiu, L.F.; Liu, H.F.; Li, M.H. Heat Capacity of Alkanolamines by Differential Scanning Calorimetry. *J. Chem. Eng. Data* **1999**, *44*, 631-636.
118. Ditmars, D.A.; Ishihara, S.; Chang, S.S.; Bernstein, G.; West, E.D. Enthalpy and Heat-Capacity Standard Reference Material: Synthetic Sapphire (α -Al₂O₃) from 10 to 2250 K. *J. Res. Nat. Bur. Stand.* **1982**, *87*, 159-163.

119. Arashiro, E.Y.; Demarquette, M.R. Use of Pendant Drop Method to Measure Interfacial Tension between Molten Polymers. *Material Research* **1999**, *2*, 23-32.
120. Marlin, T.E. *Process Control – Designing Processes and Control Systems for dynamic performance*, 2nd ed.; Mc Graw Hill: Boston. 2000
121. Osborne, N.S; Sitmson, H.F.; Ginning, D.C. Measurement of Heat Capacity and Heat of Vaporization of Water in the Range 0 °C to 100 °C. *J. Res. Nat. Bur. Stand.* **1939**, *23*, 197-260.
122. Song, H.J.; Lee, S.; Park, K.; Lee, J.; Spah, D.C.; Park, J.W.; Filburn, T.P. Simplified Estimation of Regeneration Energy of 30 wt % Sodium Glycinate Solution for Carbon Dioxide Absorption. *Ind. Eng. Chem. Res.* **2008**, *47*, 9925-9930.
123. Weiland, R.H.; Dingman, J.C.; Cronin, D.B. Heat Capacity of Aqueous Monoethanolamine, Diethanolamine, N-Methyldiethanolamine-Based Blend with Carbon Dioxide. *J. Chem. Eng. Data* **1997**, *42*, 1004-1006.
124. Eustathopoulos, N., Nicholas, M.G.; Drevet, B. *Wettability at High Temperatures*; Pergamon: Oxford. 1999.
125. Li, M.H.; Shen, K.P. Densities and Solubilities of Solution of Carbon Dioxide in Water + Monoethanolamine + N-Methyldiethanolamine. *J. Chem. Eng. Data* **1992**, *37*, 299-290.
126. Rocca, E. Apparatus for Refining Oil. U.S. Patent No. 699,572, 1902.
127. Lopez, F.; Castells, F. Influence of tray Geometry on Scaling Up Distillation Efficiency from Laboratory Data. *Ind. Eng. Chem. Res.* **1999**, *38*, 2747-2753.

128. Zhu, L.; Yu, X.; Yao, K.; Wang, L.; Wei, K.; Wang, W. Promotions for Further Improvements in Multiple Downcomer Tray Performance. *Ind. Eng. Chem. Res.* **2004**, *43*, 6484-6489.
129. Biddulph, M.W.; Burton, A.C. Mechanism of Recirculating Liquid Flow on Distillation Sieve Plates. *Ind. Eng. Chem. Res.* **1994**, *33*, 2706-2711.
130. Biddulph, M.W.; Burton, A.C.; Lavin, T.J. Distillation trays using noncircular perforations. *Ind. Eng. Chem. Res.* **1993**, *32*, 2373-2378.
131. Millard, R.B. Bubble Tower. U.S. Patent No. 1,605,263, 1926.
132. Nutter, I.E. Valve Mechanism for Fluid and Liquid Contact Apparatus. U.S. Patent No. 2,718,900, 1955.
133. Nutter, I.E. Valve Mechanism for Fluid and Liquid Contact Apparatus. U.S. Patent No. 2,951,691, 1960.
134. Nutter, I.E. Valve Mechanism for Fluid and Liquid Contact Apparatus. U.S. Patent No. 3,287,004, 1966.
135. Treybal R.E. Adiabatic Gas Absorption and Stripping in Packed Towers. *Ind. Eng. Chem.* 1969, *61*, 36-41.
136. Chan, H.; Fair, R.J. Prediction of Point Efficiency on Sieve Tray. 1. Binary System. *Ind. Eng. Process Des. Dev.* **1984**, *23*, 814-819
137. Chan, H.; Fair, R.J. Prediction of Point Efficiency on Sieve Tray. 2. Multi component System. *Ind. Eng. Process Des. Dev.* **1984**, *23*, 820-827.
138. Barnicki, S.D.; Davis, J.F. Designing Sieve-Tray Columns, Part 2: Column Design and Verification, *Chem. Eng.* **1989**, *96*, 202-212.

139. Sinnott, R.K. *Coulson & Richardson's Chemical Engineering Vol. 6*, 3rd ed.; Butterworth-Heinemann: Oxford. 2003.
140. Lee, L.B. A Vapour-Liquid Equilibrium Model for Natural Gas Sweetening Process. Ph.D. Dissertation, University of Oklahoma, United States of America, 1996.
141. Yaws, K.L. *Yaws' Handbook of Thermodynamic and Physical Properties of Chemical Compounds*; Knovel: New York. 2003.
142. Jones, J.H.; Froning, H.R.; Clayton, E.E.Jr. Solubility of Acidic Gases in Aqueous Monoethanolamine. *J.Chem Eng. Data* **1959**, *4*, 85-92.
143. Perry, R.H; Green, D.W. *Perry's Chemical Engineers' Handbook*, 7th ed.; Mc. Graw Hill: New York. 1997.
144. Kim, I; Svendsen, H.F. Heat of Absorption of Carbon Dioxide (CO₂) in Monoethanolamine (MEA) and 2-(aminoethyl)ethanolamine (AEEA) Solutions. *Ind Eng. Chem. Res.* **2007**, *46*, 5803-5809.
145. Fair, J.R. How to Predict Sieve Tray Entrainment and Flooding. *Petro/Chem. Eng.* **1961**, *33*, 45.
146. Monnery, W. D.; Svrcek, W. Y. Successfully Specify Three-Phase Separators. *Chemical Engineering Progress* **1994**, *September*, 29-40.
147. Lockett, M.J.; Banik, S. Weeping from sieve trays. *Ind. Eng. Chem. Process Dev.* **1986**, *25*, 561-569.
148. Kister, H.Z.; Haas, J.R. Entrainment from sieve trays in the froth regime. *Ind. Eng. Chem. Res.* **1988**, *27*, 2331-2341.

PUBLICATION

JOURNAL

1. Harris, F.; Kurnia, K.A.; Mutalib, M.I.A; Thanapalan, M. Solubilities of Carbon Dioxide and Densities of Aqueous Sodium Glycinate Solutions before and after CO₂ Absorption. *J. Chem. Eng. Data* **2009**, *54*, 144-147.
2. Harris, F.; Kurnia, K.A.; Abdul Mutalib, M.I.; Thanapalan, M. Heat Capacity of Aqueous and CO₂-Loaded Sodium Glycinate Solutions. *In Correction, J. Chem. Eng. Data*, **June 2009**.

SYMPOSIUM

1. Harris, F.; Mutalib, M.I.A; Thanapalan, M. Development of New Solvent for Acid Gas Absorption based on Amino Acid Salt. SHELL Inter-Varsity Student Paper Presentation (S-SPEC), Universiti Teknologi Malaysia (UTM), Malaysia. **2008**.

APPENDIX A

MATERIAL AND ENERGY BALANCE AROUND ABSORBER

The material and energy balance calculation around absorber was done based on the simplified design procedure as proposed by Kohl [5]. The calculation involves several iterations. The result for the final iteration is presented below.

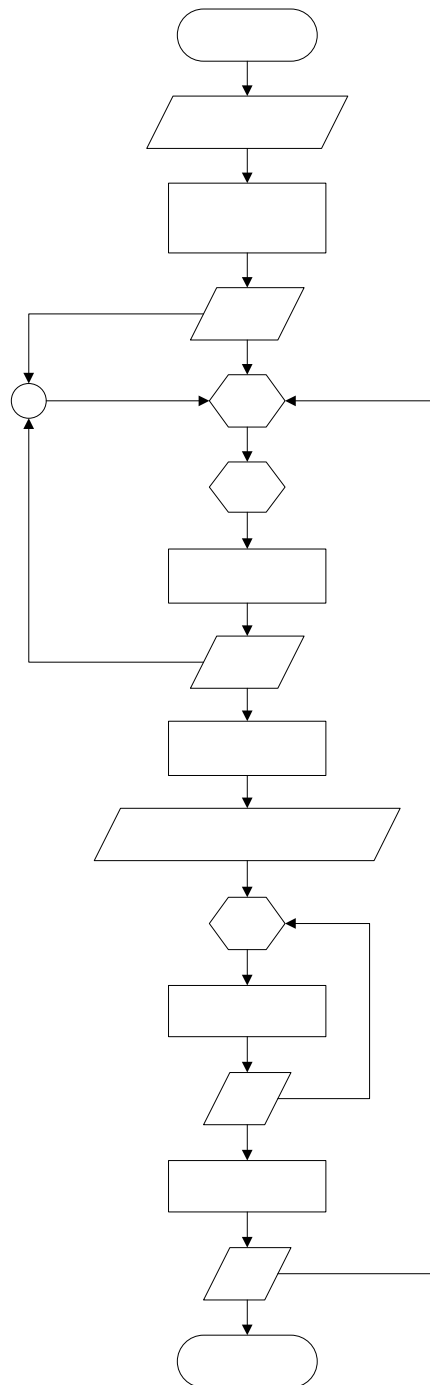


Figure A1. Flow diagram for the material and energy balance around absorber

For *monoethanolamine* (MEA) system:

1. Define the inlet regenerated absorbent condition.

Absorbent inlet condition and composition:

$$\text{Temperature, } T_L = 318.70 \text{ K}$$

$$\begin{aligned} \text{Composition, } x & : \text{MEA} : 5.06 \% \text{ mol} = 15.3 \text{ wt. \%} \\ & \text{H}_2\text{O} : 94.94 \% \text{ mol} = 84.7 \text{ wt. \%} \end{aligned}$$

$$\begin{aligned} \text{Molecular weight, } Mr & : \text{MEA} = 61.08 \text{ kg.kmol}^{-1} \\ & \text{H}_2\text{O} = 18.015 \text{ kg.kmol}^{-1} \end{aligned}$$

$$\text{Acid gas loading, } \alpha_L = 0.12$$

2. Specify the feed gas condition.

Feed gas condition and composition:

$$\text{Pressure, } P_F = 2000 \text{ kPa}$$

$$\text{Temperature, } T_F = 313.15 \text{ K}$$

$$\text{Molar flowrate, } M_F = 1000 \text{ kmol.h}^{-1}$$

$$\text{Mass flowrate, } m_F = 21644 \text{ kg.h}^{-1}$$

$$\text{Molecular weight, } Mr_F = 21.644 \text{ kg.kmol}^{-1}$$

$$\begin{aligned} \text{Composition, } x & : \text{CH}_4 : 79.59 \% \text{ mol} = 58.99 \text{ wt. \%} \\ & \text{CO}_2 : 20.00 \% \text{ mol} = 40.67 \text{ wt. \%} \\ & \text{H}_2\text{O} : 0.41 \% \text{ mol} = 0.34 \text{ wt. \%} \end{aligned}$$

$$\text{Acid gas molar flowrate, } M_{F,AG} = x_{\text{CO}_2} \cdot M_F = 200 \text{ kmol.h}^{-1}$$

$$\text{Acid gas mass flowrate, } m_{F,AG} = 8801.98 \text{ kg.h}^{-1}$$

$$\text{Water mass flowrate, } m_{F,\text{H}_2\text{O}} = 73.89 \text{ kg. h}^{-1}$$

Latent heat of evaporation:

$$\Delta H_{vF} = 5.2053 \times 10^7 (1 - T_r)^{0.3199 - 0.212T_r + 0.25795T_r^2} = 2406.32 \text{ kJ.kg}^{-1}$$

3. Calculate total acid gas content and partial pressure of acid gas in feed gas.

$$P_{F\text{CO}_2} = y_{\text{CO}_2} P = 0.2 \cdot 2000 \text{ kPa} = 400 \text{ kPa}$$

4. Set initial value for spent solution temperature.

$$\text{Set } T_{R,i} = 346.00 \text{ K}$$

5. Assume acid gas loading of the spent solution.

- The acid gas component in the feed gas is CO₂ only therefore the CO₂ loading is equal with acid gas loading of the spent solution.

$$\alpha_R = \alpha_{CO_2} = 0.635$$

- Calculate the acid gas partial pressure of spent solution at its temperature based on the available VLE data [81, 125] and the following equation:

$$\ln P_R^o = \ln P_1^o + \left[\frac{\frac{1}{T_1} - \frac{1}{T_R}}{\frac{1}{T_1} - \frac{1}{T_2}} \right] \ln \left(\frac{P_2^o}{P_1^o} \right)$$

$$\text{For } \alpha_{CO_2} = 0.635 \text{ and } T_R = 346.00 \text{ K, } P_R^o = 400 \text{ kPa}$$

- Adjust the acid gas loading until the calculated acid gas partial pressure equal with acid gas partial pressure of the feed.

$$P_R^o = 400 \text{ kPa} = p_{FCO_2}$$

6. Calculate the required inlet flow rate of the regenerated absorbent based on the total acid gas pick up (AGPU) of the absorbent.

$$AGPU = \alpha_R - \alpha_L = 0.635 - 0.12 = 0.515$$

Inlet absorbent mass flowrate:

$$m_L = \frac{100 M_{F,AG} \cdot Mr_{MEA}}{AGPU \cdot \%wt_{MEA}} = 155035 \text{ kg.hr}^{-1}$$

7. Determine the product gas condition.

Total acid gas removal is one of the main assumptions in this method. So the product gas contains hydrocarbon gas and water vapour.

$$M_{P,CH_4} = M_{F,CH_4} = x_{F,CH_4} \cdot M_F = 0.7959 \cdot 1000 = 795.9 \text{ kmol.h}^{-1}$$

Water vapour content:

$$y_i P = x_i P_i^{sat}$$

The water saturation pressure is calculated from Equation 5.6. $P_i^{sat} = 9.90 \text{ kPa}$

$$y_{H_2O} = 0.000250394$$

$$M_{P,H_2O} = 0.199338 \text{ kmol.h}^{-1}$$

$$m_{P,H_2O} = 3.59 \text{ kg.h}^{-1}$$

$$\Delta H_{vp} = 2394.59 \text{ kJ.kg}^{-1}$$

8. Calculate the heat of absorption, Q_{abs} .

$$Q_{abs} = M_{F,AG} \cdot \Delta H_{abs}$$

for ΔH_{abs} of MEA system is obtained from published data [5].

$$Q_{abs} = 1.7 \text{ e}07 \text{ kJ.h}^{-1}$$

9. Calculate the heat of water evaporation or condensation.

- Calculate the amount of water evaporated or condensed:

$$\Delta H_{2O} = m_{F,H_2O} - m_{P,H_2O} = 70.30 \text{ kg.h}^{-1}$$

- Calculate the heat of water evaporation or condensed

$$Q_{H_2O} = m_{F,H_2O} \cdot \Delta H_{vF} - m_{P,H_2O} \cdot \Delta H_{vP} = 169206.4 \text{ kJ.h}^{-1}$$

- Calculate the spent solution mass flowrate.

$$m_R = m_L + m_{F,AG} + \Delta H_{2O} = 163907.2 \text{ kg.h}^{-1}$$

10. Calculate the actual spent solution temperature based on enthalpy balance around absorber.

$$T_R = \frac{m_L c_{pL} (T_L - T_F) - m_P c_{pP} (T_P - T_F) + Q_{abs} + Q_{H_2O}}{m_R c_{pR}} + T_F$$

The heat capacity of gases and liquid is calculated from available data [5, 143].

The actual spent solution temperature, $T_R = 346.00 \text{ K}$

11. Compare the actual temperature of the spent solution with initial value from step 4.

$$T_R = T_{R,i} = 346.00 \text{ K}$$

For *Sodium glycinate* (SG) system:

1. Absorbent inlet condition and composition:

Temperature, T_L	= 318.70 K
Composition, x	: SG : 3.17 % mol = 15.00 wt. % H ₂ O : 96.83 % mol = 85.00 wt. %
Molecular weight, Mr	: SG = 97.05 kg.kmol ⁻¹ H ₂ O = 18.015 kg.kmol ⁻¹
Acid gas loading, α_L	= 0.12

2. Feed gas condition and composition:

Pressure, P_F	= 2000 kPa
Temperature, T_F	= 313.15 K
Molar flowrate, M_F	= 1000 kmol.h ⁻¹
Mass flowrate, m_F	= 21644 kg.h ⁻¹
Molecular weight, Mr_F	= 21.644 kg.kmol ⁻¹
Composition, x	: CH ₄ : 79.59 % mol = 58.99 wt. % CO ₂ : 20.00 % mol = 40.67 wt. % H ₂ O : 0.41 % mol = 0.34 wt. %

$$M_{F,AG} = 200 \text{ kmol.h}^{-1}$$

$$m_{F,AG} = 8801.98 \text{ kg.h}^{-1}$$

$$m_{F,H_2O} = 73.89 \text{ kg. h}^{-1}$$

$$\Delta H_{vF} = 2406.32 \text{ kJ.kg}^{-1}$$

3. $p_{FCO_2} = 400 \text{ kPa}$

4. Set $T_{R,i} = 323.7 \text{ K}$

5. $\alpha_R = \alpha_{CO_2} = 0.967$

For $\alpha_{CO_2} = 0.967$ and $T_R = 323.7 \text{ K}$, $P_R^o = 400 \text{ kPa}$

$$P_R^o = 400 \text{ kPa} = p_{FCO_2}$$

6. $AGPU = 0.847$

$$m_L = 152768 \text{ kg.hr}^{-1}$$

7. $M_{P,CH_4} = 795.9 \text{ kmol.h}^{-1}$

$$y_{H_2O} = 0.000157021$$

$$M_{P,H_2O} = 0.124992 \text{ kmol.h}^{-1}$$

$$m_{P,H_2O} = 2.25 \text{ kg.h}^{-1}$$

$$\Delta H_{vp} = 2394.59 \text{ kJ.kg}^{-1}$$

8. $Q_{abs} = 3222447 \text{ kJ.h}^{-1}$

9. $\Delta H_{2O} = 71.64 \text{ kg.h}^{-1}$

$$Q_{H_2O} = 172413.6 \text{ kJ.h}^{-1}$$

$$m_R = m_L + m_{F,AG} + \Delta H_{2O} = 161641.5 \text{ kg.h}^{-1}$$

10. $T_R = 323.7 \text{ K}$

11. $T_R = T_{R,i} = 323.7 \text{ K}$

APPENDIX B

DIAMETER OF ABSORBER CALCULATION

The calculation for absorber diameter and geometry is done for plate absorber according to method proposed by R.K. Sinnott [139]. The calculation is based on trial and error approach using empirical correlation and some rule of thumb. All stream flow rate and properties used is calculated in Appendix A. The result for the final iteration is presented below.

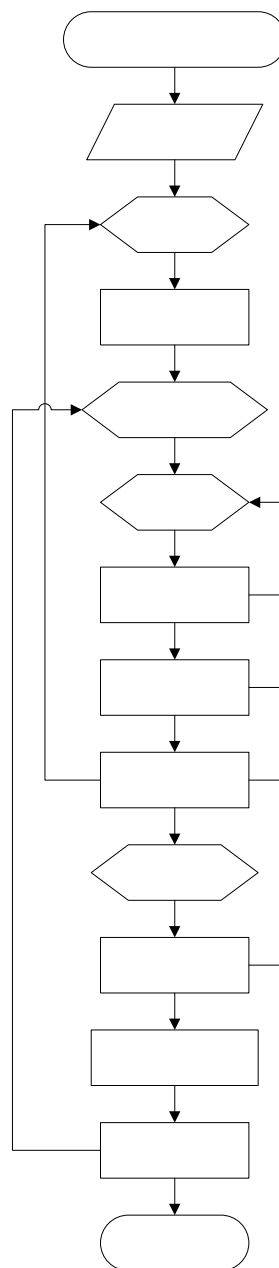


Figure B1. Flow diagram for diameter of absorber calculation

For *monoethanolamine* (MEA) system:

1. Calculate the maximum and minimum vapour and liquid flow rate for turn down ratio.

Stream flowrate:

Feed gas	: M_F	= 1000 kmol.h ⁻¹
	m_F	= 21644 kg.h ⁻¹ = 6.012 kg.s ⁻¹
Inlet absorbent	: M_L	= 7677.5 kmol.h ⁻¹
	m_L	= 155035 kg.h ⁻¹ = 43.065 kg.s ⁻¹
Product gas	: M_P	= 796.096 kmol.h ⁻¹
	m_P	= 12772.19 kg.h ⁻¹ = 3.548 kg.s ⁻¹
Spent solution	: M_R	= 7881.433 kmol.h ⁻¹
	m_R	= 163907 kg.h ⁻¹ = 45.53 kg.s ⁻¹
Turn down ratio	: TD	= 90 %

2. Collect or estimate the system physical properties.

Feed gas density, ρ_F	= 17.39 kg.m ⁻³
Inlet absorbent density, ρ_L	= 995.19 kg.m ⁻³
Inlet absorbent surface tension, σ_L	= 0.0654 N.m ⁻¹
Product gas density, ρ_P	= 12.41 kg.m ⁻³
Spent solution density, ρ_R	= 995.19 kg.m ⁻³
Spent solution surface tension, σ_R	= 0.0613 N.m ⁻¹

3. Select trial plate spacing.

Set tray spacing, $S = 0.9$ m

4. Estimate the column diameter based on flooding consideration.

- Calculate liquid vapour flow factor: $F_{LV} = \frac{L_w}{V_w} \left(\frac{\rho_G}{\rho_L} \right)^{0.5}$. The calculation is done for top section and bottom section of the absorber.

For top part, $F_{LVT} = 1.0769$

Bottom part, $F_{LVB} = 1.0201$

- Determine the K_1 constant based on Figure 5.5. Correction factor for liquid surface tension other than 0.02 N.m⁻¹: $K_1' = K_1 \left(\frac{\sigma}{0.02} \right)^{0.2}$

For top part, $K_1' T = 0.044 \cdot 1.2675 = 0.0558$

$$\text{Bottom part, } K_{1B}' = 0.045 \cdot 1.2512 = 0.0563$$

- Calculate the flooding velocity: $u_f = K_1 \left(\frac{\rho_L - \rho_G}{\rho_G} \right)^{0.5}$

$$\text{For top part, } u_{fT} = 0.4963 \text{ m.s}^{-1}$$

$$\text{Bottom part, } u_{fB} = 0.4314 \text{ m.s}^{-1}$$

Set maximum vapour velocity at 85 % of flooding velocity: $\hat{u}_T = 0.85 u_f$

$$\text{For top part, } \hat{u}_T = 0.4218 \text{ m.s}^{-1}$$

$$\text{Bottom part, } \hat{u}_B = 0.3666 \text{ m.s}^{-1}$$

- Calculate required column area: $A_n = \frac{m}{\rho \cdot \hat{u}}$

$$\text{For top part, } A_{NT} = 0.6777 \text{ m}^2$$

$$\text{Bottom part, } A_{NB} = 0.9432 \text{ m}^2$$

Set downcomer design factor, $kA_d = 0.12$

$$\text{Actual column area } A = \frac{A_n}{kA_d}$$

$$\text{For top part, } A_T = 0.7701 \text{ m}^2$$

$$\text{Bottom part, } A_B = 1.0718 \text{ m}^2$$

- Calculate required column diameter: $D = \left(\frac{4A}{\pi} \right)^{0.5}$

$$\text{For top part, } D_T = 0.9902 \text{ m}$$

$$\text{Bottom part, } D_B = 1.1682 \text{ m}$$

Since the calculated diameter for bottom section of the absorber is larger than the top section therefore the calculation of absorber diameter would be based on bottom section diameter.

Set absorber diameter, $D = 1.17 \text{ m}$

5. Decide the liquid flow arrangement.

Set liquid flow arrangement for single pass

6. Make trial plate layout. The layout include downcomer area, active area, hole area, hole size, and weir height.

Provision tray layout:

$$\text{Column area, } A_c = \frac{\pi}{4} D^2 = 1.0751 \text{ m}^2$$

$$\text{Downcomer area, } A_d = kA_d \cdot A_c = 0.1290 \text{ m}^2$$

Net area, $A_n = A_c - A_d = 0.9461 \text{ m}^2$

Active area, $A_a = A_c - 2 A_d = 0.8171 \text{ m}^2$

Set hole design factor, $kA_h = 0.1$

Hole area, $A_h = kA_h. A_a = 0.0817 \text{ m}^2$

Calculate downcomer height, l_w , based on Equation 5.11. $l_w = 0.8945 \text{ m}$

Downcomer subtended angle, $\theta_c = 99.23^\circ$

Set weir height, $h_w = 0.05 \text{ m}$

Hole diameter, $d_h = 0.005 \text{ m}$

7. Check weeping rate, if unsatisfactory return to step 6.

- Weep flux could be calculated using the following equation:

$$WF = 0.020Fr^{-1} - 0.030$$

$$Fr = u_h \left(\frac{\rho_G}{gh_{cl}\rho_L} \right)^{0.5}$$

Weeping occurs if weep flux equal to zero or Froude number (Fr) equal to 0.67. The minimum vapour velocity through hole could be calculated at weep flux equal to zero.

$$u_{hmin} = 3.6055 \text{ m.s}^{-1}$$

- The actual minimum vapour velocity through hole is calculated from the following equation:

$$u_h = \frac{TD \cdot m_R}{\rho_L \cdot A_h} = 3.8091 \text{ m.s}^{-1}$$

- Calculation is satisfactory if $u_h > u_{hmin}$

8. Check plate pressure drop, if unsatisfactory return to step 6.

- Calculate the liquid height over weir:

$$h_{ow} = 750 \left[\frac{L_w}{\rho_L l_w} \right] = 750 \left[\frac{m_R}{\rho_R l_w} \right] = 100.4867 \text{ mm}$$

- Calculate the dry plate pressure drop:

$$h_{dry} = \frac{\epsilon \rho_G u_s^2}{2\rho_L g} \left(\frac{1}{\beta^2} - 1 \right) = 4.5344 \text{ mm}$$

- Calculate the residual head:

$$h_{residual} = \frac{4\sigma}{d_h \rho_L g} = 4.8248 \text{ mm}$$

- The weir height, $h_w = 0.05 \text{ m}$

- The tray pressure drop, $h_t = 159.8459$ mm
9. Check downcomer back up, if too high return to step 6 or step 3.
- Calculate the head loss in downcomer:

$$h_{dc} = 166 \left(\frac{L_{wd}}{\rho_L A_m} \right)^2 = 249.5340 \text{ mm}$$

- Calculate downcomer back up:

$$h_b = h_w + h_{ow} + h_t + h_{dc} = 559.8666 \text{ mm}$$

10. Decide plate layout detail. Detail plate layout includes calming zone and unperforated areas. Check hole pitch, if unsatisfactory return to step 6.

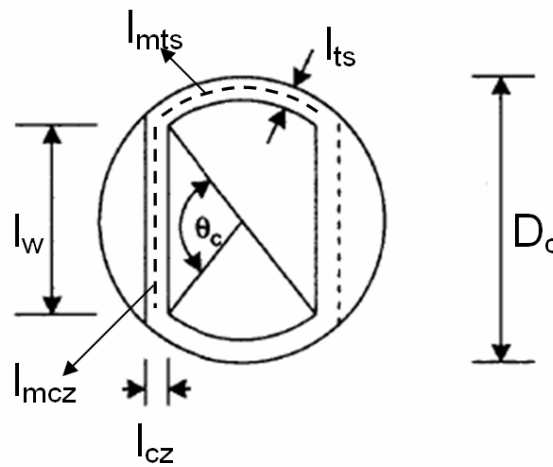


Figure A. Actual tray layout [139]

Set calming zone length, $l_{cz} = 50$ mm

Set tray support length, $l_{ts} = 50$ mm

Mean length calming zone, $l_{mcz} = (D - l_{cz}) \sin\left(\frac{\theta_c}{2}\right) = 0.8532$ m

Mean length tray support, $l_{mts} = (D - l_{ts}) \pi \left(\frac{180 - \theta_c}{180} \right) = 1.5787$ m

Calming zone area, $A_{cz} = 2 \cdot l_{cz} \cdot l_{mcz} = 0.0853$ m²

Tray support area, $A_{ts} = l_{ts} \cdot l_{mts} = 0.0789$ m²

Perforation area, $A_p = A_a - A_{cz} - A_{ts} = 0.6528$ m²

Calculate the hole pitch to hole diameter ratio. Calculation is satisfactory if the ratio above 2.5.

$$\frac{A_h}{A_p} = 0.9 \left[\frac{d_h}{l_p} \right]^2 ; \frac{l_p}{d_h} = 2.6816$$

11. Recalculate the percentage of flooding based on chosen column diameter.

$$\text{Actual vapour velocity, } u_v = \frac{m_R}{\rho_R A_n} = 0.3655 \text{ m.s}^{-1}$$

$$\text{Actual flooding factor} = \frac{u_v}{u_{fB}} = 0.7365$$

12. Check entrainment, if too high return to step 4.

$$E = 3.08 \times 10^5 \left(\frac{u_s}{S - 2.5h_c} \right)^{3.2} \left(\frac{73}{\sigma} \right) = 1.7634 \text{e-}5$$

The calculation is satisfactory if $E < 0.1$

13. Optimize design. Repeat steps 3 to 12 to obtain acceptable smallest diameter and tray spacing.
14. Finalize design. Sketch plate layout and state tray specification.

For *sodium glycinate* (SG) system:

1. Calculate the maximum and minimum vapour and liquid flow rate for turn down ratio.

Stream flowrate:

Feed gas	: M_F	= 1000 kmol.h ⁻¹
	m_F	= 21644 kg.h ⁻¹ = 6.012 kg.s ⁻¹
Inlet absorbent	: M_L	= 7444.1 kmol.h ⁻¹
	m_L	= 152768 kg.h ⁻¹ = 42.436 kg.s ⁻¹
Product gas	: M_P	= 796.022 kmol.h ⁻¹
	m_P	= 12770.85 kg.h ⁻¹ = 3.547 kg.s ⁻¹
Spent solution	: M_R	= 7648.082 kmol.h ⁻¹
	m_R	= 161641.5 kg.h ⁻¹ = 44.900 kg.s ⁻¹
Turn down ratio	: TD	= 90 %

2. Collect or estimate the system physical properties.

Feed gas density, ρ_F	= 17.39 kg.m ⁻³
Inlet absorbent density, ρ_L	= 1080.632 kg.m ⁻³
Inlet absorbent surface tension, σ_L	= 0.023 N.m ⁻¹
Product gas density, ρ_P	= 12.41 kg.m ⁻³
Spent solution density, ρ_R	= 1081.864 kg.m ⁻³
Spent solution surface tension, σ_R	= 0.057 N.m ⁻¹

3. Select trial plate spacing.

Set tray spacing, $S = 0.9$ m

4. Estimate the column diameter based on flooding consideration.

- For top part, $F_{LVT} = 1.0021$
Bottom part, $F_{LVB} = 0.9695$
- For top part, $K_{1T}' = 0.046 \cdot 1.0283 = 0.0473$
Bottom part, $K_{1B}' = 0.047 \cdot 1.2330 = 0.0580$
- For top part, $u_{fT} = 0.4389$ m.s⁻¹
Bottom part, $u_{fB} = 0.4535$ m.s⁻¹

Set maximum vapour velocity at 85 % of flooding velocity: $\hat{u}_T = 0.85 u_f$

For top part, \hat{u}_T	= 0.3730 m.s ⁻¹
Bottom part, \hat{u}_B	= 0.3854 m.s ⁻¹

- For top part, $A_{NT} = 0.7663 \text{ m}^2$
 Bottom part, $A_{NB} = 0.8972 \text{ m}^2$
 Set downcomer design factor, $kA_d = 0.12$

$$\text{Actual column area } A = \frac{A_n}{kA_d}$$

- For top part, $A_T = 0.8708 \text{ m}^2$
 Bottom part, $A_B = 1.0196 \text{ m}^2$
- For top part, $D_T = 1.0529 \text{ m}$
 Bottom part, $D_B = 1.1393 \text{ m}$

Since the calculated diameter for bottom section of the absorber is larger than the top section therefore the calculation of absorber diameter would be based on bottom section diameter.

Set absorber diameter, $D = 1.14 \text{ m}$

5. Decide the liquid flow arrangement.

Set liquid flow arrangement for single pass

6. Make trial plate layout. The layout include downcomer area, active area, hole area, hole size, and weir height.

Provision tray layout:

$$\text{Column area, } A_c = 1.0207 \text{ m}^2$$

$$\text{Downcomer area, } A_d = 0.1224 \text{ m}^2$$

$$\text{Net area, } A_n = 0.8982 \text{ m}^2$$

$$\text{Active area, } A_a = 0.7757 \text{ m}^2$$

$$\text{Set hole design factor, } kA_h = 0.1$$

$$\text{Hole area, } A_h = 0.0776 \text{ m}^2$$

$$\text{Calculate downcomer height, } l_w, \text{ based on Equation 5.11. } l_w = 0.8716 \text{ m}$$

$$\text{Downcomer subtended angle, } \theta_c = 99.23^\circ$$

$$\text{Set weir height, } h_w = 0.05 \text{ m}$$

$$\text{Hole diameter, } d_h = 0.005 \text{ m}$$

7. Check weeping rate, if unsatisfactory return to step 6.

- $u_{hmin} = 3.6812 \text{ m.s}^{-1}$
- $u_h = 4.012 \text{ m.s}^{-1}$
- Calculation is satisfactory if $u_h > u_{hmin}$

8. Check plate pressure drop, if unsatisfactory return to step 6.

- $h_{ow} = 98.5272$ mm
 - $h_{dry} = 4.8259$ mm
 - $h_{residual} = 4.3009$ mm
 - The weir height, $h_w = 0.05$ m
 - The tray pressure drop, $h_t = 157.6541$ mm
9. Check downcomer back up, if too high return to step 6 or step 3.
- $h_{dc} = 235.2193$ mm
 - $h_b = 541.4006$ mm
10. Decide plate layout detail. Detail plate layout includes calming zone and unperforated areas. Check hole pitch, if unsatisfactory return to step 6.
- Set calming zone length, $l_{cz} = 50$ mm
- Set tray support length, $l_{ts} = 50$ mm
- Mean length calming zone, $l_{mcz} = 0.8303$ m
- Mean length tray support, $l_{mts} = 1.5364$ m
- Calming zone area, $A_{cz} = 0.0830$ m²
- Tray support area, $A_{ts} = 0.0768$ m²
- Perforation area, $A_p = 0.6159$ m²
- Calculate the hole pitch to hole diameter ratio. Calculation is satisfactory if the ratio above 2.5.
- $$\frac{A_h}{A_p} = 0.9 \left[\frac{d_h}{l_p} \right]^2 ; \frac{l_p}{d_h} = 2.6731$$
11. Recalculate the percentage of flooding based on chosen column diameter.
- Actual vapour velocity, $u_v = 0.3850$ m.s⁻¹
- $$\text{Actual flooding factor} = \frac{u_v}{u_{fB}} = 0.8490$$
12. Check entrainment, if too high return to step 4.
- $E = 2.1986e-05$
- The calculation is satisfactory if $E < 0.1$
13. Optimize design. Repeat steps 3 to 12 to obtain acceptable smallest diameter and tray spacing.
14. Finalize design. Sketch plate layout and state tray specification.